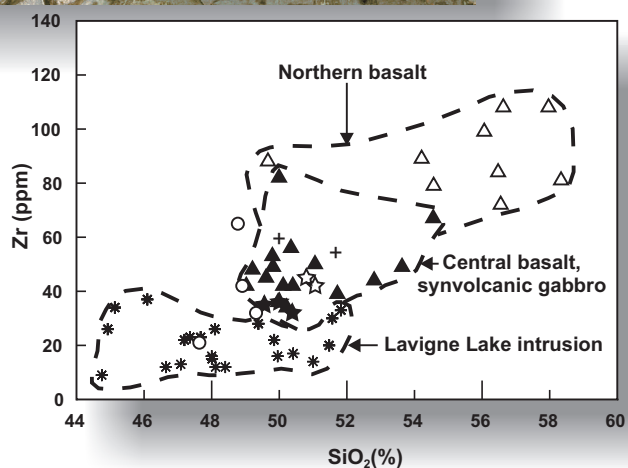
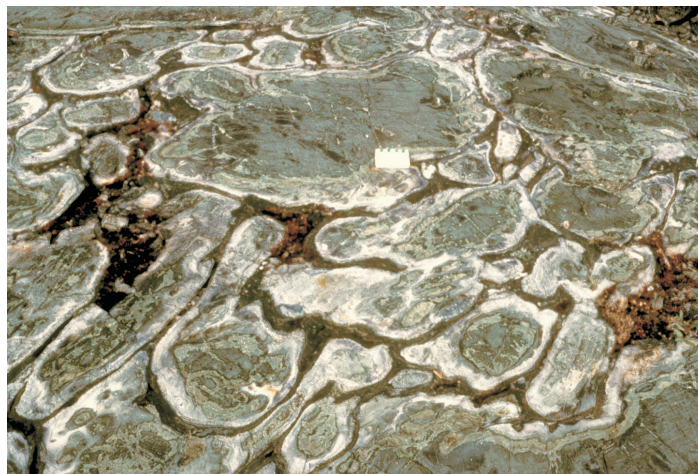




GR2004-2

GEOSCIENTIFIC REPORT

Geology and geochemistry of Archean supracrustal and intrusive rocks in the southeast Max Lake–Aswapiswanan Lake area, Manitoba (parts of NTS 53L5N, 6NW and 12SW)



By
H.P. Gilbert



Geoscientific Report GR2004-2

Geology and geochemistry of Archean supracrustal and intrusive rocks in the southeast Max Lake–Aswapiswanan Lake area, Manitoba (parts of NTS 53L5N, 6NW and 12SW)

by H.P. Gilbert
Winnipeg, 2004

Industry, Economic Development and Mines

Hon. Scott Smith
Minister

Hugh Eliasson
Deputy Minister

Mineral Resources Division

C.A. Kaszycki
Assistant Deputy Minister

Manitoba Geological Survey

E.C. Syme
Director

Every possible effort is made to ensure the accuracy of the information contained in this report, but Manitoba Industry, Economic Development and Mines does not assume any liability for errors that may occur. Source references are included in the report and users should verify critical information.

Any digital data and software accompanying this publication are supplied on the understanding that they are for the sole use of the licensee, and will not be redistributed in any form, in whole or in part, to third parties. Any references to proprietary software in the documentation and/or any use of proprietary data formats in this release do not constitute endorsement by Manitoba Industry, Economic Development and Mines of any manufacturer's product.

When using information from this publication in other publications or presentations, due acknowledgment should be given to the Manitoba Geological Survey. The following reference format is recommended:

Gilbert, H.P. 2004: Geology and geochemistry of Archean supracrustal and intrusive rocks in the southeast Max Lake–Aswapiswanan Lake area, Manitoba (parts of NTS 53L5N, 6NW and 12SW); Manitoba Industry, Economic Development and Mines, Manitoba Geological Survey, Geoscientific Report GR2004-2, 52 p.

NTS grid: 53L5N, 53L6NW, 53L12SW

Keywords: Manitoba, Precambrian, Archean, Superior Province, island arcs, basalts, calc-alkalic composition, geochemistry, komatiite, oceanic crust, rare earths, rhyolites, tholeiite, economic geology, Max Lake, Aswapiswanan Lake, MacVicar Lake, Max Lake belt, Ralph Anderson Lake belt

Published by:

Manitoba Industry, Economic Development and Mines
Manitoba Geological Survey
360-1395 Ellice Avenue
Winnipeg, Manitoba
R3G 3P2 Canada

Telephone: (800) 223-5215 (General Enquiry)
(204) 945-4154 (Publication Sales)
Fax: (204) 945-8427
E-mail: minesinfo@gov.mb.ca
Website: www.gov.mb.ca/itm/mrd

Cover illustration: Aphyric basalt of ocean-floor affinity, showing silicic and epidotic alteration of amoeboid pillows, close to the west end of Ralph Anderson Lake. The geochemical plot (zirconium versus silica) shows mafic volcanic and gabbroic rocks in the southeast Max Lake area; the central and northern volcanic suites are spatially separated by the geochemically distinct Lavigne Lake intrusion of inferred postvolcanic age.

Abstract

The Ralph Anderson Lake greenstone belt constitutes a branch of the Archean 'Max Lake belt' within the Superior Province of Manitoba. This greenstone belt extends for a distance of approximately 50 km from Logan Lake in the west to Aswapiswanan Lake in the east. The belt is monoclinial and consists mainly of arc-type mafic volcanic rocks, with subordinate felsic volcanic and sedimentary units.

The Ralph Anderson Lake belt consists of three distinct components: the 'southern', 'central' and 'northern' sections. The 'southern' section is pervasively intruded by a 1.2 km thick gabbro sill and consists of a series of skialithic enclaves of basalt, rhyolite, heterolithic debris flows and turbidite. The 'central' and 'northern' sections, which are the main supracrustal components of the belt, consist mainly of basalt; these two sections are separated by a conspicuous mafic to ultramafic sill ('Lavigne Lake gabbro'), which extends for over 24 km through the core of the belt. The 'southern', 'central' and 'northern' sections are characterized by distinctive stratigraphic and geochemical attributes. The north part of the 'northern' section includes a felsic volcanosedimentary formation, together with an associated subvolcanic porphyry sill.

Mafic volcanic rocks, which consist mainly of pillowed aphyric basalt, are characterized by widespread sea-floor-type hydrothermal alteration. A prominent, garnetiferous, silicic alteration zone in the northwest part of the map area is coincident with an oxide-facies iron formation and is interpreted as a site of early hydrothermal alteration.

Sulphide-rich zones dominated by pyrite occur in various stratigraphic/structural settings. Stratabound mineralization in both the 'northern' and 'southern' arc-type sections offers one of the best exploration prospects. The mineralization occurs in chert-siltstone units and magnetiferous iron formations intercalated with the mainly basaltic volcanic rocks. The most significant locality of this type is a pervasively altered, garnetiferous metasedimentary unit in the northwest part of the map area. Further south, the faulted contact between the southern and central stratigraphic sections contains sporadic pyritic zones that may represent prospects for gold mineralization.

TABLE OF CONTENTS

	Page
Abstract	iii
Introduction	1
MacVicar Lake–Ralph Anderson Lake area	7
Ocean-floor–type supracrustal rocks (central section)	7
Mafic volcanic rocks of ocean-floor affinity and metamorphic equivalents (unit O1)	7
Aphyric basalt; minor plagioclase-phyric basalt and related gabbro (subunit O1a)	7
Basaltic pillow-fragment breccia, flow-top breccia (subunit O1b)	8
Gabbro, locally plagioclase phyric, megaphyric or glomeroporphyritic; minor hornblende (subunits O1c, O1d)	8
Alteration in massive to fragmental basaltic rocks of ocean-floor affinity	8
Juvenile-arc–type supracrustal rocks (northern and southern sections)	9
Mafic volcanic rocks of juvenile volcanic-arc affinity and metamorphic equivalents (unit J1)	9
Aphyric basalt; minor plagioclase-phyric basalt and related gabbro (subunit J1a)	9
Basaltic pillow-fragment breccia, flow-top breccia (subunit J1b)	10
Gabbro, locally plagioclase phyric; minor hornblende (subunit J1c)	10
Amphibolite, related gneiss and schist (subunit J1e)	11
Spherulitic pillowed basalt (subunit J1f)	11
Alteration in massive to fragmental basaltic rocks of juvenile-arc affinity	11
Northern section	12
Southern section	12
Sedimentary rocks: feldspathic greywacke, siltstone and related paragneiss; oxide-facies iron formation; altered supracrustal rocks (unit J2)	13
Oxide-facies iron formation (subunit J2a)	13
Northern section	13
Southern section	13
Siltstone, feldspathic greywacke; minor chert (subunit J2b)	13
Northern section	13
Southern section	15
Altered garnetiferous supracrustal rocks (subunit J2c)	16
Heterolithic volcanic breccia and associated tuff; related sedimentary rocks (unit J3)	16
Heterolithic volcanic breccia and tuff (subunits J3a, J3b); volcanic-derived conglomerate, feldspathic greywacke and siltstone (subunit J3c)	17
Felsic volcanic rocks of juvenile-arc affinity; minor sedimentary rocks and felsic porphyry (unit J4)	19
Rhyolite, massive to fragmental (subunit J4a); heterolithic volcanic breccia and tuff (subunit J4b); volcanic-derived conglomerate, feldspathic greywacke and siltstone (subunit J4c)	19
Northern section	20
Southern section	20
Plagioclase±quartz porphyry (subunit J4d)	21
Franklin Murray Lake–Aswapiswanan Lake area	22
Stratigraphy	22
Ocean-floor–type supracrustal rocks (central section)	22
Mafic volcanic rocks of ocean-floor affinity and metamorphic equivalents (unit O1)	22
Juvenile-arc–type supracrustal rocks (southern section)	22
Mafic volcanic rocks of juvenile volcanic-arc affinity and metamorphic equivalents (unit J1); heterolithic volcanic breccia (unit J3)	22
Intrusive rocks	24
Introduction	24
Gabbro, minor pyroxenite, peridotite and hornblende; quartz diorite to diorite; diabase (unit P5)	24
McLeod Narrows intrusion	24
Lavigne Lake intrusion	24
Diabase (subunit P5c)	25

	Page
Granitoid and related gneissic rocks: tonalite, granodiorite, granite; quartz diorite to diorite; minor plagioclase porphyry, pegmatite, aplite; hybrid gneiss (unit P6)	25
Leucogabbro, diabase (unit P7)	25
Geochemistry	26
Intermediate to mafic volcanic rocks	26
Gabbroic rocks	26
Intermediate to felsic volcanic rocks and related porphyry intrusions	30
Metamorphism	38
M ₁ metamorphism	38
M ₂ metamorphism	38
M ₃ metamorphism	39
Structural geology	41
D ₁ deformation	41
D ₂ deformation	43
D ₃ deformation	43
D ₄ deformation	44
Discussion	45
Economic geology	46
Stratabound mineralization associated with iron formation and basalt (type 1, Table 7)	46
Stratabound mineralization associated with chert (types 2A, 2B, 2C, Table 7)	46
Associated with felsic porphyry dikes (type 3, Table 7)	46
Associated with gabbro (type 4, Table 7)	46
Mafic volcanic rock (type 5, Table 7)	46
Faulted contact (type 6, Table 7)	49
Intrusive or structural contact (type 7, Table 7)	49
Exploration prospects	49
Acknowledgments	49
References	50

FIGURES

Figure 1: Regional geology of the Max Lake area, showing the location of the project area at the junction of the Gods Lake and Molson Lake domains	1
Figure 2: Simplified geology of the MacVicar Lake–Ralph Anderson Lake area	2
Figure 3: Simplified geology of the Franklin Murray Lake–Aswapiswanan Lake area	3
Figure 4: Stratigraphic and structural details in the vicinity of MacVicar Lake in the northwest part of the project area	4
Figure 5: North-northeast–south-southwest section through the Ralph Anderson Lake belt	5
Figure 6: Aphyric pillowed basalt with pervasive interpillow autoclastic breccia	8
Figure 7: Altered 1 m wide basaltic flow-top breccia	9
Figure 8: Pseudohexagonal plagioclase phenocrysts in glomeroporphyritic gabbro	9
Figure 9: Zonal silicic and epidotic alteration of pillows in basalt	10
Figure 10: Epidotization of pillow cores in amygdaloidal basalt	10
Figure 11: Stratabound cordierite porphyroblasts oriented parallel to S ₁ in the northern sedimentary formation	14
Figure 12: S ₀ -S ₁ discordance in a cordierite-bearing siltstone-greywacke bed within the northern sedimentary formation	14
Figure 13: Flame structure in a chert layer within the northern sedimentary formation	14
Figure 14: White chert and black magnetite laminae within intermediate to argillaceous, garnetiferous siltstone	15
Figure 15: Graded turbidite deposit	15
Figure 16: Disrupted garnetiferous amphibolite in zone of silicic alteration	16
Figure 17: North-south stratigraphic sections through the Lavigne Lake–McLeod Narrows supracrustal enclave	17
Figure 18: Transverse north-south sections through the lower part of the Lavigne Lake–McLeod Narrows supracrustal enclave	18
Figure 19: Heterolithic volcanic breccia containing unsorted, sporadic large blocks within less coarse volcanic detritus	19
Figure 20: 'Primitive mantle'-normalized extended-element plots of mafic volcanic and gabbroic rocks	27
Figure 21: Plots of Th-Zr-Nb	28
Figure 22: Plot of Th/Nb versus Nb/Y for mafic volcanic rocks in the central and northern sections	28
Figure 23: Plots of TiO ₂ versus MgO	29
Figure 24: Plots of FeO ^T /MgO versus SiO ₂ for mafic volcanic and gabbroic rocks	30

Figure 25: Ternary Al_2O_3 –($\text{FeO}^{\text{t}}+\text{TiO}_2$)– MgO diagram for mafic to felsic volcanic rocks and related intrusive rocks.....	31
Figure 26: Plot of Zr versus SiO_2 for mafic volcanic and gabbroic rocks	32
Figure 27: Plots of Al_2O_3 –($\text{FeO}^{\text{t}}+\text{TiO}_2$)– MgO , $\text{FeO}^{\text{t}}/\text{MgO}$ versus REE, and Al_2O_3 versus $\text{FeO}^{\text{t}}/[\text{FeO}^{\text{t}}+\text{MgO}]$ for various localities throughout the Lavigne Lake intrusion.....	33
Figure 28: 'Primitive mantle'–normalized extended-element plots for the Lavigne Lake intrusion	34
Figure 29: Chondrite-normalized rare earth element plots	35
Figure 30: $(\text{La}/\text{Yb})_{\text{N}}$ versus Yb_{N} plot of felsic volcanic rocks and related plagioclase-quartz-porphyry intrusions	36
Figure 31: Plot of Zr versus TiO_2 for felsic volcanic rocks and related plagioclase-quartz porphyry intrusions.....	37
Figure 32: Ovoid aggregates of pinitized cordierite porphyroblasts are coplanar with S_1 and deformed by an F_2 minor fold	39
Figure 33: Photomicrograph of a rotational M_1 garnet porphyroblast in magnetite-bearing paragneiss	39
Figure 34: Photomicrograph of fascicular M_2 anthophyllite porphyroblasts, overprinting the S_1 micaceous foliation in pebble conglomerate	40
Figure 35: Photomicrograph of a pinitized M_1 cordierite porphyroblast with later M_2 biotite and anthophyllite in siltstone ..	40
Figure 36: Photomicrograph of randomly oriented M_2 biotite within an altered M_1 cordierite porphyroblast in siltstone	40
Figure 37: Minor F_1 fold in bedded turbidite.....	41
Figure 38: Minor F_1 fold in oxide-facies iron formation	42
Figure 39: Sequential north-south transverse sections showing the proposed structural model for the evolution of the Ralph Anderson Lake greenstone belt	42
Figure 40: Lower-hemisphere stereographic projection of F_2 minor fold axes and b lineations	43
Figure 41: F_2 folding and dislocation of S_1 foliation and related lamination, due to dextral strike-slip movement in strongly attenuated volcanic rocks	44
Figure 42: F_1 – F_2 fold interference pattern in layered metasedimentary rocks.....	44
Figure 43: Boudinage in laminated amphibolite derived from mafic volcanic flows at the north margin of the Ralph Anderson Lake belt.....	44

TABLES

Table 1: Geological map units in the southeast Max Lake–Aswapiswanan Lake area	6
Table 2: Features that distinguish the northern section from the central section, MacVicar Lake–Ralph Anderson Lake area	11
Table 3: Lithology and stratigraphic association of volcanic fragmental rocks and associated conglomerate at the south margin of the Ralph Anderson Lake greenstone belt	19
Table 4: Averages of selected geochemical parameters for mafic volcanic rocks and major gabbroic intrusions in the southeast Max Lake–Aswapiswanan Lake area.....	31
Table 5: Averages of selected geochemical parameters for felsic volcanic and related intrusive rocks, southeast Max Lake area	36
Table 6: Summary of the structural and metamorphic histories of the southeast Max Lake–Aswapiswanan Lake area	38
Table 7: Selected geochemical data for mineralized rock samples from the Ralph Anderson Lake greenstone belt	47

APPENDIX

Major-, minor- and trace-element data for volcanic and intrusive rocks in the southeast Max Lake–Aswapiswanan Lake area	A-1
-------------------------------------------------------------------------------------------------------------------------------	-----

MAPS

GR2004-2-1 Geology of the southeast Max Lake area, Manitoba (parts of NTS 53L5NW and 12SW), scale 1:20 000.....	in back pocket
GR2004-2-2 Geology of the western Aswapiswanan Lake area, Manitoba (parts of NTS 53L5NE and 6NW), scale 1:20 000.....	in back pocket
GR2004-2-3 Geology of the eastern Aswapiswanan Lake area, Manitoba (part of NTS 53L6NW), scale 1:20 000.....	in back pocket

Introduction

The southeast Max Lake area is located 120 km east-northeast of Norway House, at the junction of the Archean Gods Lake and Molson Lake domains (Manitoba Energy and Mines, 1987). The project area extends from MacVicar Lake in the west to Aswapiswanan Lake in the east, and encompasses part of the approximately 3 km wide Ralph Anderson Lake belt that extends east from Logan Lake for approximately 50 km (Figure 1). West of Logan Lake, the supracrustal rocks extend intermittently for a further 120 km to Cross Lake; to the east, the Ralph Anderson Lake belt is on strike (across a drift-covered area) with supracrustal rocks in the Goose Lake-Beaver Hill Lake area (Elbers and Marten, 1973). The supracrustal rocks between Cross Lake in the west and Goose Lake in the east constitute a near-continuous linear belt at the south margin of the Gods Lake Domain, where it is in contact with granitoid rocks of the Molson Lake Domain (Manitoba Energy and Mines, 1996).

A two-year mapping program was initiated in 1999 to upgrade previous 1:250 000-scale maps (Currie, 1961; Manitoba Energy and Mines, 1987) and to provide a detailed map as a base for possible future geological studies. Previous geological maps in the southeast Max Lake area show only the rudiments of stratigraphic and structural information (Currie, 1961; Elbers, 1973a, b; Schledewitz, 1980). Forest fires throughout most of the map area in 1989 resulted in a significant increase in the amount and quality of bedrock exposure, and thus increased the scope for detailed mapping. In the mid-1990s, attention was focused on the economic prospects of the area as a result of regional multimedia geochemical surveys in the north part of the Superior Province (Fedikow et al., 1996, 1997a, b). A conspicuous, altered sedimentary unit, discovered during the 1996 survey in the northeast part of MacVicar Lake, was characterized by base-metal and gold anomalies. Similar anomalies were recorded elsewhere in the southeast Max Lake area (Fedikow and Nielsen 1997a, b; Fedikow et al., 1997a, b; Fedikow and Nielsen, 1998; Fedikow et al., 1999). In 1999, geological mapping was initiated by the author in the MacVicar Lake–Ralph Anderson Lake area, southeast of Max Lake (Figure 2); the map area was extended in 2000 eastward to the Franklin Murray Lake–Aswapiswanan Lake area (Figure 3) and also further west in the MacVicar Lake area (Gilbert, 2000). Concurrent investigations were carried out on stratigraphy and structure, the geochemistry of volcanic rocks and the setting of mineralization at various localities. A 36 m wide, garnetiferous, silicified zone in the northwest part of the map area ('MacVicar Lake alteration zone', Figure 4) was the subject of particular attention (Gilbert, 1999a).

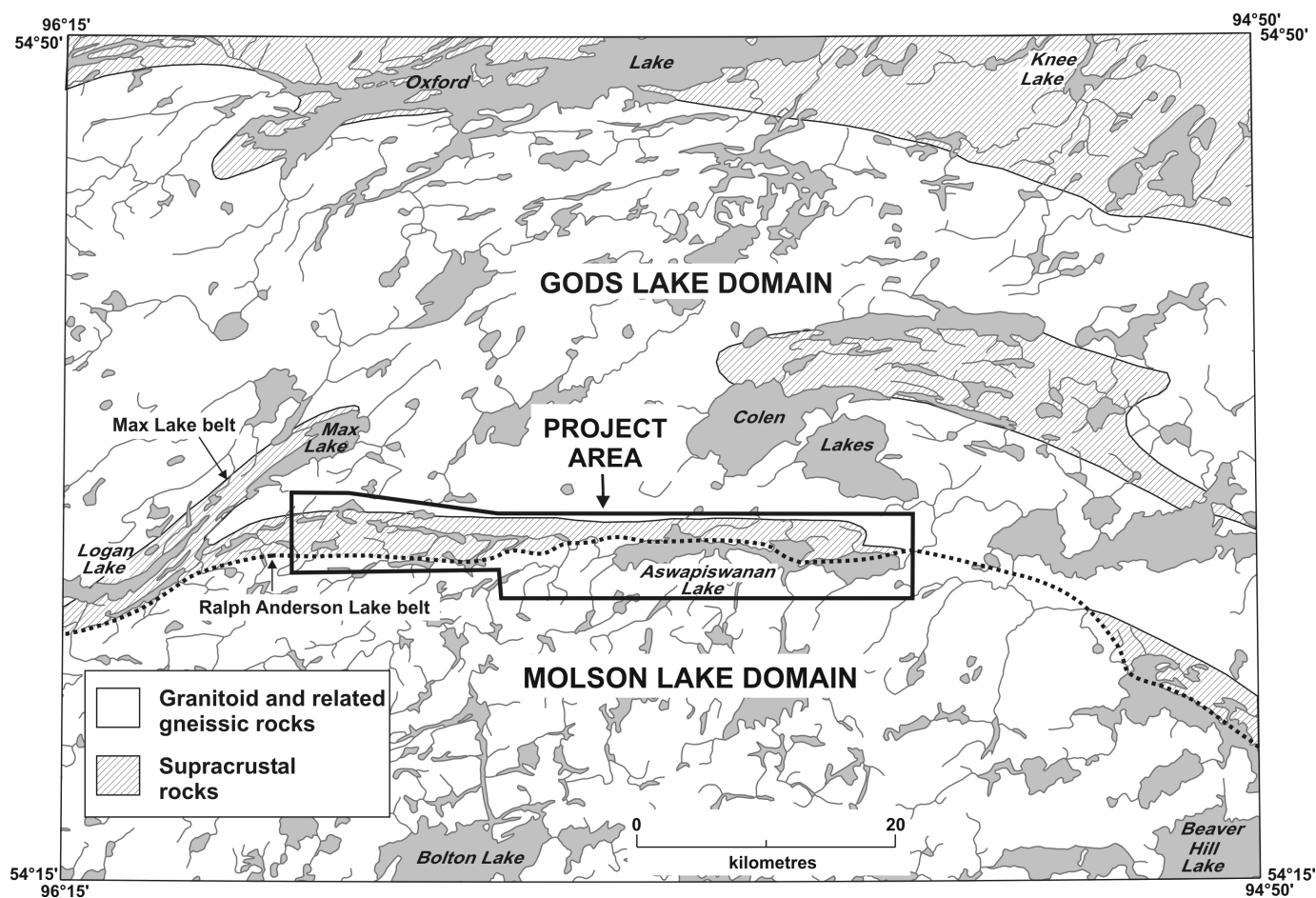


Figure 1: Regional geology of the Max Lake area, showing the location of the project area at the junction of the Gods Lake and Molson Lake domains.

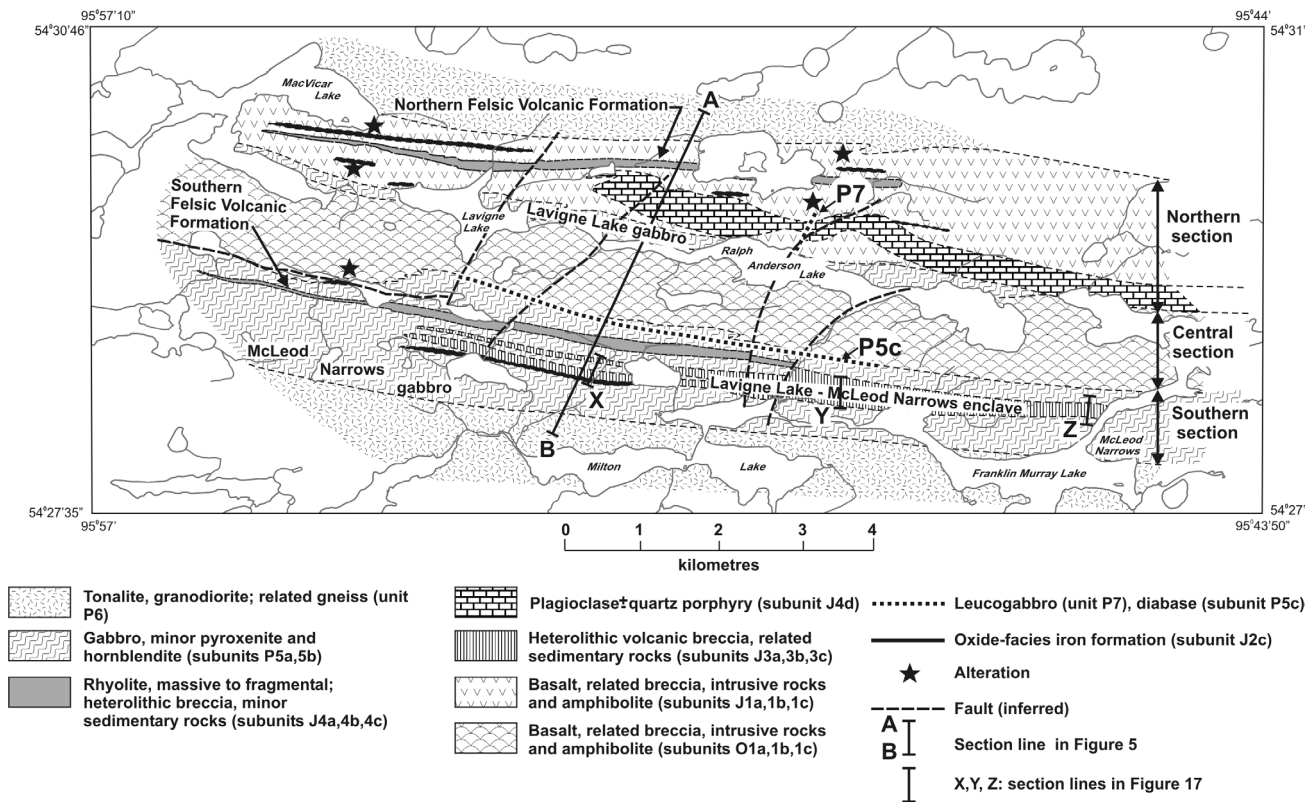


Figure 2: Simplified geology of the MacVicar Lake–Ralph Anderson Lake area.

Geochronological and geochemical investigations in the northwest part of the Superior Province (Sachigo Subprovince) have interpreted the supracrustal belt that extends between Cross Lake and Goose Lake as a mainly oceanic arc at the south margin of the Munro Lake Terrane, a late Archean crustal component bounded by the Gods Lake Narrows Shear Zone to the north and the Pipestone Lake Shear Zone to the south (Thurston et al., 1991; Corkery et al., 1992; Skulski et al., 2000; Percival et al., 2000). This supracrustal belt varies in width from 1 to 10 km, due to stratigraphic variations, tectonic attenuation and possible faulting that may locally have removed some components. In the southeast Max Lake area, the belt is relatively narrow (3 km) and consists mainly of arc tholeiite and related gabbro, subdivided into a lower depleted basalt suite overlain by more evolved tholeiitic-calcalkaline volcanic rocks. Further east in western Ontario, the 10 km wide Sachigo Lake–Ponask Lake greenstone belt, approximately 180 km along strike from the Ralph Anderson Lake belt, contains both an oceanic-arc assemblage and a platform sequence (komatiite–marble–quartz arenite) that were deposited on the north margin of the North Caribou craton (Skulski et al., 2000). In the area west of Max Lake, the Cross Lake belt (120 km along strike from the Ralph Anderson Lake belt) consists of three tectonically distinct components: the 2760 Ga Pipestone Lake Group of arc tholeiite (geochemically similar and probably correlative with the Ralph Anderson Lake section) and the overlying Gunpoint and Cross Lake groups, which are predominantly sedimentary and have no counterparts in the southeast Max Lake area (Corkery, 1985; Corkery et al., 1992; Corkery, pers. comm., 2002). Thus, supracrustal belts along strike to the east and west of the Ralph Anderson Lake belt are generally thicker and characterized by more diverse stratigraphy; in contrast, the contiguous Munro Lake–Colon Lake belt, just 30 km northeast of Ralph Anderson Lake (across a granitoid terrane) is stratigraphically similar and possibly correlative with the Ralph Anderson Lake sequence. Specific comparison between the Ralph Anderson Lake and Munro Lake–Colon Lake rocks is not possible due to the absence of geochemical data for the latter area; however, it is possible that the two belts were originally a single crustal component that was subsequently divided in two as a result of granitoid plutonism.

The rocks of the southeast Max Lake area are similar to supracrustal rocks in the Hayes River Group, originally defined by Wright (1928, 1932) and subsequently redefined by Hubregtse (1985a). This term was widely applied to the oceanic-arc component of supracrustal belts throughout the Gods Lake Domain, and in the Island Lake Domain to the south, until the application of precise U-Pb zircon dating revealed significant age differences between the volcanic suites in different belts (e.g., 2760 Ga at Cross Lake; 2830 Ga at Knee Lake; 2860 Ga at Island Lake). Whereas the supracrustal Ralph Anderson Lake belt is stratigraphically and geochemically similar to the oceanic-arc component of some other belts in the Sachigo Subprovince, the term ‘Hayes River Group’ is avoided here, pending a reassessment of the use of this term (Corkery, pers. comm., 2003).

The Ralph Anderson Lake belt consists mainly of basaltic pillow lavas with subordinate felsic volcanic rocks and heterolithic breccia and epiclastic deposits, flanked by granitoid rocks to the north and a 1.2 km wide gabbroic intrusion (McLeod Narrows gabbro) to the south (Figures 2, 5; Table 1). The margins of the belt are characterized by contact zones in which the supracrustal

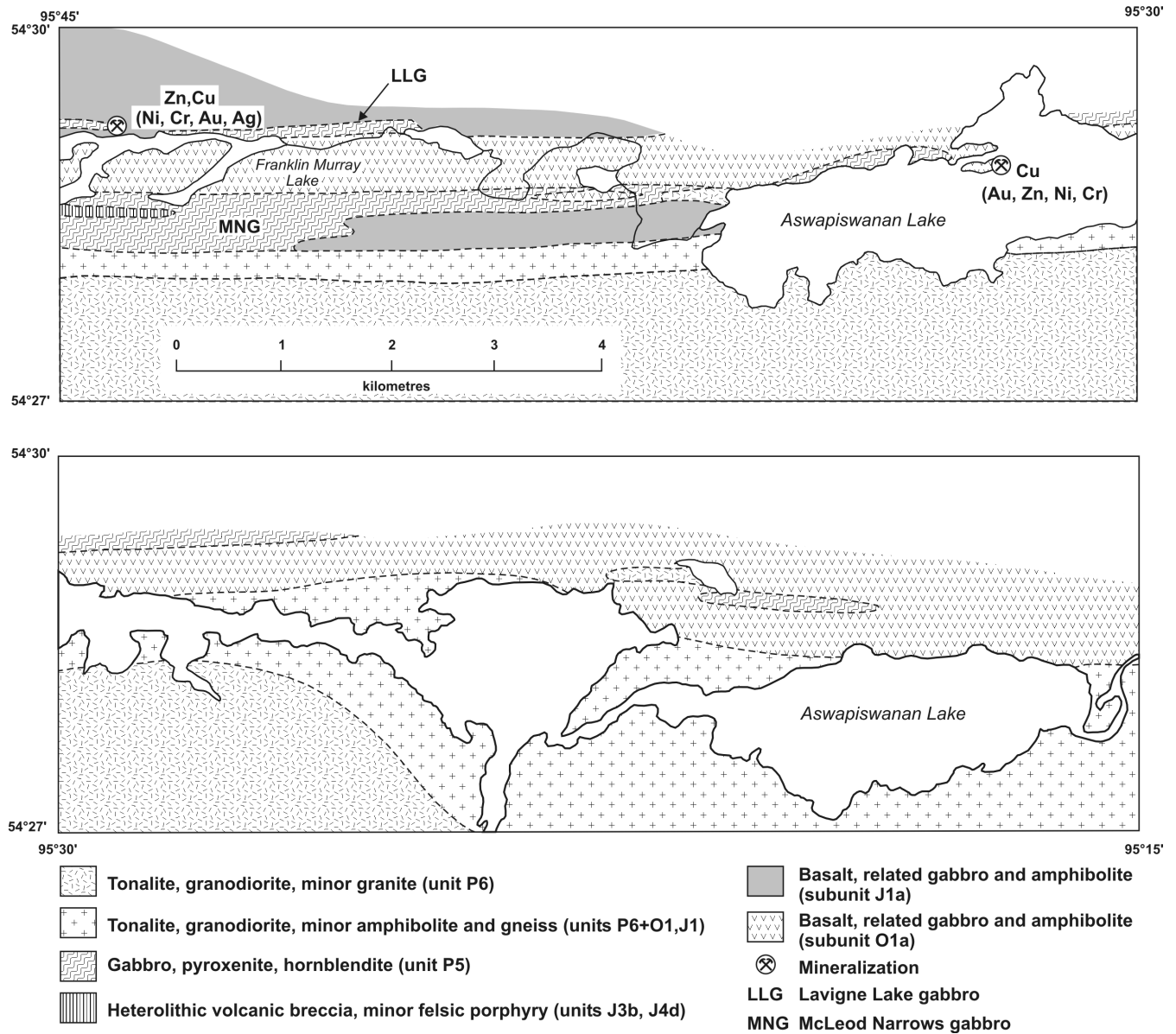


Figure 3: Simplified geology of the Franklin Murray Lake–Aswapiswanan Lake area.

rocks are intruded by conformable units derived from the flanking plutonic terranes. The volcanic sequence is divided into a central suite of transitional mid-ocean ridge basalt (MORB)- to arc-like rocks and a northern suite of more evolved, arc-tholeiitic rocks. The central section is devoid of sedimentary intercalations, whereas the northern section contains subordinate turbidite deposits and sporadic oxide-facies iron formation. The contrasting central and northern sections are interpreted as back-arc and arc components of a juvenile oceanic-arc system that has been deformed and tectonically reassembled. The narrow terrane between the central and northern sections, which contains a series of elongate lakes, is occupied by a sinuous mafic-ultramafic intrusion (Lavigne Lake gabbro) that apparently exploited the tectonic break between the two volcanic suites. The relative ages of the central and northern volcanic rock suites are unknown, but they are assumed to be in correct (north-facing) stratigraphic order.

A third supracrustal component in the Ralph Anderson Lake belt (southern volcanic suite) is represented by skialithic remnants (up to 300 m thick) within the McLeod Narrows gabbro, a prominent (>1 km thick) mafic sill that extends along the south flank of the Ralph Anderson Lake belt (Figure 2). This intrusion is geochemically similar to basalt in the central volcanic suite and is assumed to be penecontemporaneous with the volcanism. The supracrustal enclaves within the gabbro are lithologically diverse and include mafic to felsic volcanic rocks and related fragmental deposits. Limited data indicate these rocks (southern volcanic suite) are geochemically akin to the northern volcanic suite.

Abundant facing directions, indicated by pillow structure and sporadic top indicators in epiclastic rocks, are almost exclusively to the north throughout the Ralph Anderson Lake greenstone belt. The sequence (notwithstanding the geochemical breaks between volcanic rock suites) is interpreted as a series of tectonically intercalated regional nappe folds, parts of which have been

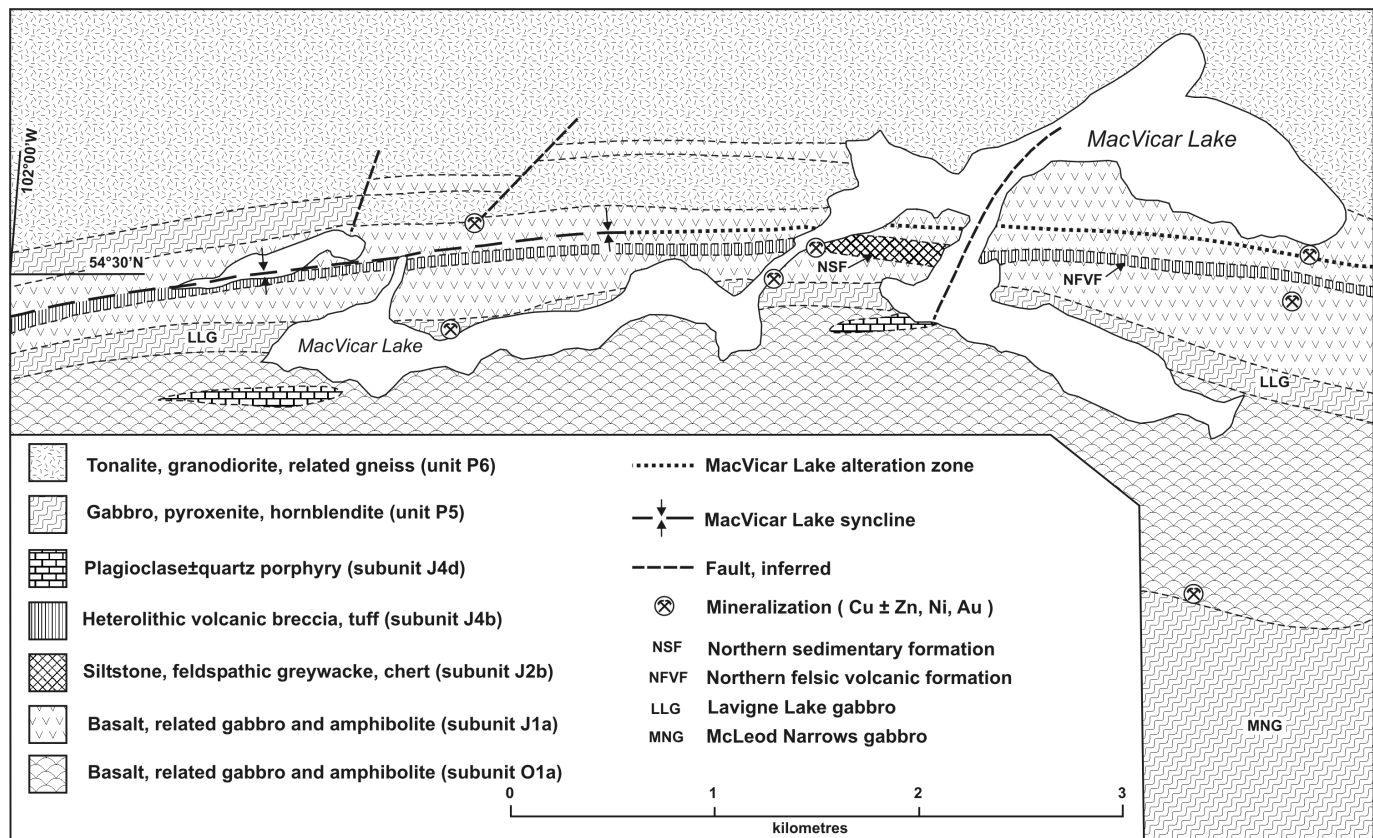


Figure 4: Stratigraphic and structural details in the vicinity of MacVicar Lake in the northwest part of the project area.

removed by major early thrust faults. A synclinal fold near the north margin of the belt is indicated by a south-facing turbidite deposit in the west part of the project area (Figure 4). In the southwest part of the area, a major fault is inferred along the south margin of the central volcanic section, at the contact with the McLeod Narrows gabbro and supracrustal rocks of the southern section.

Ninety rock samples from volcanic and related intrusive map units were analyzed for major, trace and rare earth elements. Mafic to felsic volcanic and associated intrusive rocks of the northern and southern volcanic suites are geochemically akin to modern arc tholeiite, whereas the central volcanic suite consists of modified, ocean-floor-type basalt and related gabbro. Both arc and ocean-floor volcanic types are characterized by marked negative Nb anomalies and flat to negatively sloping rare earth element (REE) profiles due to decoupling of large-ion lithophile elements (LILE) from high-field-strength elements (HFSE); TiO_2 values are generally less than 1%. Interflow gabbroic sills are compositionally similar to contiguous mafic-volcanic flow units.

The McLeod Narrows gabbro is geochemically akin to basaltic flows and associated sills in the central volcanic suite, consistent with the inferred synvolcanic age of emplacement of the intrusion. The Lavigne Lake intrusion in the central part of the belt consists of pyroxenite and melanocratic gabbro, and is geochemically distinct from any mafic volcanic rocks in the Ralph Anderson Lake belt. The age of the sill is uncertain: although the intrusion could represent a primitive fraction of the source magma of the volcanic rocks, a postvolcanic intrusive age is indicated by the structural setting interpreted for the intrusion (*see* 'Structural geology' section).

Most mineral occurrences in the southeast Max Lake area occur within the northern, upper part of the volcanic sequence, where base-metal mineralization is associated with both a felsic volcanic formation and a conspicuous, hydrothermally altered sedimentary unit close to the margin of the belt. A gold-bearing iron formation at this locality also represents a potential exploration target. Base-metal sulphide showings (\pm trace Au) also occur at the north margin of the southern stratigraphic section, both in the west part of the belt and further east at Aswapiswanan Lake. The central section is devoid of base-metal sulphide showings, consistent with the modified MORB-like geochemical profile of the rock suite, which suggests the basalt was extruded in a back-arc basin or ocean-floor setting.

This report provides lithostratigraphic descriptions of the geological map units, together with accounts of the geochemistry of volcanic and intrusive rocks, the metamorphic and structural histories, and the economic geology of the area. The economic potential of the belt is discussed, with reference to the geochemistry of the volcanic rocks. The stratigraphy of the better exposed, west part of the greenstone belt (MacVicar Lake–Ralph Anderson Lake area) is described first, followed by that of the east part (Franklin Murray Lake–Aswapiswanan Lake area). The lithological descriptions of rock units in this report are organized according to the

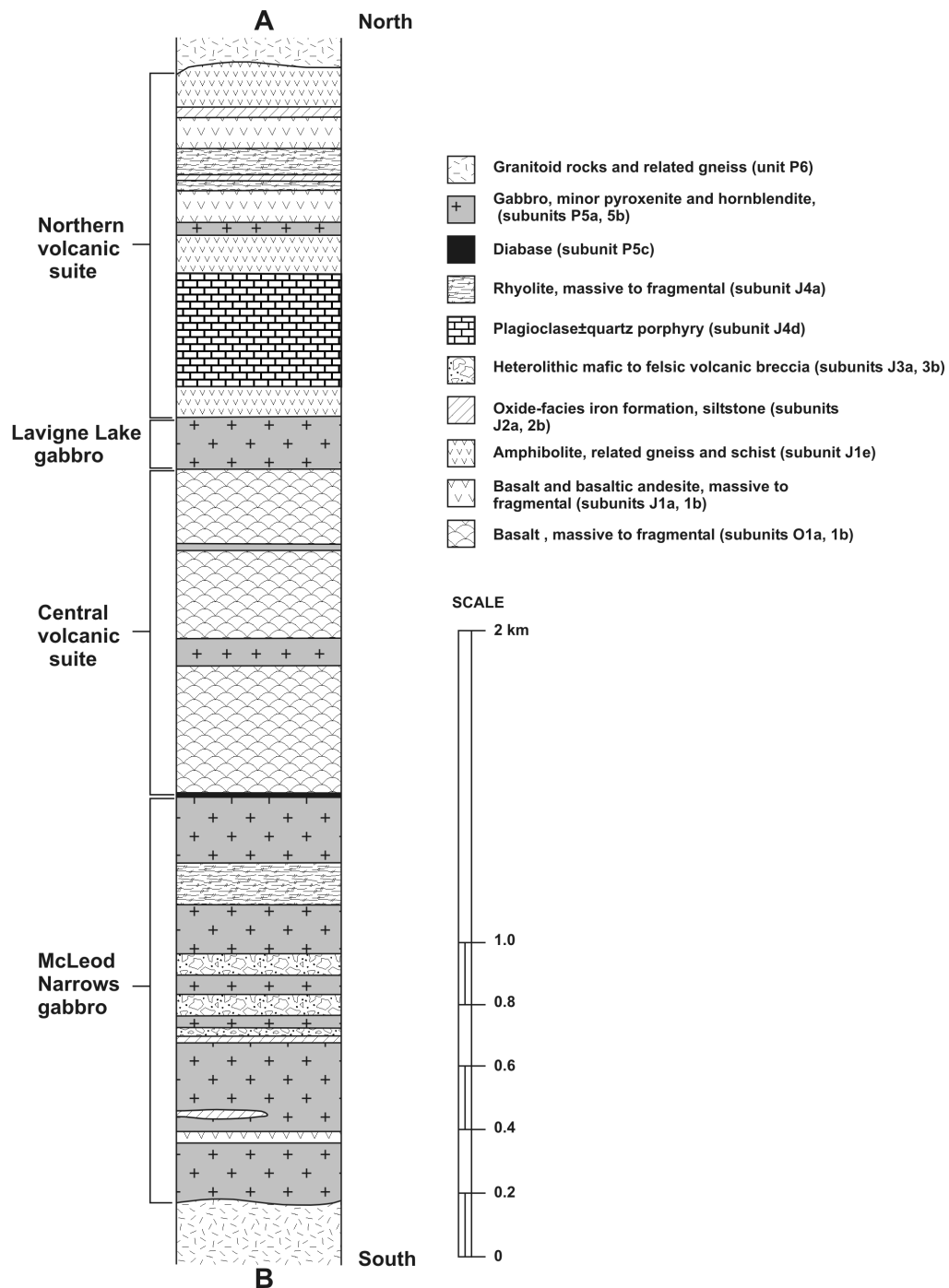


Figure 5: North-northeast-south-southwest section through the Ralph Anderson Lake belt (see Figure 2 for location).

three tectonostratigraphically defined sections (i.e., the [ocean-floor] central section, followed by the [juvenile arc] northern and southern sections). Throughout this report, the terms ‘central’, ‘northern’ and ‘southern’ are also applied to lithological entities such as ‘volcanic suite’ and ‘basalt’; in these cases, the descriptors are used to indicate affiliation with the analogous, tectonostratigraphically defined section.

Table 1: Geological map units in the southeast Max Lake–Aswapiswanan Lake area.

INTRUSIVE ROCKS

P7	Leucogabbro, diabase
P6	Granitoid rocks and related gneiss: tonalite, granodiorite, granite; minor plagioclase porphyry, pegmatite, aplite; hybrid gneiss
(P6a)	Granite, massive; related aplite and pegmatite
(P6b)	Granodiorite and granite, massive to gneissoid; minor K-feldspar–blastic granodiorite–granite; minor pegmatite
(P6c)	Tonalite and granodiorite, gneissoid
(P6d)	Hornblende quartz diorite to diorite
(P6e)	Tonalite, plagioclase phyric; minor felsitic lits
(P6f)	Hybrid gneiss (derived from units O1, J1 and P6)
P5	Gabbro, minor pyroxenite, peridotite and hornblendite (McLeod Narrows intrusion, Lavigne Lake intrusion); diabase
(P5a)	Gabbro, mesocratic to melanocratic
(P5b)	Pyroxenite, hornblendite; peridotite
(P5c)	Diabase
(P5d)	Magnetiferous quartz diorite, diorite

VOLCANIC AND SEDIMENTARY ROCKS

VOLCANIC AND SEDIMENTARY ROCKS OF JUVENILE ARC AFFILIATION

J4	Rhyolite, massive to fragmental; heterolithic breccia, minor related sedimentary rocks; plagioclase±quartz porphyry
(J4a)	Rhyolite, massive to fragmental
(J4b)	Heterolithic volcanic breccia and tuff
(J4c)	Volcanic-derived conglomerate, feldspathic greywacke and siltstone
(J4d)	Plagioclase±quartz porphyry
J3	Heterolithic volcanic breccia and associated tuff; related sedimentary rocks
(J3a)	Heterolithic volcanic breccia and tuff, mafic to felsic fragments
(J3b)	Heterolithic volcanic breccia and tuff, felsic and minor intermediate fragments
(J3c)	Volcanic-derived conglomerate, feldspathic greywacke and siltstone
J2	Sedimentary rocks; altered supracrustal rocks
(J2a)	Oxide-facies iron formation
(J2b)	Siltstone, feldspathic greywacke, minor chert
(J2c)	Altered garnetiferous supracrustal rocks
J1	Basalt, related fragmental and synvolcanic intrusive rocks; derived laminated amphibolite, schist and gneiss
(J1a)	Aphyric basalt; minor plagioclase-phyric basalt and related gabbro
(J1b)	Basaltic pillow-fragment breccia, flow-top breccia
(J1c)	Gabbro, locally plagioclase phyric; minor hornblendite
(J1d)	Gabbro, megaphyric
(J1e)	Amphibolite, related gneiss and schist
(J1f)	Spherulitic pillowed basalt

VOLCANIC ROCKS OF OCEAN-FLOOR AFFILIATION

O1	Basalt, related fragmental and synvolcanic intrusive rocks; derived laminated amphibolite, schist and gneiss
(O1a)	Aphyric basalt; minor plagioclase-phyric basalt and related gabbro
(O1b)	Basaltic pillow-fragment breccia, flow-top breccia
(O1c)	Gabbro, locally plagioclase phyric; minor hornblendite
(O1d)	Gabbro, megaphyric or glomeroporphyritic
(O1e)	Amphibolite, related gneiss and schist

MacVicar Lake–Ralph Anderson Lake area

The south part of the Ralph Anderson Lake greenstone belt consists of a series of skialithic enclaves within the McLeod Narrows gabbro that constitute the stratigraphic ‘southern section’ (Figures 2, 4). An enclave of aphyric, pillowed basalt (95 m thick) close to the south limit of mapping is succeeded northwards by heterolithic volcanic breccia and associated sedimentary rocks (up to 300 m thick) and, further north, by a felsic volcanic rock formation (85 m thick). The lithostratigraphy and geochemical profile of the southern section are consistent with a juvenile-arc volcanic affinity; map unit numbers of basaltic rocks are identified with the prefix ‘J’.

The ‘central section’ of the greenstone belt is the supracrustal sequence that extends from the north margin of the McLeod Narrows gabbro to the Lavigne Lake gabbro in the core of the belt. This stratigraphic panel, approximately 1 km wide, consists exclusively of mafic volcanic flows, related fragmental rocks and associated gabbro sills; sedimentary strata are absent. The geochemical profile of the basaltic rocks indicates an ocean-floor-type affinity; map unit numbers of these rocks are identified with the prefix ‘O’.

The ‘northern section’ of the belt (north of the Lavigne Lake gabbro) is up to 1 km wide and consists largely of mafic volcanic rocks and related gabbro, together with derived schist and gneiss. As in the southern section, the lithostratigraphy and geochemical profile of the northern section are consistent with a juvenile-arc volcanic affinity, and northern volcanic units are distinguished from those in the central section with the prefix ‘J’. Basaltic flows and related gabbro intrusions of juvenile-arc type (in both the southern and northern sections) are stratigraphically associated with diverse felsic volcanic and sedimentary rocks, unlike the ocean-floor-type mafic volcanic rocks in the more uniform central section. A felsic volcanic formation within the northern section, up to 115 m thick and at least 7 km along strike, is interpreted as the extrusive equivalent of a conspicuous, underlying, felsic porphyry sill (Figure 2, subunit J4d). The felsic intrusion may be directly connected with the extrusive rocks at one locality northwest of Ralph Anderson Lake, where the contact between these map units is obscured by a small lake (Map GR2004-2-1, in back pocket). The ‘northern felsic volcanic formation’ consists of massive to fragmental rhyolite and heterolithic volcanic breccia, locally associated with subordinate greywacke-siltstone and conglomerate. A prominent 36 m wide garnetiferous zone of highly altered and sheared sedimentary and volcanic rocks, together with minor oxide-facies iron formation, occur within mafic volcanic rocks approximately 0.2 km south of the north margin of the Ralph Anderson Lake greenstone belt. Iron formation also occurs sporadically within the underlying mafic volcanic sequence in the northern section.

Ocean-floor-type supracrustal rocks (central section)

Mafic volcanic rocks of ocean-floor affinity and metamorphic equivalents (unit O1)

Aphyric basalt; minor plagioclase-phyric basalt and related gabbro (subunit O1a)

Mafic volcanic rocks in the central section, which are compositionally similar to some modern ocean-floor basalt flows, are mainly pillowed and contain sporadic pillow-fragment breccia intercalations. Subordinate nonpillowed basalt flows and related gabbroic sills are interlayered with pillowed units at a scale of 2–25 m; flow contacts are locally marked by thin (2–5 cm) chilled margins or discrete flow-top breccia units. Pillows are undeformed or only moderately deformed, except toward the south margin of the central section, where the basaltic rocks are increasingly attenuated. The ocean-floor-type basalt units weather medium to dark grey-green, similar to arc-type mafic flows (except where the latter are altered).

Pillowed flows in the central section are characterized by ovoid to amoeboid pillows (0.5–2 m in diameter), locally interspersed with large ‘mattress’ pillows (up to 6 m by 2 m) in the lower parts of some flow units. Whereas plagioclase phenocrysts occur in less than 5% of mafic flows, amygdules (with quartz±plagioclase or rare chlorite fill) are widespread, randomly distributed or concentrated in the marginal zones of pillows. Ovoid vugs (2–12 cm long), locally filled with carbonate, are common in the central parts of pillows. The flows are also characterized by interpillow hyaloclastite or (less commonly) carbonate or chert. Rare concentric cooling fractures occur within pillows and analogous thermal contraction cracks occur at the upper margins of some flows, with fracture spacing decreasing toward the flow contact.

Basalt of the central section is geochemically identified as a transitional MORB- to arc-type suite that is similar to some types of modern back-arc basin basalt (see ‘Geochemistry’ section). Their geochemical signature and stratigraphic association suggest they were not extruded in an arc-type environment. For example, they consist solely of mafic flows, related breccia and gabbro, whereas arc volcanic sequences are characterized by lithologically more diverse assemblages containing mafic to felsic flows, volcanic fragmental rocks and associated epiclastic deposits. A deep-water, ocean-floor environment is also considered unlikely for the central basalt, because the abundance of amygdules and large gas cavities within these flows is more consistent with extrusion at a shallow or intermediate water depth. Abundance of vesicles in basaltic magma has been shown to increase progressively with decreasing water depth (Jones, 1969; Moore, 1970), although this relationship is not unequivocal. In summary, a back-arc basin environment is considered the most likely setting for the central volcanic section.

Basaltic pillow-fragment breccia, flow-top breccia (subunit O1b)

Monolithic volcanic fragmental rocks are intercalated with massive flows and constitute approximately 5–10% of the mafic volcanic sequence in the central section of the Ralph Anderson Lake belt. The autoclastic breccia deposits occur in conformable, discontinuous zones, typically 1–8 m wide, that are intercalated with mafic flows, and as lensoid to irregular deposits up to 35 m by 10 m. Amygdules are commonly abundant in all types of volcanic fragmental rock, reflecting high volatile content in the original magma. The fragmental rocks are intimately intercalated with pillowed flows in several ways. Some flow-breccia deposits are laterally gradational with pillowed basalt; at one locality just north of the McLeod Narrows gabbro, the marginal part of a breccia unit is pervasive into the margins of a contiguous basalt flow, and pillows are partly detached and incorporated into the fragmental unit (Figure 6). Elsewhere, basaltic amoeboid pillow breccia contains angular, tabular or highly irregular, amoeboid pillow fragments, up to 30 cm by 12 cm, in a hyaloclastic matrix. The conditions that led to gravitational instability of pillowed flow units and the incorporation of discrete pillows and pillow fragments in the breccia deposits were probably controlled by such factors as the slope of the underlying terrane, and the viscosity and rate of supply of the basaltic magma.

In contrast to pillow-fragment breccia, flow-top breccia units are relatively thin (0.2–1 m) and contain angular fragments that are due to rapid chilling and fragmentation of the upper margins of lava flows during extrusion. Flow-top breccia displays gradational contacts with underlying flow units, whereas contacts with overlying units are sharply defined (Figure 7). These thin breccia units are relatively incompetent compared to contiguous massive or pillowed basalt, and are commonly sheared and variously epidotized or silicified.

Gabbro, locally plagioclase phyrlic, megaphyric or glomeroporphyritic; minor hornblendite (subunits O1c, O1d)

Synvolcanic gabbro units, ranging from minor intrusions to conspicuous sills over 80 m thick, constitute approximately 20% of the central volcanic section (Map GR2004-2-1, in back pocket). The gabbro intrusions are massive and mesocratic to melanocratic, and commonly display chilled margins; the mafic rocks are medium to coarse grained, and commonly display ‘spotted’ texture due to prominent equant hornblende crystals. Rare porphyritic zones with plagioclase phenocrysts up to 2 cm long occur in some intrusions.

A megaphyric to glomerophyric gabbro sill (subunit O1d), approximately 45 m thick, occurs at the top of the central section, and extends for over 2 km along the south shore of Ralph Anderson Lake. The upper (north) part of the sill consists of gabbro with conspicuous pseudo-hexagonal plagioclase megacrysts and glomerocrysts up to 13 cm across (Figure 8) and hornblende pseudomorphs after pyroxene (2–15 mm), each of which constitutes up to 20% of the rock. The plagioclase megacrysts are partly saussuritized and diminish in size and abundance southwards, toward melanocratic gabbro and hornblendite in the basal part of the sill. Some megaphyric basalt flows are texturally analogous to intercalated porphyritic gabbro units, suggesting that they may be extrusive counterparts of the mafic sills.

Alteration in massive to fragmental basaltic rocks of ocean-floor affinity

Early, synvolcanic alteration is widespread in pillowed basalt of the central section. Pillows commonly display altered zones defined by secondary minerals (quartz, epidote, amphibole and chlorite), whereas nonpillowed, massive flows display little or no alteration. Silicification of pillow margins was accompanied by intrapillow alteration, initiated by the growth of chlorite+actinolite within radially oriented cooling fractures, and followed by epidotization that extended along internal fractures toward pillow

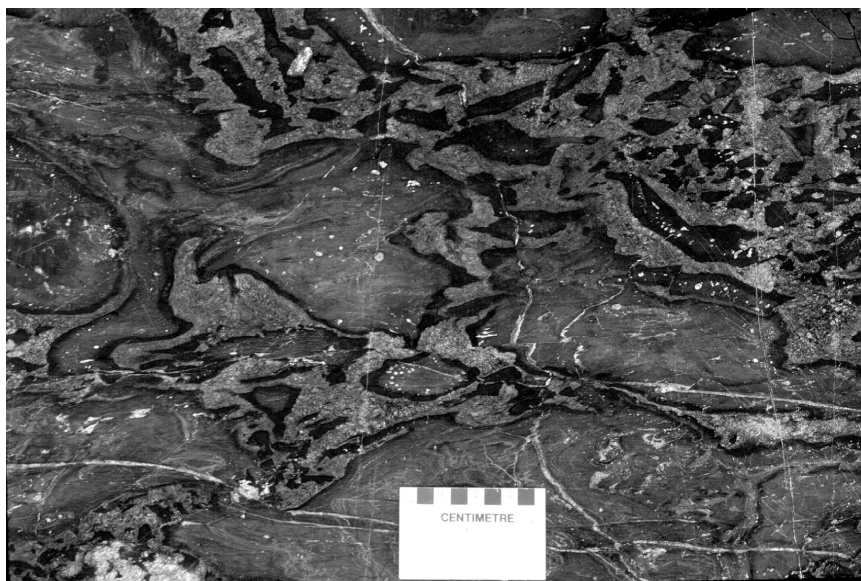


Figure 6: Aphyric pillowed basalt with pervasive interpillow autoclastic breccia (subunit O1b), 1 km south of the west end of Ralph Anderson Lake.

cores. The altered pillows display progressive concentric zonation, defined by an outer (pale grey/white) silicified zone, inner (pale yellow) epidosite domain, and unaltered, green pillow core (Figure 9). More pervasive alteration in a minority of basalt flows resulted in the complete replacement of selected small pillows by silica. Many flows are characterized by variable epidotic alteration in pillow cores, without attendant silicification (Figure 10); selective epidote replacement of pillow selvages has also affected some units.

Narrow interflow fragmental units, interpreted as flow-top breccia (0.2–1 m wide), are invariably partly epidotized and/or silicified. These units are typically in sharp contact with overlying unaltered basalt, consistent with a synvolcanic age of alteration (Figure 7). In addition to the intrapillow and flow-top breccia alteration types within the central section, epidotic alteration is also represented by sporadic pods, stringers and diffuse epidosite domains within the basaltic rocks. These latter features are probably due to both syngenetic sea-floor alteration and later hydrothermal processes or regional greenschist-facies metamorphism.

Carbonatization of postvolcanic age occurs at the base of the central section, in the area south of Lavigne Lake (Map GR2004-2-1, in back pocket). At that locality, highly contorted basalt is pervasively carbonatized over a 16 m wide zone immediately north of the contact with the McLeod Narrows gabbro. The alteration postdates both the deformation of the basalt and the metamorphic fabric of a diabase dike that intrudes the mafic volcanic flows.

Juvenile-arc-type supracrustal rocks (northern and southern sections)

Mafic volcanic rocks of juvenile volcanic-arc affinity and metamorphic equivalents (unit J1)

Aphyric basalt; minor plagioclase-phyric basalt and related gabbro (subunit J1a)

Basalt of juvenile-arc affinity is typically aphyric and medium to dark grey-green weathering, although alteration has commonly resulted in paler green to grey weathered surfaces. A north to northeast facing direction is indicated at a few localities where pillows (0.4–2 m) are relatively undeformed; however, most flows are too attenuated for the determination of stratigraphic tops. Amygdules (quartz, plagioclase or, less commonly, hornblende±chlorite) are common, but these are never as abundant as in the ocean-floor-type basalt in the central section. The vesicle fillings are typically ovoid (0.2–2 mm) and localized in the upper parts or margins of pillows; radial pipe amygdules (1–2 cm long) and irregular vugs in pillow cores are both rare. Plagioclase phenocrysts are inconspicuous



Figure 7: Altered 1 m wide basaltic flow-top breccia (subunit O1b), 0.9 km south-southwest of the west end of Lavigne Lake. Fragments are spalled from underlying pillows. The top of the pale grey-weathering, silicified breccia unit is in sharp contact with overlying dark green, unaltered massive basalt (not shown).

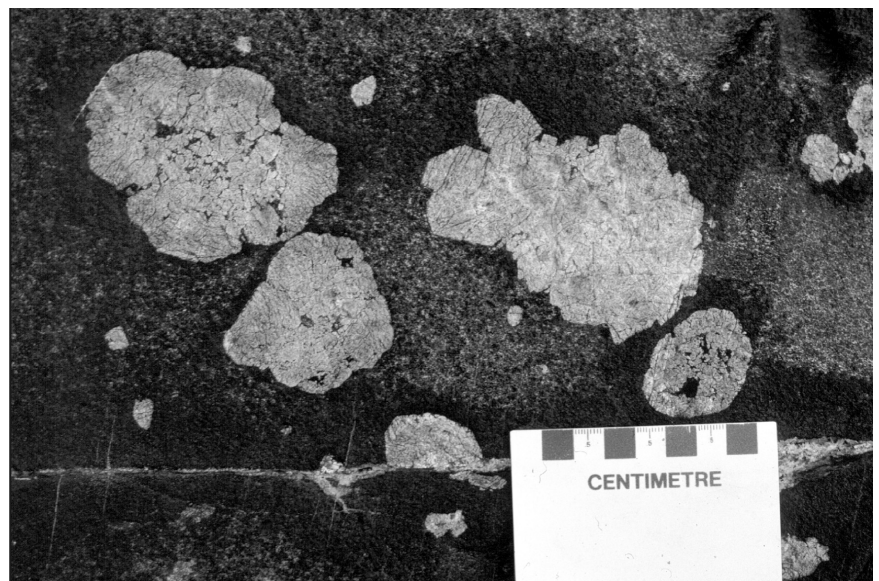


Figure 8: Pseudohexagonal plagioclase phenocrysts in glomeroporphyritic gabbro (subunit O1c), south shore, central part of Ralph Anderson Lake.

and occur only sporadically in the arc-type basalt flows (0.5–2 mm, 5–10% of the rock). Parallel thermal contraction cracks are prominent in several mafic flow units; the fractures are filled with plagioclase+epidote and are spaced at 10–25 cm intervals (decreasing toward the margins of the flow unit). Features that distinguish juvenile-arc basalt from ocean-floor types are listed in Table 2.

Basaltic pillow-fragment breccia, flow-top breccia (subunit J1b)

Basaltic breccia is rarely preserved within the northern volcanic section, in contrast to the central section where this map unit is more conspicuous. This may, in part, reflect selective destruction of these less competent units by shearing and obliteration of primary textures in the northern section. Nevertheless, despite such alteration due to deformation, basaltic breccia is significantly less abundant in undeformed parts of the northern volcanic section, compared with the central section.

Basaltic breccia (subunit J1b) was observed at only two localities in the northern section. North of the west end of MacVicar Lake, a 10 m wide zone of monolithic, mafic volcanic breccia occurs within pillowed to massive basalt, immediately north of the garnetiferous supracrustal rocks (subunit J2c) shown on Map GR2004-2-1 (in back pocket). The rock contains strongly attenuated basalt fragments (up to 25 cm by 2 cm) in a fine-grained, amphibolitic matrix. Both the breccia and associated pillowed basalt are gradational with laminated amphibolite (subunit J1e) at that locality. A second occurrence of monolithic basaltic breccia (subunit J1b) is located approximately 1 km north of the east part of Ralph Anderson Lake (Map GR2004-2-1, in back pocket). This breccia unit, which is at least 40 m thick, is characterized by a dark green amphibolitic matrix and very pale grey fragments that are interpreted as silicified basalt. The clasts are tectonically flattened, but were originally cobbles to small boulders in size; the largest fragment measures 50 cm by 3 cm. The breccia is stratigraphically associated with massive to pillowed basalt, laminated amphibolite and gabbro.

Gabbro, locally plagioclase phyric; minor hornblende (subunit J1c)

Synvolcanic gabbro (subunit J1c) constitutes approximately 15% of the northern volcanic section. Compared to gabbroic units within the central section (subunit O1c), the mafic sills intercalated with northern basalt are generally smaller (typically 1 to 10 m in thickness, rarely up to 40 m). Lithologically, the gabbro in both the northern and central sections is very similar: the rocks are medium to coarse grained and meso- to melanocratic, and display either speckled texture (due to randomly distributed hornblende

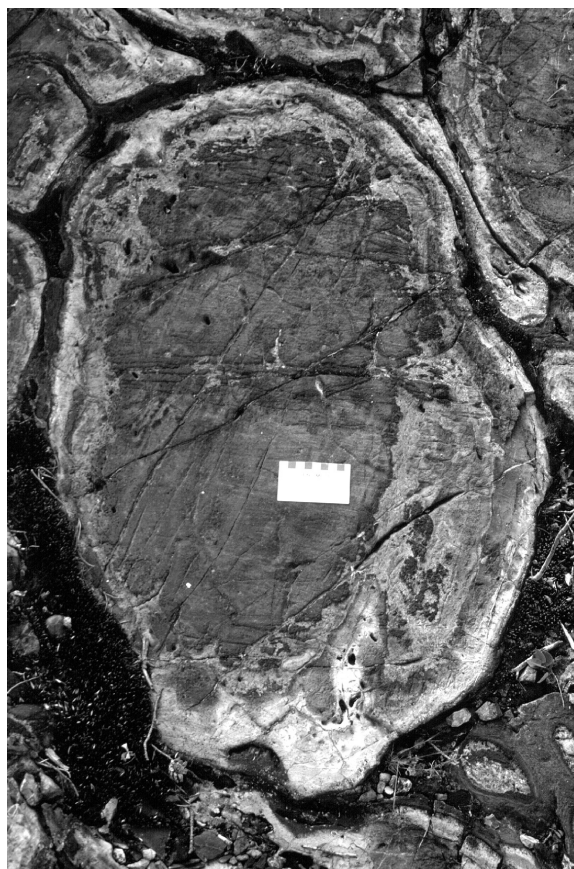


Figure 9: Zonal silicic and epidotic alteration of pillows in basalt (subunit O1a), close to the west end of Ralph Anderson Lake.

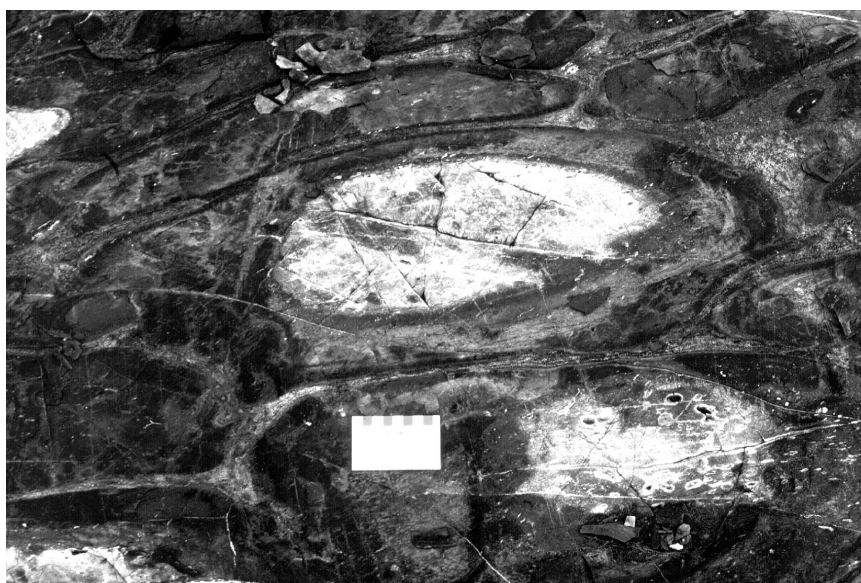


Figure 10: Epidotization of pillow cores in amygdaloidal basalt (subunit O1a), close to the south-east end of MacVicar Lake.

Table 2: Features that distinguish the northern section (ocean-floor-type supracrustal rocks) from the central section (juvenile-arc-type supracrustal rocks), MacVicar Lake–Ralph Anderson Lake area.

1. Northern basalt (juvenile-arc type) is geochemically distinct from MORB-like central basalt, which is characterized by lower SiO₂, LREE, LILE and (La/Yb), and higher MgO, Ni and Cr.
2. In the northern section, pillowed flows are subordinate to nonpillowed units; autoclastic breccia and amygdaloidal basalt are less common than in the central section. A spherulitic flow occurs in the northern basalt, but this texture is apparently absent in the central volcanic suite.
3. Oxide-facies iron formation occurs at four stratigraphic levels within the northern section but is absent in the central section. Magnetiferous units also occur in the southern section: within supracrustal enclaves at the north margin and in the central part of the McLeod Narrows gabbro.
4. Alteration of volcanic rocks consists mainly of epidotization and carbonatization, and occurs typically in concordant, 1–5 m wide zones. Concentric, zonal silicic-epidotic alteration of pillows, widespread in the central volcanic suite, is not characteristic of the northern basalt.
5. Deformation is more significant and increases toward the north margin of the greenstone belt (pillow elongation typically ranges from 4:1 to 10:1). Basalt is altered to finely laminated amphibolite and locally recrystallized to epidote-amphibole gneiss.

prisms) or spotted texture (due to more equant amphibole crystals). Gabbro in the northern volcanic section (subunit J1c) is equigranular; there are no counterparts of the plagioclase-phyric and megaphyric gabbro sills (subunits O1c, O1d) from the central volcanic section. Chilled margins are characteristic of some mafic sills. The margins are also locally foliated, but otherwise the intrusive units are generally massive, even where intercalated basaltic units are strongly foliated or metamorphically laminated.

Amphibolite, related gneiss and schist (subunit J1e)

A 0.4 km wide zone of volcanic-derived amphibolitic gneiss and mafic schist extends along the north margin of the Ralph Anderson Lake belt, in the area north of Lavigne and Ralph Anderson lakes (Map GR2004-2-1, in back pocket). Gneiss and schist (subunit J1e) are also intercalated with massive basalt and gabbro (subunits J1a, J1c) throughout the northern section in the west part of the belt, which is attenuated and reduced in width by approximately 50%. Further east, in the area north of Ralph Anderson Lake, deformation is less pronounced and alteration of basalt to gneiss and schist is relatively minor. The gneissic rocks are interpreted as the products of localized strain and metamorphism in discrete tectonic zones within the basalt-gabbro sequence. These zones are assumed to have developed at incompetent stratigraphic horizons such as lithological contacts, altered localities or earlier shear zones.

Fine-grained amphibolitic gneiss commonly contains subparallel, branching epidotic laminae that are locally recognized as pillow selvage remnants, but generally the rocks are devoid of any traces of original volcanic features. The gneissic amphibolite consists mainly of green hornblende and plagioclase, locally with sporadic subhedral clinopyroxene grains that are interpreted as porphyroblasts. These rocks typically display mafic, epidotic or siliceous laminae that are assumed to be derived from compositionally distinct components in the original rock (assumed to be an altered basalt flow), such as pillow selvages and variously altered domains within the pillows. In addition, the amphibolitic gneiss is characterized by diffuse epidotic zones and quartz-plagioclase-epidote (\pm carbonate) stringers. At the margin of the Ralph Anderson Lake belt north of Lavigne and Ralph Anderson lakes, the mafic gneiss is strongly foliated and displays conspicuous boudinage. The south margin of the amphibolite-gneiss-schist zone is gradational with relatively undeformed, pillowed to massive basaltic flows (subunit J1a) that constitute the south part of the northern section. Thin (20–50 cm wide) tectonic breccia interlayers occur locally within the amphibolitic gneiss. The breccia, which contains randomly oriented, angular fragments of the gneiss in a saussuritic quartzofeldspathic matrix, is attributed to late brittle deformation.

Spherulitic pillowed basalt (subunit J1f)

Pillowed, spherulitic basalt occurs within aphyric basalt and gabbro (subunits J1a, J1c) in the northern section, approximately 1 km north of the east part of Ralph Anderson Lake (Map GR2004-2-1, in back pocket). The unit is at least 20 m wide and was traced along strike for approximately 100 m. Pillows are moderate to large (up to 3.5 m by 0.75 m) and contain elongate (lineated) spherulites measuring 1–6 cm long and 2–15 mm in diameter. The spherulites coalesce toward pillow cores due to an increase in their size and abundance. This original distribution has been preserved, in spite of subsequent recrystallization and the conspicuous lineation of the spherulites. These structures are typically dark green and concentrically zoned, with hornblende-rich cores and pale green, very fine grained amphibolite rims. Elsewhere in the same map unit, the spherulites are locally pale green weathering due to epidotic alteration, in contrast to a darker weathering, chloritized basalt matrix. The characteristic spherulitic texture of this unit, which is unique within the southeast Max Lake area, is assumed to be due to devitrification of an originally glassy precursor that resulted from very rapid cooling of the lava.

Alteration in massive to fragmental basaltic rocks of juvenile-arc affinity

Early hydrothermal alteration, interpreted as coeval with subaqueous volcanism, occurs throughout the Ralph Anderson Lake belt but is most widely developed in arc-type volcanic rocks of the northern and southern sections. This alteration is interpreted to

result from the interaction between hydrothermal fluids, brines and volcanic rocks at the sea floor or in the immediate substrate. The main alteration products — quartz, epidote, chlorite and sericite — are locally associated with base-metal sulphide minerals. Within basalt, the alteration is more conspicuous in pillowed flows than in massive flows. At outcrop scale, the alteration is typically manifested by irregular to concordant, silicified or epidotized zones that occur sporadically within the mafic flows or are spatially associated with pillows or interflow-breccia units. Major alteration zones (35–75 m) also occur in both the northern and southern sections.

Northern section

A major semiconformable zone of hydrothermal alteration (MacVicar Lake alteration zone, Figure 4) occurs close to the north margin of the Ralph Anderson Lake greenstone belt, where a 36 m wide garnetiferous gneiss unit is interpreted as being derived from sedimentary and basaltic rocks at the top of the northern stratigraphic section (*see* ‘Altered garnetiferous supracrustal rocks’ section).

Numerous, less conspicuous localities of early alteration occur elsewhere in the northern section, where original volcanic features have been partially or completely lost due to metasomatism and recrystallization. Epidote, the most widespread alteration product, occurs in polygonal (fracture-controlled) epidosite domains and/or ovoid to amoeboid zones that commonly originate in pillow cores. In rare cases, pillow selvages are the focus of epidotization; more commonly, selvages are the site of chloritic alteration or carbonatization. With advanced alteration, pillow structure is lost and the flow is transformed into fine-grained amphibolite with randomly distributed, ovoid epidosite bodies (10–40 cm) characterized by tiny (0.1–1 mm) blebs of exsolved quartz and thin, chloritic rims. Rare flow-brecciated zones within the basalt are invariably epidotized and/or silicified.

Silicification in basalt (unit J1) of the northern section is attributed to early, sea-floor hydrothermal alteration. The silicified domains are locally associated with disseminated pyrite; in some flows, this alteration and mineralization are localized, either in pillow cores or at pillow rims. More extensive silicification, locally accompanied by epidotization, occurs in conformable alteration zones (typically 0.2–2 m wide). These zones are most common in the lower (south) part of the northern volcanic section, in the area immediately north of the Lavigne Lake gabbro. Within this stratigraphic interval, the conformable alteration zones are typically strongly foliated and contiguous basalt is recrystallized to amphibolitic gneiss, due to postvolcanic deformation and metamorphism.

A conspicuous, 10 m wide alteration zone occurs within the northern section, 0.3 km north of the Ralph Anderson Lake felsic porphyry (subunit J4d; Figure 2). The beige-grey-weathering basalt at that locality is affected by pervasive silicification, epidotization and pyrite mineralization that is attributed to sea-floor hydrothermal activity. Subsequent M_1 - M_2 regional metamorphism resulted in sporadic garnet porphyroblasts and irregular recrystallized zones of medium-grained, ‘speckled’ amphibolite within fine-grained basalt. Extensive carbonatization postdates the M_2 regional metamorphism and is interpreted to be a product of late, retrogressive (M_3) alteration (*see* ‘Metamorphism’ section). Elsewhere in the northern section, pervasive chloritic alteration (\pm carbonatization) is characteristic of late shear zones (D_3), where basaltic rocks have been altered to mafic schist. Saussuritic alteration is pervasive in discrete tectonic breccia units (0.2–0.4 m) that are attributed to a locally more brittle style of D_3 deformation.

Southern section

A 75 m wide zone of silicic and epidotic alteration occurs at the north (upper) margin of the southern stratigraphic section in the area directly south of the east end of MacVicar Lake (Map GR2004-2-1, in back pocket), where the arc-type volcanic rocks are in fault contact with ocean-floor-type central basalt. In the north part of this zone, discrete shear zones up to 10 m wide contain laminated, quartz-sericite-chlorite-epidote (\pm anthophyllite \pm cordierite) schist and siliceous gneiss that alternate with variously altered, massive basalt. Deformation is most intense in the protomylonitic, central part of the zone; the south part of the zone consists of silicified, heterolithic volcanic breccia. The sericitic schist and gneiss in the alteration zone locally contain stringers of base-metal sulphides (pyrite-chalcopyrite-pyrrhotite). Original volcanic textures have been largely obliterated by metasomatism and recrystallization. The alteration and mineralization are interpreted as being due to hydrothermal activity penecontemporaneous with subaqueous volcanism, but this zone may also have been influenced by later, low-grade metamorphism associated with faulting between the southern and central volcanic sections. Regional metamorphism has resulted in irregular porphyroblastic zones with cordierite (M_1) and anthophyllite (M_2) that postdate the hydrothermal alteration (*see* ‘Metamorphism’ section).

At least three types of postvolcanic alteration have been recognized in the arc-type basaltic rocks of the southern section:

- Carbonatization is a minor but widely distributed alteration type in basaltic rocks, and is commonly pervasive at pillow selvages or in the matrix of volcanic breccia. Whereas some carbonate alteration is probably syngenetic, a postvolcanic age is observed elsewhere, such as in the (previously described) 10 m wide zone of alteration in the south-central part of the northern section, where carbonate overprints the M_2 metamorphic assemblage.
- Retrogressive metamorphism resulted in greenschist-facies mineral assemblages (chlorite \pm sericite \pm epidote \pm carbonate). These secondary minerals occur throughout the map area as a result of regional (M_3) greenschist-facies metamorphism, but are best

developed in discrete, 0.5–2 m wide shear zones and along lithological contacts between intrusive and supracrustal rocks.

- Silicic-epidotic alteration and veining in narrow (0.1–0.5 m) layers of fault breccia are attributed to late brittle deformation (D₃).

Sedimentary rocks: feldspathic greywacke, siltstone and related paragneiss; oxide-facies iron formation; altered supracrustal rocks (unit J2)

Sedimentary rocks (unit J2) are subordinate yet economically significant components of the Ralph Anderson Lake belt. They include both fine-grained clastic and chemical sediments (chert and iron formation), are locally mineralized with stratabound base-metal sulphides and, within the northern section, contain sporadic traces of gold. The sedimentary rock units occur only in association with arc-type volcanic rocks, and are thus confined to the northern and southern sections.

Within the northern section, turbidite-type sedimentary intercalations up to 85 m thick occur within the volcanic sequence in the vicinity of MacVicar Lake (Map GR2004-2-1, in back pocket), and similar deposits occur as subordinate components of the ‘northern felsic volcanic formation’ (Figure 4). Fine-grained sedimentary rocks in the southern section occur both as minor skialiths (up to 20 m thick) within the McLeod Narrows gabbro and as subordinate interlayers within larger enclaves of volcanic fragmental and felsic volcanic rocks (units J3 and J4). At least six stratigraphically distinct, oxide-facies iron formations (subunit J2a) occur within the arc-type volcanic sequences of the northern and southern sections.

Oxide-facies iron formation (subunit J2a)

Northern section

Four oxide-facies iron formations occur within arc-type basaltic flows and derived amphibolite in the northern section. These formations, which extend for up to 6 km along strike, occur both above and below the northern felsic volcanic formation, located in the central part of the section (Figure 2). The northernmost iron formation, approximately 150 m above the felsic volcanic rocks, consists of two thinly layered magnetite+chert units (1.3 and 1 m thick), separated by up to 10 m of laminated amphibolite (subunit J1e); these units occur a few metres north of a prominent garnetiferous alteration zone (subunit J2c) close to the northeast corner of MacVicar Lake. The alteration zone itself contains two narrow (<1 m wide) magnetite+chert units. Similar oxide-facies iron formations occur 200 and 400 m below the felsic volcanic formation.

The iron formations consist of thinly laminated magnetiferous chert and massive magnetite, locally accompanied by chloritic amphibolite interlayers or thin chloritic partings. Laminae are 2–20 mm thick (rarely up to 6 cm). Siliceous siltstone and intermediate, garnetiferous siltstone are associated with several magnetiferous units. The iron formations are locally highly contorted, with steeply plunging, partly disrupted folds. Surficial iron staining due to alteration of pyritic zones within the magnetiferous rocks is locally characteristic of these formations.

Southern section

Oxide-facies iron formations occur both in the lower part and close to the top of the southern section, in the areas south of Lavigne and MacVicar lakes, respectively (Figure 2). The latter unit is thin (0.3 m) and of limited lateral extent, in contrast to the formation in the lower part of the southern section, which consists of four magnetiferous layers (0.5–1.5 m thick) intercalated with siltstone over a 14 m wide section that extends for at least 2 km along strike. The magnetiferous units consist of alternating, 2–30 mm thick laminae of magnetite-chlorite schist, chert, siltstone (±garnet) and very fine grained amphibolite. The intervening, laminated siltstone beds contain anthophyllite blades and fascicular aggregates, and cordierite as lensoid to elongate porphyroblasts up to 3 cm long, in stratabound zones 20–80 cm wide. The iron formation is locally tightly folded and disrupted.

Siltstone, feldspathic greywacke; minor chert (subunit J2b)

Northern section

Fine-grained turbidite-type deposits (subunit J2b) constitute 10–20% of the northern section in the vicinity of MacVicar Lake, close to the north margin of the greenstone belt (Map GR2004-2-1, in back pocket). The sedimentary units, typically 2–20 m thick, are intercalated with arc-type ‘northern’ volcanic rocks; the largest deposit (‘northern sedimentary formation’ in Figure 4) is 85 m thick and is located on the peninsula in central MacVicar Lake. This formation, a diverse assemblage of siltstone, feldspathic greywacke, chert and related paragneiss, wedges out to the west, where the sedimentary rocks are laterally gradational with felsic fragmental deposits (subunit J4b) of inferred mass-flow origin. To the east, the northern sedimentary formation is also apparently gradational with felsic volcanic rocks (‘northern felsic volcanic formation’ in Figure 4). The northern sedimentary formation is located approximately 75 m south of the hinge line of a synclinal fold, and is thus close to the top of the stratigraphic sequence in the northern section of the greenstone belt (see ‘Structural geology’ section).

Intermediate siltstone, greywacke and minor argillaceous siltstone (subunit J2b) display well-defined bedding (2–40 cm) and local very fine lamination (2–10 mm). Some layers are garnetiferous and/or characterized by stratabound cordierite and

anthophyllite. Ovoid cordierite of M_1 age constitutes up to 65% of porphyroblastic, 10–50 cm thick layers; the elongate blasts (up to 3 cm by 1 cm) are aligned parallel to S_1 (Figure 11) and locally lineated parallel to minor F_1 folds (Figure 12). Randomly oriented, euhedral anthophyllite constitutes a later metamorphic overprint (M_2). Sporadic graphitic, argillaceous siltstone beds, commonly associated with amphibolitic interlayers, are characterized by surficial iron staining due to pyrite oxidation.

Laminated chert is intercalated with greywacke and siltstone close to the south margin of the northern sedimentary formation, where chert beds up to 30 cm thick locally display flame structures at the contact with overlying greywacke (Figure 13). Chert also

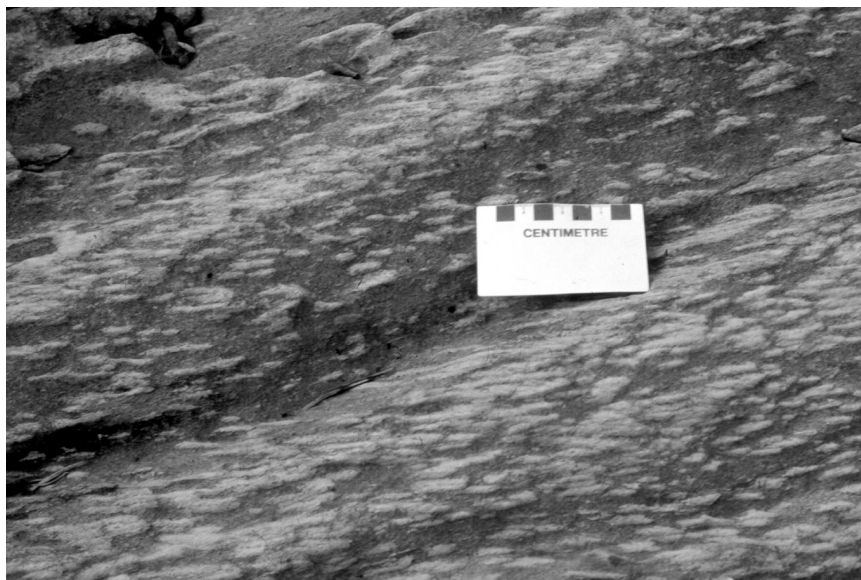


Figure 11: Stratabound cordierite porphyroblasts oriented parallel to S_1 in the northern sedimentary formation (unit J2), located on the peninsula in the centre of MacVicar Lake.



Figure 12: S_0 - S_1 discordance in a cordierite-bearing siltstone-greywacke bed (subunit J2b) within the northern sedimentary formation, located on the peninsula in the centre of MacVicar Lake. Cordierite is lineated parallel to F_1 folds.

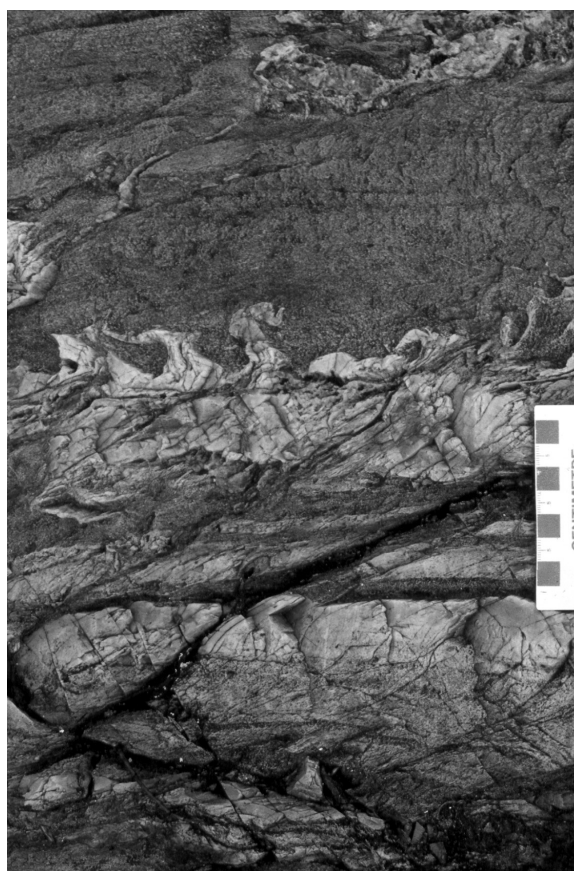


Figure 13: Flame structure in a chert layer (subunit J2b) within the northern sedimentary formation, located on the peninsula in the centre of MacVicar Lake.

occurs close to the north margin of the formation, where garnetiferous siltstone contains thin white chert and black massive magnetite laminae (Figure 14). In addition, chert occurs as a subordinate component of garnetiferous mafic gneiss units (subunit J2c) near both the north and south margins of the northern sedimentary formation.

A 6 m thick, south-facing turbidite layer (subunit J2b) occurs within laminated amphibolite (subunit J1e) close to the top of the northern stratigraphic section, 60 m south of the amphibolite-tonalite contact in the northwest corner of the map area (Map GR2004-2-1, in back pocket). This structurally important, south-facing sedimentary unit consists of well-graded feldspathic greywacke and siltstone that display A-D Bouma divisions (Figure 15). The siltstone locally contains stratabound cordierite, lineated parallel to F_1 minor fold axes.

The base of the mainly basaltic northern section at Franklin Murray Lake is marked by an 11 m thick sedimentary deposit (subunit J2b) that consists of chert and related siliceous siltstone (Map GR2004-2-1, in back pocket). The south margin of the sedimentary unit is mineralized with base-metal sulphides (Cu, Zn) and Au (*see* 'Economic geology' section). The north margin of this unit is intruded by a plagioclase porphyry sill (subunit J4d), whereas the contact relationship between the siliceous sedimentary unit and ocean-floor-type basalt to the south (central section) is unknown.

Southern section

A sedimentary deposit (subunit J2b), up to 50 m thick, that extends along strike for at least 1 km is intercalated with basalt at the north margin of the southern section, in the area south of MacVicar Lake (Map GR2004-2-1, in back pocket). The sedimentary unit is interpreted to be a shear-bounded structural slice. Extensive alteration, shearing and local protomylonite, which are characteristic of this unit, probably reflect its location at the major stratigraphic-structural break between the southern and central sections of the Ralph Anderson Lake greenstone belt. To the north, the sedimentary unit is bounded by relatively undeformed and unaltered ocean-floor-type basalt and related gabbro of the central section. To the south, the unit is in contact with tectonized and extensively silicified and epidotized arc-type basalt and heterolithic volcanic fragmental rocks of the southern section.

Siltstone is the principal lithological type in the sedimentary deposit south of MacVicar Lake. The north margin of this unit is porphyroblastic over a 3 m wide zone, where ovoid cordierite and subhedral anthophyllite blasts constitute up to 40% of the metamorphosed rock. The siltstone-basalt contact at the north margin of the unit displays extensive surficial iron staining due to

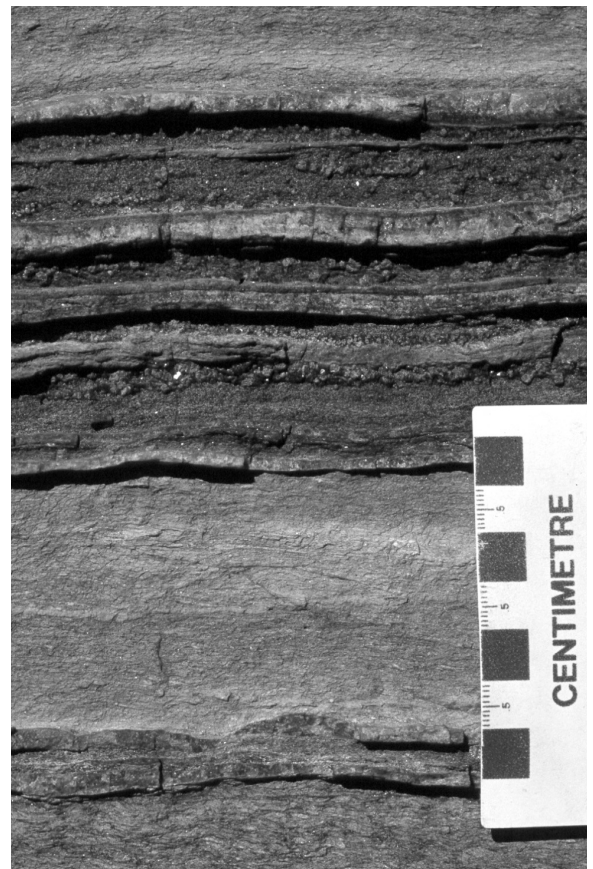


Figure 14: White chert and black magnetite laminae within intermediate to argillaceous, garnetiferous siltstone (subunit J2b), close to the north margin of the northern sedimentary formation, located on the peninsula in the centre of MacVicar Lake.



Figure 15: Graded turbidite deposit (subunit J2b), close to the margin of the Ralph Anderson Lake belt in the northwest part of the map area.

the weathering of a 2 m wide zone of disseminated pyrite mineralization that contains minor Cu and Ni (see 'Economic geology' section).

Feldspathic greywacke, pebbly wacke and siltstone occur in several narrow (approximately 20 m wide) skialithic enclaves within the McLeod Narrows gabbro, 600 m north of the southwest end of Milton Lake (Map GR2004-2-1, in back pocket). Greywacke-siltstone units are characterized by well-layered, locally graded beds (10–70 cm thick) of probable turbidite origin. Stratigraphically equivalent siltstone beds at the narrows between Milton and Franklin Murray lakes contain elongate anthophyllite and cummingtonite prisms, and ovoid cordierite porphyroblasts up to 1 cm long, which occur in lensoid aggregates measuring up to 12 cm by 1 cm.

Altered garnetiferous supracrustal rocks (subunit J2c)

A mineralized alteration zone occurs within 'northern' basalt and amphibolite at MacVicar Lake (Figure 4), approximately 150 m south of the north margin of the greenstone belt (Gilbert, 1999a, 2000). The lateral extent of the 'MacVicar Lake alteration zone', together with stratigraphically equivalent oxide-facies iron formation to the east, is over 10 km; the thickness of the zone diminishes from a maximum of 36 m in the northeast part of MacVicar Lake to 5 m at the west end of the lake. The alteration zone is coincident with a sedimentary unit, which occupies the core of the MacVicar Lake syncline (Figure 4) and thus overlies the mafic volcanic sequence in this part of the greenstone belt (see 'Structural geology' section). The sedimentary unit consists of siltstone and subordinate, locally magnetiferous chert, intercalated with massive to laminated amphibolite. Whereas some amphibolite is interpreted as basalt derived, finely laminated hornblendic laminae within siltstone units are probably sedimentary in origin. Extensive silicic alteration and surficial iron staining due to the weathering of widely disseminated pyrite are characteristic of both the siltstone and the amphibolite. The alteration and sulphide mineralization are interpreted to be the result of early hydrothermal activity, probably contemporaneous with volcanism and related felsic porphyry intrusions. Minor Cu and Zn (<0.5%) and traces of Au occur in silicified basalt, chert and felsitic intrusive rocks (see 'Economic geology' section). Subsequent regional metamorphism resulted in extensive recrystallization of the altered rocks to coarse-grained garnetiferous gneiss, which was later folded and disrupted by sinistral, strike-slip movement. Localized tectonic breccia within this zone is attributed to late brittle deformation.

Siliceous rocks constitute 20–40% of the alteration zone and can mostly be traced to basaltic precursors, which occur as intercalated concordant units and irregular, dark green, massive to laminated remnants within the altered rocks (Figure 16). Horizons of intense alteration and deformation are characterized by pervasive quartz veins (\pm massive magnetite laminae), sporadic garnets (up to 2 cm), blastic garnetiferous trails, and massive, highly contorted garnetite layers up to 15 cm thick. Minor, disrupted plagioclase porphyry and siltstone units also occur locally in the alteration zone.

Layered garnetiferous gneissic zones, approximately 1–4 m wide and similar to the MacVicar Lake alteration zone, occur close to both the north and south margins of the northern sedimentary formation (see 'Siltstone, feldspathic greywacke; minor chert' section). These zones, which display surficial iron staining, are strongly deformed and characterized by pervasive metasomatism that resulted in silicic, hornblendic and chloritic alteration, extensive garnet blastesis, and development of massive garnetite. The garnetiferous zones appear to be mainly of sedimentary origin, but some amphibolitic layers may be derived from intrusive units.

Heterolithic volcanic breccia and associated tuff; related sedimentary rocks (unit J3)

Heterolithic volcanic fragmental rocks (unit J3) constitute approximately half of the southern section of the Ralph Anderson Lake belt. These rocks occur as skialithic components of a major supracrustal enclave that extends for at least 8 km through the central part of the McLeod Narrows gabbro (Lavigne Lake–McLeod Narrows enclave, Figure 2). Limited structural data indicate the sequence is a north-facing monocline. The heterolithic deposits consist mainly of mafic to felsic, volcanic fragmental detritus (Figure 17), with subordinate reworked sedimentary rocks (subunit J3c). The stratigraphic sequence of the supracrustal enclave south of western Ralph Anderson Lake consists of a basal, 14 m thick deposit of oxide-facies iron formation and siltstone (subunits J2a, J2b), overlain by over 200 m of volcanic breccia and tuff (subunits J3a, J3b) that contain subordinate gabbroic intercalations. In the



Figure 16: Disrupted garnetiferous amphibolite in zone of silicic alteration (subunit J2c), northeast MacVicar Lake.

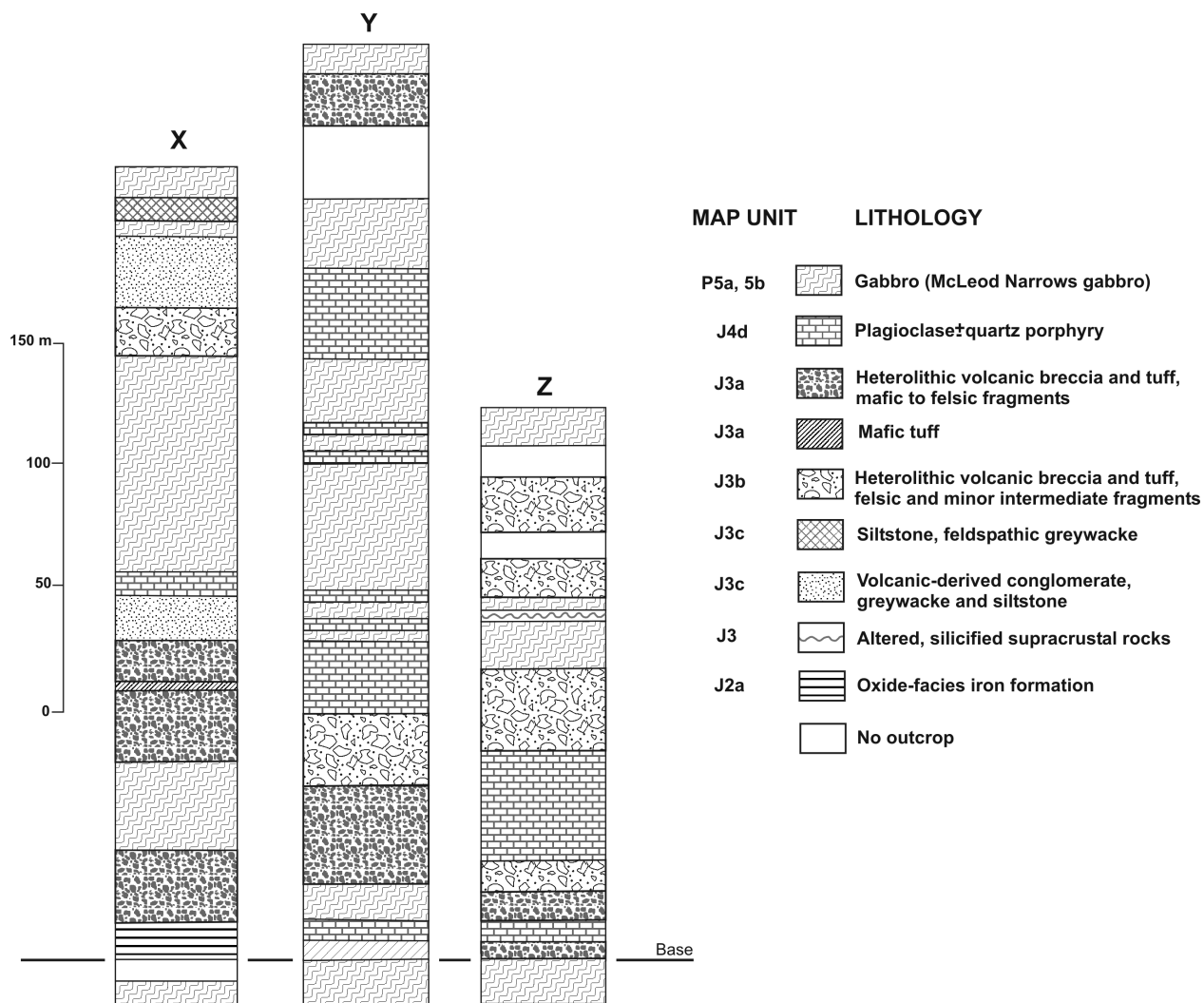


Figure 17: North-south stratigraphic sections through the Lavigne Lake–McLeod Narrows supracrustal enclave (see Figure 2 for location): **X**) northwest of Milton Lake (305 m section); **Y**) north of the west end of Franklin Murray Lake (355 m section); and **Z**) at McLeod Narrows (195 m section).

lower part of the section, the breccia is characterized by an upward increase in the relative amount of felsic detritus; mafic fragments are confined to the lowest part of the breccia unit (Figure 18).

Heterolithic volcanic breccia and tuff (subunits J3a, J3b); volcanic-derived conglomerate, feldspathic greywacke and siltstone (subunit J3c)

Heterolithic volcanic breccia (subunits J3a, J3b) consists of an assemblage of diverse volcanic fragments (with variously porphyritic, aphyric or rare amygdaloidal textures) within a mafic to intermediate, tuffaceous matrix (Table 3). Subunit J3a is composed of mafic to felsic fragments, whereas J3b consists mainly of felsic fragments. The fragments, which typically constitute 40–65% of the rock, are deformed and attenuated (elongation ratios typically range from 5:1 to 20:1); the original, mainly angular fragment shapes are only locally preserved. Individual breccia deposits are up to 35 m thick, but their original true thickness may be several times that amount, based on the degree of attenuation of the fragments. The fragmental rocks are generally poorly sorted or unsorted. Crude sorting at one locality is defined by a lower 10 m wide zone of coarse breccia that grades upward to a 12 m zone of alternating breccia and lapilli tuff. More typically, sporadic large blocks (mostly felsic and up to 1.8 m by 0.5 m in size) are distributed randomly within breccia that contains mostly smaller, unsorted fragments, typically 5–30 cm long (Figure 19). Rarely, conspicuous large blocks occur along stratigraphic horizons in otherwise unsorted volcanic breccia. Tuff and lapilli tuff intercalations constitute approximately 10% of the section.

Sedimentary deposits (subunit J3c) within the southern section of the Ralph Anderson Lake belt are largely confined to the west part of the Lavigne Lake–McLeod Narrows enclave (Figure 2; Figure 17, section X). Northwest of Milton Lake, greywacke, siltstone and conglomerate (subunit J3c) occur in the central part of the supracrustal sequence. The sedimentary rocks, which are

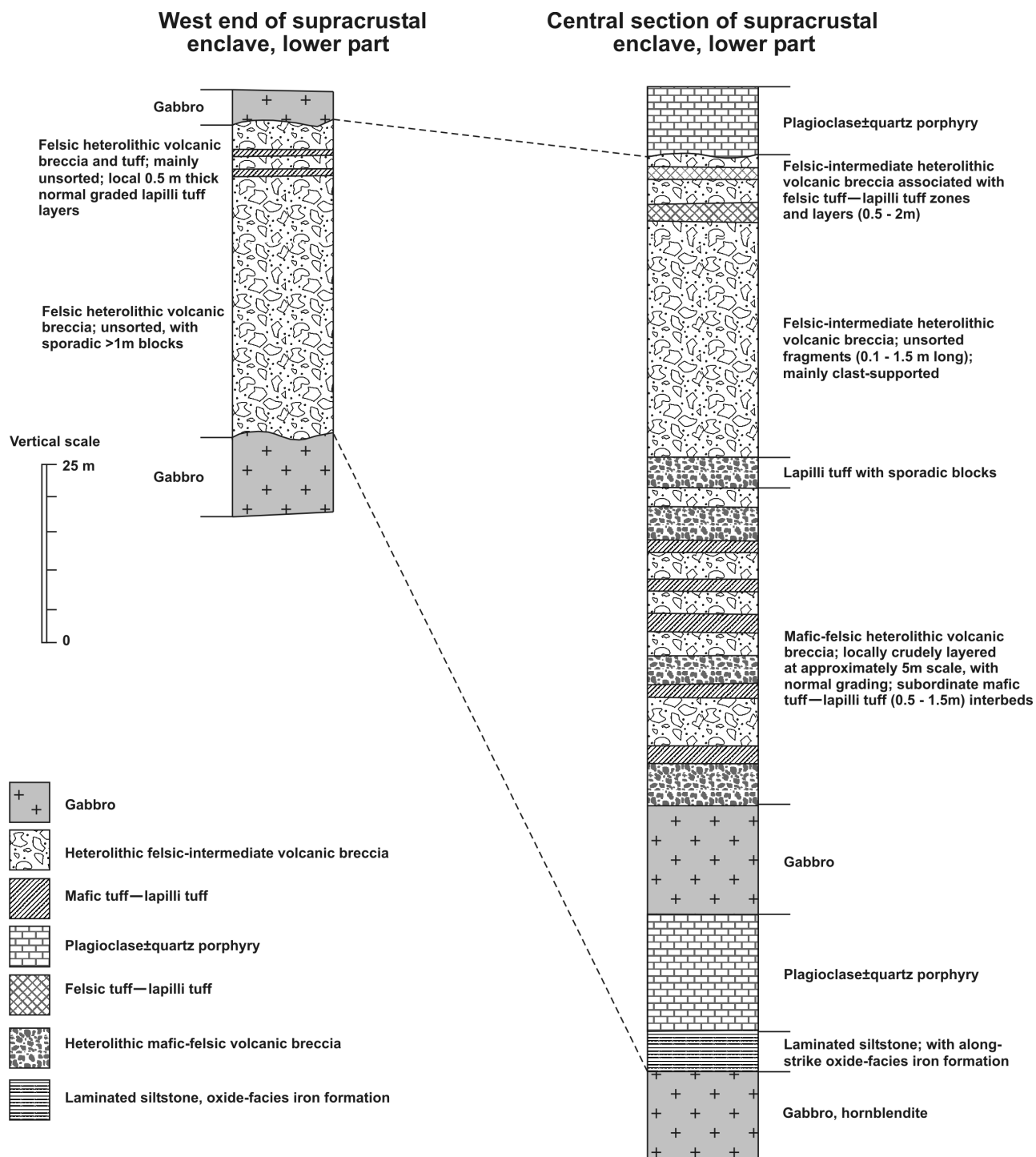


Figure 18: Transverse north-south sections through the lower part of the Lavigne Lake–McLeod Narrows supracrustal enclave.

compositionally similar to and gradational with the underlying breccia and tuff (subunit J3a), are distinguished by well-defined layering and graded bedding consistent with a turbidite origin (Table 3). The sedimentary deposits are characterized by 0.1–0.5 m thick cyclic units that consist of basal conglomerate overlain by pebbly greywacke and uppermost fine-grained greywacke and siltstone. The approximately 20 m thick turbidite section is intruded at the north margin by felsic porphyry and a 90 m thick gabbro sill (Figure 17, section X). North of the gabbro, the uppermost 30 m of the supracrustal sequence also consist of fine-grained sedimentary rocks: greywacke, porphyroblastic siltstone and conglomerate.

Heterolithic volcanic breccia and associated tuff (subunits J3a, J3b) are interpreted as reworked volcanoclastic deposits emplaced by debris flows, possibly initiated by the slumping of unconsolidated volcanic detritus on unstable slopes. Diagnostic features that suggest a mass-flow mode of origin (Fisher and Schmincke, 1984) include the following:

Table 3: Lithology and stratigraphic association of volcanic fragmental rocks (subunits J3a, J3b) and associated conglomerate (subunit J3c) at the south margin of the Ralph Anderson Lake greenstone belt.

Rock type (map unit)	Fragment type	Fragment shape and size	Clast volume (%)	Sorting	Matrix type	Associated clastic units	Inferred origin
Heterolithic volcanic breccia, (subunit J3a)	Felsic to mafic (aphyric to porphyritic)	Angular or tabular to flattened (up to 1.85 m x 0.5 m)	20-75%, typically >50%	Unsorted to rarely sorted; rarely graded	Mafic-intermediate tuff, crystal tuff	Tuff and lapilli tuff (<10% of map unit)	Mass flow, subaqueous
Heterolithic volcanic breccia (subunit J3b)	Felsic, minor intermediate (mainly plagioclase±quartz phryic)				Felsic-intermediate tuff, crystal tuff		
Volcanic-derived conglomerate (subunit J3c)	Felsic to mafic (aphyric to porphyritic)	Subangular to subrounded, flattened, pebble- to cobble-size	35-75%	Well sorted; locally graded, with cyclic bedding	Greywacke-siltstone	Greywacke, pebbly greywacke, siltstone	Reworked by water (below storm-wave base)

- Depositional units are thick (5–35 m) and unsorted to poorly sorted (Figure 18).
- There is a wide range of fragment size with unimodal variation; normal and (less commonly) reverse size-grading of fragments occur locally.
- Sporadic large blocks within the breccia occur well above the base of depositional units.
- Original clast shapes, where preserved, are mainly angular.

The stratigraphic association of sedimentary rocks with heterolithic volcanic breccia (Figure 17) indicates a subaqueous depositional environment. Minor graded bedding and cyclic interlayering of conglomerate and greywacke-siltstone within the breccia sequence are attributed to reworking by turbidity currents.

Felsic volcanic rocks of juvenile-arc affinity; minor sedimentary rocks and felsic porphyry (unit J4)

Rhyolite, massive to fragmental (subunit J4a); heterolithic volcanic breccia and tuff (subunit J4b); volcanic-derived conglomerate, feldspathic greywacke and siltstone (subunit J4c)

Felsic volcanic rocks are conspicuous components of the arc-related, northern and southern sections in the Ralph Anderson Lake belt. In the northern section, massive to fragmental rhyolite (‘northern felsic volcanic formation’) is associated with an inferred, subvolcanic felsic porphyry sill (subunit J4d) that is emplaced obliquely within the underlying basalt (Figure 2). The analogous ‘southern felsic volcanic formation’ in the southern section consists of a major skialithic enclave and several minor inclusions within the McLeod Narrows gabbro. The dimensions of both northern and southern felsic volcanic formations are similar: up to 130 m thick and 11 km along strike. These two formations may be stratigraphically equivalent, based on the regional structural interpretation (see ‘Structural geology’ section).

The rhyolitic rocks are moderately to strongly attenuated and original flow structures are generally not preserved; however, the southern formation is relatively undeformed in the area due south of Lavigne Lake, where it consists of a fragmental lava flow with remnant layers and irregular lobes of massive rhyolite. The northern felsic volcanic formation consists of relatively more homogeneous, massive extrusive rocks (subunit J4a), overlain by unsorted heterolithic breccia with mainly felsic volcanic fragments. Massive flows are thickest in the central parts of both northern and southern formations (i.e., at northern Lavigne Lake and at a small lake directly south of Lavigne Lake, respectively; Map GR2004-2-1, in back pocket). In both the northern and

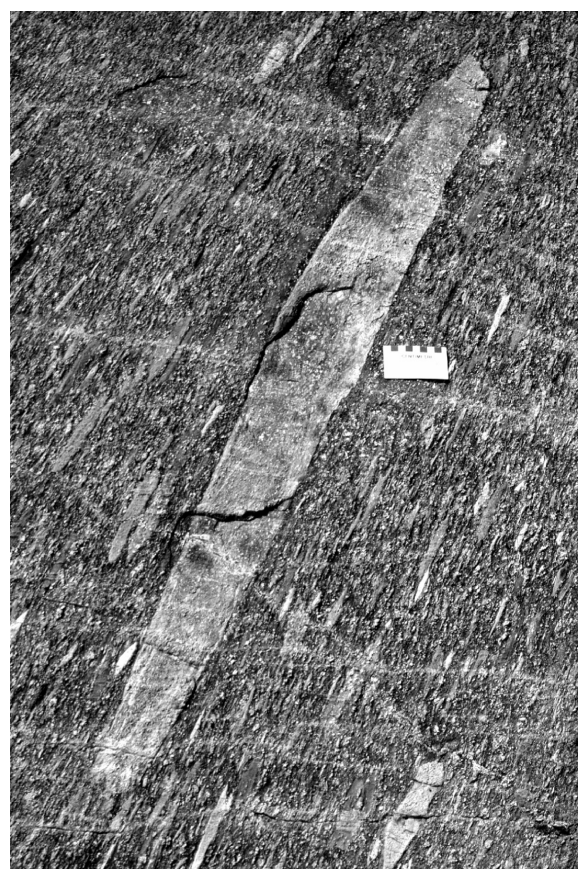


Figure 19: Heterolithic volcanic breccia (subunit J3a) containing unsorted, sporadic large blocks within less coarse volcanic detritus, located 1.8 km south of the west end of Ralph Anderson Lake.

southern felsic volcanic formations, subordinate volcanoclastic rocks (subunits J4b, J4c) either overlie or are laterally gradational with the massive rhyolite components, and are thus areally more extensive than the massive rock units. The distribution of these facies types is consistent with a depositional model in which the original felsic volcanic edifice consisted of a proximal massive extrusion that was flanked by related felsic breccia and tuff. The coarse volcanic fragmental rocks and more distal tuffaceous deposits are interpreted as having been locally redeposited in an adjacent sedimentary basin as a result of mass flows and turbidity currents.

Northern section

The northern felsic volcanic formation is especially well exposed on the north shore of Lavigne Lake, where massive and fragmental rhyolitic rocks are intimately intercalated. Subordinate conglomerate and greywacke-siltstone deposits (subunit J4c) up to 25 m thick occur both within and directly below the felsic volcanic rocks (Map GR2004-2-1, in back pocket). The sequence at Lavigne Lake consists of a lower zone, 50 m thick, of largely massive rhyolite (subunit J4a) overlain by at least 65 m of heterolithic volcanic breccia that consists of predominantly felsic fragments (subunit J4b). The lower massive unit contains sporadic fragmental zones that are attributed to flow brecciation; localized subparallel, evenly spaced, chlorite-filled joints are interpreted as thermal contraction cracks. The rocks contain sparse to abundant plagioclase phenocrysts (3–25%), and are locally characterized by fine tectonic laminae (1–5 mm) and diffuse concordant zones of recrystallized plagioclase and hornblende.

Heterolithic volcanic breccia (subunit J4b) that directly overlies the massive rhyolite unit at northern Lavigne Lake contains aphyric to plagioclase-phyric volcanic fragments, typically 5–40 cm long, together with sporadic large blocks up to 0.15 m by 1.3 m. Clasts are predominantly felsic but include subordinate (<15%) intermediate rock types. The fragments are moderately to strongly flattened, but traces of original angular shapes are locally preserved. The breccia matrix is tuffaceous and similar to rare felsic tuff and lapilli tuff layers (approximately 1 m thick) that occur within the fragmental unit. The breccia is generally unsorted but, in the area west of Lavigne Lake, the coarse fragmental detritus is gradational upwards into lapilli tuff.

A lithostratigraphic transition occurs along strike from Lavigne Lake, west to MacVicar Lake; this transition is considered to represent a change from a proximal to a more distal depositional environment. The northern felsic volcanic formation thins rapidly over a distance of 1.5 km from the Lavigne Lake locality (115 m thick) west to the northeast part of MacVicar Lake (Map GR2004-2-1, in back pocket; Figure 2), where it is represented by a 40 m thick heterolithic volcanic breccia deposit (subunit J4b). The breccia, which is more diverse and slightly less coarse than at Lavigne Lake, contains approximately equal amounts of felsic and intermediate fragments with minor (5%) mafic types, within a tuffaceous matrix. Clasts (mainly 5–25 cm long) are subangular to strongly flattened; blocks up to 80 cm by 25 cm occur sporadically within the breccia, which is unsorted in units up to 10 m thick. Subordinate tuff and lapilli tuff interlayers, which constitute approximately 20% of the formation at MacVicar Lake, are moderately well layered (at a scale of 0.2–1.5 m) and locally graded, possibly due to redeposition by subaqueous density currents. Conglomerate and siltstone (subunit J4c) occur along strike to the west of the heterolithic breccia deposit.

A diverse assemblage of fine-grained sedimentary rocks (subunits J2b, J2c) up to 85 m thick ('northern sedimentary formation') occurs on the peninsula in central MacVicar Lake, directly to the west and along strike from the northern felsic volcanic formation in the east part of MacVicar Lake (Figure 4). The sedimentary rocks are, in turn, succeeded along strike by heterolithic breccia (subunit J4b), up to 34 m thick, that extends to the limit of mapping in the northwest part of the project area (Map GR2004-2-1, in back pocket). The latter, 'western' breccia deposit may be derived from a felsic volcanic centre, located along strike to the west of the project area, which is separated from the felsic volcanic centre at Lavigne Lake by fine-grained turbidite ('northern sedimentary formation', Figure 4). The 'western' breccia is apparently slightly younger in age than the turbidite, because this sedimentary rock is overlain by the fragmental volcanic strata on the peninsula in the central part of MacVicar Lake (Map GR2004-2-1, in back pocket).

Southern section

The southern felsic volcanic formation, near the south margin of the belt, is truncated to the east by a fault in the area north-east of Milton Lake (Figure 2); the west end of the formation appears to wedge out in the area south of MacVicar Lake. Porphyritic rhyolite and related monolithic flow breccia (subunit J4a), up to 85 m thick, are well preserved at the small lake due south of Lavigne Lake, where massive rhyolite occurs as concordant layers (typically 1–3 m thick) and sporadic lenses and lobes (up to 9 m by 2.5 m) within the breccia. Massive units display both sharp and gradational contacts with the associated fragmental rocks, which constitute approximately 80% of the formation at that locality. Massive rhyolite is white to cream-grey weathering, in contrast to felsic clasts in the associated breccia, which range from white to grey or beige, probably due to secondary epidote or carbonate content. The breccia is characterized by unsorted 10–30 cm long clasts and sporadic blocks up to 1.5 m by 0.5 m; the felsic-tuff-crystal-tuff matrix constitutes 25–70% of the rock. Rhyolite fragments are moderately to strongly attenuated (elongation ratios range from 4:1 to >20:1), but angular clast shapes are locally preserved. Both massive and fragmental units contain ubiquitous plagioclase phenocrysts (0.5–3.0 mm long; 5–20% of the rock).

Northwest of the narrows between Milton and Franklin Murray lakes (Figure 2), the southern felsic volcanic formation consists of a 90 m thick section of massive to fragmental, locally porphyroblastic rhyolite (subunit J4a). A 30 m wide zone in the

north part of the formation is characterized by ovoid to elongate, pinitized cordierite porphyroblasts and randomly oriented, chloritized anthophyllite blasts. Cordierite porphyroblasts are 0.5–3.0 cm long and occur in aggregates, measuring up to 11 cm by 7 cm, that constitute 5–30% of the rock. A densely porphyroblastic felsic rock that contains 70–80% cordierite occurs in a 1 m wide zone at the north margin of the southern felsic volcanic formation, where it is in contact with gabbro.

Between the above two massive rhyolite localities, the southern felsic volcanic formation consists of approximately 120 m of volcanic-derived conglomerate, feldspathic greywacke and siltstone (subunit J4c), with subordinate (<10%) massive rhyolite flow-sill units (subunit J4a) up to 8 m thick (Map GR2004-2-1, in back pocket). The sedimentary rocks are intercalated at a scale of 1–12 m, and are interpreted as reworked, subaqueous mass-flow deposits. The conglomerate contains strongly attenuated pebble- to boulder-sized rhyolite clasts (up to 0.1 m by 1.85 m) that locally display traces of original subangular shapes; the clasts range from aphyric to sparsely or densely plagioclase phyrlic. The fragments are unsorted, except for rare, narrow (0.5 m) pebbly horizons within coarser conglomerate. The sedimentary deposits are porphyroblastic in the south (lower) part of the section, where lenticular to elongate stratabound cordierite blasts up to 2 cm by 5 cm constitute 10–50% of the rock in zones up to 2.5 m wide. Ovoid anthophyllite rosettes (1–2 cm) are less widespread; epidotic alteration postdates the porphyroblastesis.

The two felsic volcanic formations (northern and southern) in the Ralph Anderson belt are equivalent in their dimensions and are also very similar both in their lithological and geochemical composition and in their stratigraphic association. These formations are interpreted as products of felsic volcanism in a juvenile-arc-type setting, in which massive intrusive-extrusive rhyolite units are associated with monolithic flow breccia, heterolithic mass-flow deposits and more distal, tuffaceous turbidites. Although the two formations cannot be positively identified as parts of the same original volcanic terrane, the field data are consistent with such a correlation; this topic is discussed further in the ‘Structural geology’ section.

Plagioclase±quartz porphyry (subunit J4d)

A prominent plagioclase±quartz porphyry sill (subunit J4d), up to 0.5 km thick and 7 km along strike, occurs within the northern volcanic suite in the area north of Ralph Anderson Lake (Figure 2). The sill, which is interpreted as a subvolcanic intrusion, is oblique to the stratigraphy, and cuts ‘up section’ to the northwest. The northwest end of the sill may be continuous with felsic volcanic flows in the northern felsic volcanic formation; however, the contact relationships are obscured by a small lake at that locality, 0.5 km north of the west end of Ralph Anderson Lake. The felsic porphyry is massive and homogeneous, and contains 1–3 mm phenocrysts of plagioclase (10–20% of the rock) and rare quartz. Ovoid to subhedral epidote pseudomorphs after feldspar (0.5–3.0 cm across), which constitute up to 20% of the rock, are confined to less than a quarter of the intrusion.

Plagioclase±quartz porphyry dikes (subunit J4d) up to 25 m thick occur in all three stratigraphic sections and throughout the southeast Max Lake map area, but are most abundant in the central and north parts of the greenstone belt. The dikes, which trend mainly east-west, include several texturally distinct types based on phenocryst size. Plagioclase phenocrysts are typically 1–3 mm long and constitute 10–40% of the rock; in some intrusions, the feldspars are up to 1 cm long. Quartz phenocrysts, where present, are subordinate to plagioclase and are typically 1–2 mm across (rarely, up to 8 mm). The felsic dikes are interpreted as contemporaneous with arc-type volcanism, because they are geochemically and petrographically similar to volcanic rocks of subunits J4a and J4b (*see* ‘Geochemistry’ section). Nevertheless, some of the more coarsely porphyritic felsic dikes, which truncate the metamorphic fabric of foliated basaltic host rocks, are postvolcanic.

Franklin Murray Lake–Aswapiswanan Lake area

Stratigraphy

The stratigraphic sequence defined in the MacVicar Lake–Ralph Anderson Lake area extends eastward to the vicinity of Franklin Murray Lake. Further to the east, stratigraphic details are incomplete due to the displacement and/or assimilation of supracrustal rocks by granitoid intrusions, more intense deformation and metamorphism, and an extensive cover of glacial drift; however, geochemical data indicate that the juvenile arc ‘southern’ section and ocean-floor ‘central’ section extend through Aswapiswanan Lake and further east, to beyond the confines of the map area (Figure 3; Maps GR2004-2-1, GR2004-2-2, GR2004-2-3, in back pocket). The ‘southern’ and ‘central’ volcanic rocks occur in an area that is flanked to the north by a gabbro-pyroxenite sill, assumed to be the on-strike equivalent of the Lavigne Lake gabbro on the basis of its similar geochemical profile. The terrane immediately north of the gabbro-pyroxenite sill, where the northern volcanic section might be anticipated, is poorly exposed and apparently occupied mainly by granitoid rocks. Thus, the northern section in that area is either covered by glacial drift and swamp, or has been assimilated by granitoid intrusions that are part of an extensive tonalite-granodiorite and granitoid gneiss terrane north of the greenstone belt (Hubregtse, 1985b). Within the Franklin Murray Lake–Aswapiswanan Lake area, the greenstone belt is increasingly more attenuated and disrupted by pervasive granitoid intrusions toward the east. At the south margin of the belt, a 100–300 m wide hybrid zone between the supracrustal rocks and the granitoid terrane immediately to the south contains amphibolite, granitoid rocks and derived gneiss.

Ocean-floor-type supracrustal rocks (central section)

Mafic volcanic rocks of ocean-floor affinity and metamorphic equivalents (unit O1)

Aphyric basalt (subunit O1a) is the principal rock type in the greenstone belt in the west part of the Aswapiswanan Lake area (Map GR2004-2-2, in back pocket). This unit is geochemically equivalent to ocean-floor basalt within the central section at Ralph Anderson Lake, directly along strike to the west. The mafic flows at western Aswapiswanan Lake, which are at least 0.6 km thick, are intercalated with gabbro (subunit O1c) and fine-grained, laminated amphibolite (subunit O1e). North-facing pillows were observed at one locality within this section, but the mafic volcanic rocks are generally too attenuated for stratigraphic tops to be determined; pillow elongations typically range from 8:1 to 15:1. In the central and eastern parts of Aswapiswanan Lake, bedrock exposure of the ocean-floor basaltic rocks is generally poor, except for a sequence of mafic flows close to the east end of the lake, which extend north from the lakeshore for at least 1.2 km.

Amygdaloidal zones (with plagioclase±quartz, or carbonate amygdules) occur sporadically in the basaltic flows. Epidotic alteration is common, either in pillow cores or toward the margins; silicic, pillow-rim alteration is more sporadic. In strongly deformed zones, the basalt is altered to gneiss (subunit O1e) that contains thin (1–15 mm), compositionally distinct laminae (hornblende±chlorite, epidote±quartz±feldspar). This tectonometamorphic lamination is interpreted as having been derived from contrasting domains in the original volcanic flows (e.g., zones of early epidotic or silicic alteration and chloritic pillow selvages). The gneiss is also characterized by stringers and aggregates of epidote (±quartz±carbonate±garnet) that postdate the fine lamination. Elsewhere, where metamorphism was not accompanied by strong deformation, the basaltic rocks (subunit O1a) locally contain diffuse, recrystallized domains of fine- to medium-grained plagioclase+hornblende.

Narrow (10–40 cm thick) alteration zones with surficial iron staining and silicification (± garnet porphyroblasts) occur in several mafic flow units. Similar gossan zones occur sporadically within the gabbro sill (subunit P5a) at western Aswapiswanan Lake. These zones locally contain disseminated pyrite and sulphidic stringers with minor base-metal sulphides (*see* ‘Economic geology’ section).

Juvenile-arc-type supracrustal rocks (southern section)

Mafic volcanic rocks of juvenile volcanic-arc affinity and metamorphic equivalents (unit J1); heterolithic volcanic breccia (unit J3)

Sporadic basaltic enclaves (subunits J1a, J1e) within the granitoid terrane along the south shore of Aswapiswanan Lake are interpreted as representatives of the southern volcanic section at Ralph Anderson Lake, based on their analogous, juvenile-arc geochemical signature. The mafic volcanic rocks occur as sporadic blocks and skialithic enclaves up to 20 m thick; the hosting granitoid rocks consist of tonalite, granodiorite, feldspar porphyry and associated gneiss. The basalt is typically aphyric to locally sparsely plagioclase phyrlic; pillows are conspicuous at one locality, and remnants of pillow selvages occur elsewhere in tectonically attenuated flow units. Primary features are generally not preserved in the mafic flows, however, due to deformation and recrystallization of the volcanic rocks to mafic gneiss (subunit J1e).

A minor but texturally distinctive megaphyric gabbro unit, interpreted as a synvolcanic dike (subunit J1d), occurs at the west end of Aswapiswanan Lake, close to the south margin of the juvenile-arc basalt section (Map GR2004-2-2, in back pocket). This >3 m thick intrusion contains 1–2.5 cm plagioclase megacrysts (up to 10% of the rock) and 1–3 mm hornblende pseudomorphs after pyroxene (up to 15%). Lithologically similar megaphyric gabbro (subunit O1d) occurs as synvolcanic intrusions

within the central section at Ralph Anderson Lake.

Copper-zinc-gold-nickel-chromium mineralization occurs in the northwest part of Aswapiswanan Lake, at or close to the contact between arc-type volcanic rocks of the southern section and ocean-floor basaltic rocks to the north (Map GR2004-2-2, in back pocket). The mineralization, which is located in a mafic sill that is interpreted to be synvolcanic (subunit J1c), consists of disseminated and stringer base-metal sulphides occurring over a 0.3 m wide zone within gabbro and associated garnetiferous amphibolite (mineralization type 4 in 'Economic geology' section).

A unique occurrence of strongly deformed, intermediate volcanic breccia (subunit J3b) on an islet close to the south shore of Aswapiswanan Lake (Map GR2004-2-3, in back pocket) contains attenuated felsic fragments (up to 25 cm by 2 cm) within an intermediate matrix. The >8 m thick unit is assumed to be affiliated with heterolithic volcanic breccia of debris-flow origin, which is common within arc-type volcanic rocks in the Ralph Anderson Lake belt further to the west.

Intrusive rocks

Introduction

Intrusive rocks in the southeast Max Lake–Aswapiswanan Lake area include major granitoid plutons that intrude the margins of the Ralph Anderson Lake greenstone belt and igneous intrusions of both synvolcanic and younger ages within the belt. Previously described synvolcanic intrusive rocks, which are geochemically akin to their extrusive hostrocks, include both felsic porphyry bodies (subunit J4d) and gabbroic dikes and sills (subunits O1c, O1d, J1c, J1d). The latter intrusions, which are between 1 and 150 m thick and extend up to 3 km along strike, are dwarfed by two major gabbroic sills of uncertain age: the McLeod Narrows and Lavigne Lake intrusions (unit P5). These sills are >1 km and >0.25 km thick, respectively, and extend for at least 24 km through the south and central parts of the greenstone belt (Figures 2, 3). Leucogabbro and diabase dikes (unit P7) are the youngest intrusive rocks in the southeast Max Lake–Aswapiswanan Lake area.

Gabbro, minor pyroxenite, peridotite and hornblende; quartz diorite to diorite; diabase (unit P5)

The McLeod Narrows and Lavigne Lake intrusions (unit P5) occupy approximately 40% of the western part of the Ralph Anderson Lake belt. These major intrusions are lithologically similar, but their ages of emplacement are uncertain. The McLeod Narrows intrusion, which consists largely of mesocratic gabbro, was initially interpreted to postdate the volcanic rocks and at least one deformational event, because the large supracrustal enclaves within the sill are highly foliated and attenuated, in contrast to the largely massive host gabbro. In this view, the inclusions were deformed and metamorphosed prior to incorporation in the gabbro, and thus the mafic sill was postvolcanic (Gilbert 1999a). Subsequent field and geochemical data, however, indicate that the McLeod Narrows intrusion is probably synvolcanic (Gilbert, 2000). In the revised interpretation, tectonic strain during early regional deformation and metamorphism was confined to incompetent zones (i.e., tabular skialithic enclaves and gabbro margins). The main, nonfoliated core of the intrusion was recrystallized, but retained a massive fabric due to a lack of strain within the central part of the sill. The geochemical similarity between the McLeod Narrows gabbro and contiguous basalt of the central section is consistent with a synvolcanic age of emplacement (*see* ‘Geochemistry’ section).

In contrast to the McLeod Narrows intrusion, the Lavigne Lake sill is relatively more homogeneous and lacks skialithic enclaves of supracrustal rocks. Furthermore, the Lavigne Lake sill is not geochemically comparable with any volcanic rocks in the greenstone belt, and structural data suggest that the sill is postvolcanic and also postdates the first major deformation event in the greenstone belt (D_1).

McLeod Narrows intrusion

The McLeod Narrows sill consists largely of massive, homogeneous, mesocratic gabbro to melagabbro (subunit P5a), with subordinate altered pyroxenite and hornblende (subunit P5b). The intrusion is mesocratic to leucocratic near the north (upper) margin and contains various subordinate intrusive phases. The predominant massive equigranular gabbro phase is locally characterized by enclaves of an older, plagioclase-phyric gabbro; both these phases predate very coarse grained porphyritic gabbro dikes that contain plagioclase and hornblende crystals up to 1.5 cm long. A 35 m wide zone of magnetiferous quartz diorite to diorite (subunit P5d), at the north margin of the sill in the west part of the map area, is interpreted as a hybrid intrusive phase that was contaminated by oxide-facies iron formation. The mafic intrusion contains basaltic enclaves (unit J1; part of the southern stratigraphic section) that are locally recrystallized to massive, coarser grained amphibolite, whereas volcanic fragmental enclaves (unit J3) are strongly foliated and attenuated. Igneous layering (at a scale of 2–25 cm), defined by grain-size and/or compositional variation (e.g., feldspar/hornblende ratio), occurs sporadically in the McLeod Narrows gabbro.

Lavigne Lake intrusion

The Lavigne Lake intrusion consists largely of melanocratic gabbro and subordinate olivine-bearing pyroxenite and hornblende; minor, late gabbroic pegmatite intrusions occur at the north margin of the Lavigne Lake sill. Ultramafic rocks display textures derived from original pyroxene oikocrysts with subhedral olivine inclusions that constitute up to 25% of the rock, but pyroxene is completely altered to tremolitic amphibole. The ultramafic rocks are confined to an approximately 30 m wide zone along the north flank of the sill, and are apparently gradational with contiguous gabbro to the south that is progressively more fractionated, consistent with a southward facing direction (*see* ‘Geochemistry’ section). The opposed facing directions of the intrusion (southward) and hosting supracrustal rocks (northward) are unusual but certainly not unknown (e.g., Bailes, 1980). The most likely explanation is that the supracrustal sequence was deformed prior to emplacement of the mafic-ultramafic sill, and represents the recumbent limb of an early overturned nappe structure (*see* ‘Structural geology’ section). Igneous layering was observed at a few localities, mainly close to the south margin of the Lavigne Lake intrusion.

A lensoid ultramafic sill, up to 150 m thick, extends for over 1 km along the north side of the creek between Franklin Murray and Aswapiswanan lakes (Maps GR2004-2-1, GR2004-2-2, in back pocket). This intrusion consists of olivine-bearing pyroxenite and minor peridotite (subunit P5b) that are geochemically similar to the northern, ultramafic component of the Lavigne Lake

gabbro, along strike to the west. Close to the north margin of the sill, the rock contains original hypersthene (partly altered to blue-grey chlorite), but generally pyroxene is entirely altered to tremolite. The ultramafic rocks are homogeneous and massive, except for minor brecciated zones (up to 1 m by 5 m) characterized by ankeritic alteration. The breccia appears to be the result of brittle fracturing, possibly contemporaneous with emplacement of the intrusion, because the irregular distribution of these zones and their gradation with massive pyroxenite are not consistent with a tectonic origin. Gabbro and hornblende occur directly to the east, on strike with the ultramafic rocks.

Diabase (subunit P5c)

A prominent altered diabase dike (subunit P5c) that extends laterally for at least 4 km intrudes the north margin of the McLeod Narrows gabbro, and locally follows the contact between the gabbro and contiguous central basalt in the area south of Ralph Anderson Lake (Figure 2). The 2–9 m thick dike is largely altered to amphibolite and chloritic schist and is deeply weathered, resulting in a pronounced topographic lineament. The mafic dike displays chilled margins, and is locally deformed and partly disrupted by mesoscopic (F_2) folds and later (F_3) internal crenulations associated with fracture cleavage. The diabase is locally intruded by felsitic veins, and is pervasively carbonatized at the westernmost exposure (180 m south of the south tip of Lavigne Lake; Figure 2).

Granitoid and related gneissic rocks: tonalite, granodiorite, granite; quartz diorite to diorite; minor plagioclase porphyry, pegmatite, aplite; hybrid gneiss (unit P6)

The youngest major intrusions in the southeast Max Lake–Aswapiswanan Lake area consist of granitoid rocks. Gneissoid tonalite to granodiorite and related gneissic rocks (unit P6) in the granitoid terranes flanking the west part of the Ralph Anderson Lake belt are variously biotite±hornblende bearing, white to pale or medium grey, and characterized by diffuse layering on a 0.3–10 m scale. This layering is interpreted to reflect minor compositional variations due to contamination by supracrustal rocks. Subordinate, concordant intrusive components (0.1–2 m thick) include white alaskite, plagioclase porphyry, pink pegmatite and aplite. These intrusions occur both within the granitoid terranes and as dikes in contact zones along the margins of the Ralph Anderson Lake belt. The dikes are mostly gneissoid, but some pegmatite bodies in the granitoid terrane south of the greenstone belt are massive and undeformed.

In the east part of the project area, quartz dioritic to granitic rocks underlie the south and northeast shores of Aswapiswanan Lake, and also occur as minor intrusions within the predominantly mafic volcanic section that extends through the main part of the lake. The granitoid terrane south of the lake appears to be mainly granodioritic to granitic (subunits P6a, P6b), whereas tonalitic to granodioritic compositions (subunit P6c) are prevalent north of the lake. Localized quartz dioritic to dioritic phases (subunit P6d) are attributed to assimilation of mafic volcanic rocks by the granitoid intrusions. Strongly foliated biotite tonalite (subunit P6e), with conspicuous subhedral plagioclase phenocrysts (up to 1 cm, constituting 25% of the rock), extends intermittently along the entire south shore of Aswapiswanan Lake. The porphyritic tonalite occurs both as discrete concordant intrusions (approximately 1–10 m thick) and as a component of layered gneiss (subunit P6f) that contains diverse mafic to felsic lits. The gneissic layering, at a scale of 2–25 cm, is interpreted as a product of the earliest, regional tectonometamorphic event ($D1_1$ – M_1 event); gneissic layers are locally deformed by F_2 folds. The gneissic layering is truncated by granodiorite to granite (subunit P6b), which is itself moderately foliated as a result of a third deformational event (D_3) that resulted in folding and boudinage of related granodiorite veins. In southwestern Aswapiswanan Lake, massive to slightly foliated granite to granodiorite (subunit P6b) is featureless, except for diffuse white to pale pink banding of inferred metasomatic origin; K-feldspar porphyroblasts also occur locally in this unit.

The youngest granitoid phase is massive and undeformed, and consists of granitic rocks (subunit P6a) that occur as minor dikes within earlier granitoid intrusions. The unit includes medium-grained granite, aplite and pegmatite; these lithological types occur both as homogeneous dikes and in irregular zones within heterogeneous granitoid intrusions. Minor mafic schlieren are common within the aplitic granite. Pegmatite is characterized by graphic quartz-feldspar intergrowths up to 25 cm across, randomly oriented biotite blades and sporadic garnet porphyroblasts.

Leucogabbro, diabase (unit P7)

Massive, post-tectonic leucogabbro (unit P7) represents the youngest intrusive unit in the southeast Max Lake–Aswapiswanan Lake area (Gilbert, 1999a). The most conspicuous intrusion consists of an ovoid 25 m by 40 m stock on the north-central shore of Ralph Anderson Lake. A zoned, 8 m thick dike of this unit extends north from the stock and intrudes the adjacent felsic porphyry sill (subunit J4d; Figure 2). The north-northeast-trending dike is characterized by a 4 m wide leucogabbro core, flanked by 2 m wide, plagioclase-phyric diabase zones that grade outwards to aphyric margins. The leucogabbro is medium grained and subophitic, with approximately 25% hornblende and 65% plagioclase; sporadic xenoliths of plagioclase porphyry and medium-grained tonalite occur locally in the dike. Several sparsely porphyritic diabase dikes occur adjacent and parallel to the zoned intrusion. Quartz-feldspar-carbonate veins locally intrude the margin of the mafic dike.

Several minor, north-northeast-trending aphyric diabase dikes (unit P7) occur within gneissoid granodiorite (subunit P6b) at southwestern Aswapiswanan Lake (Map GR2004-2-2, in back pocket). The dikes truncate the foliation of the host rock and contain an internal, northeast-trending foliation that is attributed to local strain during emplacement of the diabase.

Intermediate to mafic volcanic rocks

A prime objective of this project was the collection of geochemical data, in order to establish the stratigraphic relationships and tectonic affinities of the main geological components in the study area. Approximately 130 sites were sampled for the geochemical investigation, from which 90 volcanic and related intrusive rocks were selected for major, trace and rare earth element (REE) analysis. Initial crushing and preparation of rock powder samples was undertaken by the Rock Preparation Laboratory of Manitoba Industry, Economic Development and Mines; subsequent inductively coupled plasma–mass spectrometry (ICP-MS) and inductively coupled plasma–optical emission spectrometry (ICP-OES) analyses were carried out by Activation Laboratories Ltd. (Ancaster, Ontario). The complete geochemical data set is provided in the Appendix.

The geochemical data support the field interpretation that the predominantly north-facing supracrustal sequence in the south-east Max Lake area consists of three lithostratigraphically distinctive sections (southern, central and northern). The latter two components are separated by the elongate Lavigne Lake gabbro sill that extends through the core of the Ralph Anderson Lake belt (Figures 2, 3).

The central volcanic section, which occupies the terrane between the McLeod Narrows and Lavigne Lake gabbroic intrusions, consists entirely of subaqueous basalt and related intrusive rocks that are geochemically akin to modern normal-type mid-ocean ridge basalt (N-MORB), characteristic of ocean-ridge and back-arc basin settings. These rocks are characterized by flat incompatible-element profiles and depletion of REE relative to N-MORB values (Figure 20a). Furthermore, LILE are enriched and Th/Nb ratios are high, resulting in the basalt having a marked negative Nb anomaly in the extended trace-element plot. This Th/Nb pattern, which is more typical of arc-type magmas than MORB, has been variously attributed to contamination of MORB-type source magmas by subducted sedimentary rocks or residual sial in the crust (White and Dupré, 1986; Hawkesworth et al., 1994; Stern et al., 1995a) or, alternatively, to partial mixing of subduction-zone magmas with metasomatized sub-arc mantle wedge (Sinton and Fryer, 1987). In the case of the central section in the Ralph Anderson Lake belt, where the flat REE profile of the basaltic rocks dictates against an arc affiliation (Figure 20a), the origin of the Th/Nb anomaly cannot be determined without additional data, such as ϵ_{Nd} isotope ratios. The depleted Nb and elevated Th and Th/Nb ratios in the central basalt result in these rocks plotting in the field of juvenile-arc basalt in some discriminant diagrams (Figure 21a; Wood, 1980; Figure 22; Stern et al., 1995b). The high Th/Nb ratio of the central basalt relative to modern N-MORB, together with somewhat lower TiO_2 content (Figure 23), are consistent with a back-arc basin environment of eruption for these rocks (Sinton and Fryer, 1987; Saunders and Tarney, 1991; Stern et al., 1995b).

Unlike the central section, the northern section is lithologically heterogeneous and contains subordinate rhyolite and turbidite deposits, in addition to the predominant mafic volcanic flows. Northern basalt is geochemically akin to modern juvenile-arc tholeiite; REE profiles are negatively sloping, with pronounced LILE-HFSE decoupling and a prominent negative Nb anomaly on extended trace-element plots (Figure 20e). The main distinctions between the central and northern basalts are 1) the change from basalt to predominantly basaltic andesite composition, concomitant with tholeiitic to calcalkaline compositional change (Figures 24, 25a, 25b); 2) a decrease in MgO , Ni and Cr ; and 3) marked increases in HFSE (especially Th and Nb) and $(\text{La/Yb})_{\text{ch}}$ (Table 4). The Nb/Y ratio is an effective discriminant between the central and northern basalts, due to strongly depleted Nb in the former suite. Although these differences are consistent with a magmatic evolutionary model (for the north-facing stratigraphic sequence) from N-MORB-type central basalt to more fractionated, arc-type northern basalt, such a genetic connection between these two volcanic suites is merely conjectural because their original contact relationships are obscured by emplacement of the Lavigne Lake gabbro along their contact.

Limited geochemical data from the supracrustal enclaves that constitute the southern section of the greenstone belt (Figure 2) show these rocks to be compositionally similar to the northern, juvenile-arc-type volcanic suite (Table 4). The southern basalt is characterized by negatively sloping REE profiles, with LREE enrichment and conspicuous LILE-HFSE decoupling (Figure 20e, f). The southern and northern volcanic sections are also similar in their lithological diversity: both sections consist of mafic to felsic flows, fragmental deposits and subordinate sedimentary units. The two units do, however, differ in the ratio of flow to fragmental facies (Map GR2004-2-1, in back pocket) and there is no definitive evidence for their stratigraphic equivalence; this topic is discussed further in the ‘Structure’ section.

Gabbroic rocks

Synvolcanic gabbro intrusions of both the equigranular and glomeroporphyritic type within the central stratigraphic section are compositionally very similar to the basalt flows with which they are intercalated. Limited data for the McLeod Narrows intrusion (four rock samples), when plotted on various diagrams that reflect fractionation trends, show that this intrusion is also geochemically similar to the central basalt, and thus may be derived from a common magmatic source (Figures 20–26). The data are consistent with the suggestion that the McLeod Narrows intrusion and central basalt originated from a common, high-Mg tholeiite, MORB-like source, from which the northern volcanic suite was subsequently derived (Figure 25a, b, d).

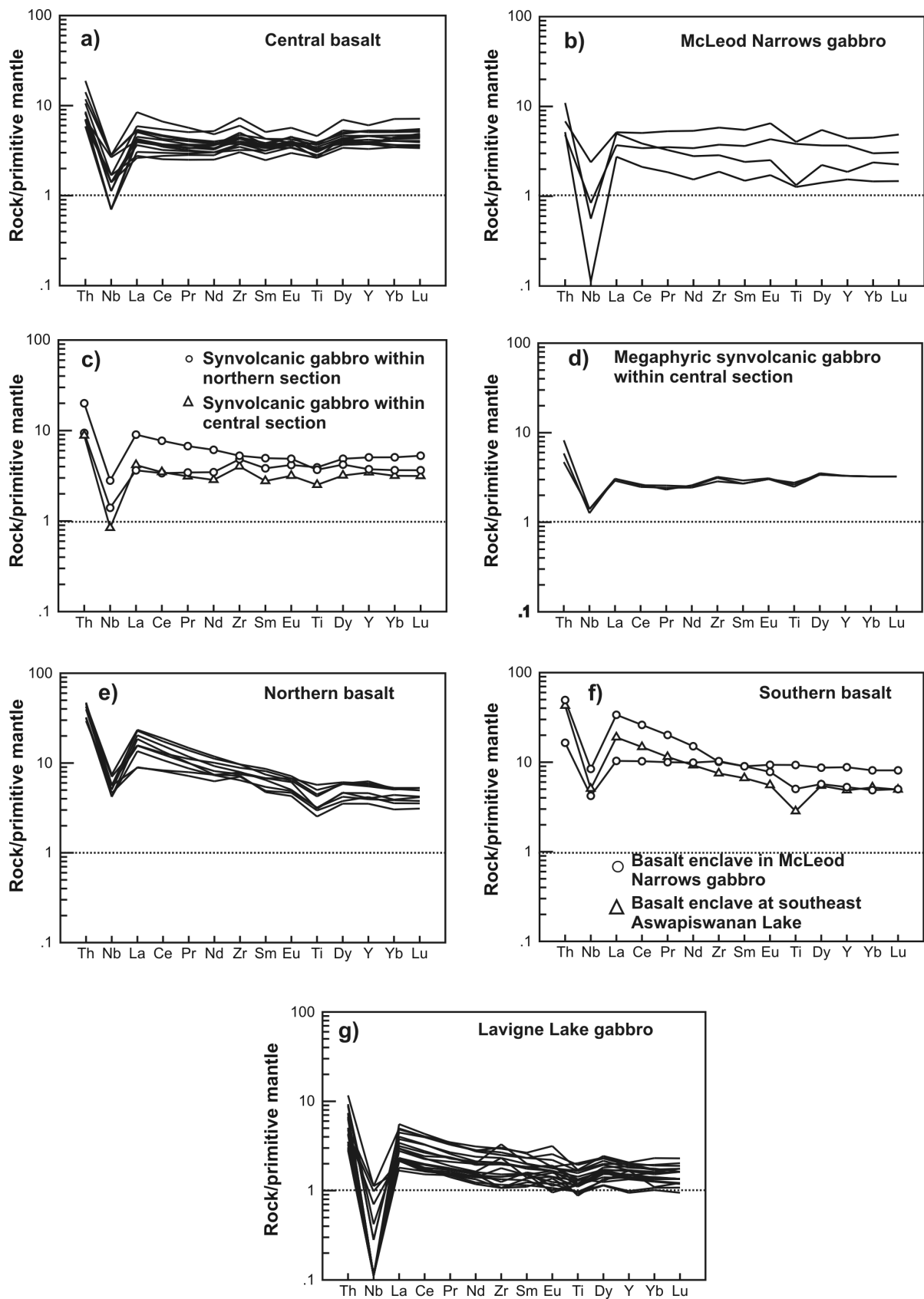


Figure 20: ‘Primitive mantle’–normalized extended–element plots of mafic volcanic and gabbroic rocks in the southeast Max Lake–Aswapiswanan Lake area, showing depleted to light rare earth element (LREE)–enriched, arc–type signatures of basalt and synvolcanic gabbro: **a)** central basalt, **b)** McLeod Narrows gabbro, **c)** synvolcanic gabbro, **d)** megaphyric synvolcanic gabbro, **e)** northern basalt, **f)** southern basalt, and **g)** Lavigne Lake gabbro. Normalizing values from Sun and McDonough (1989).

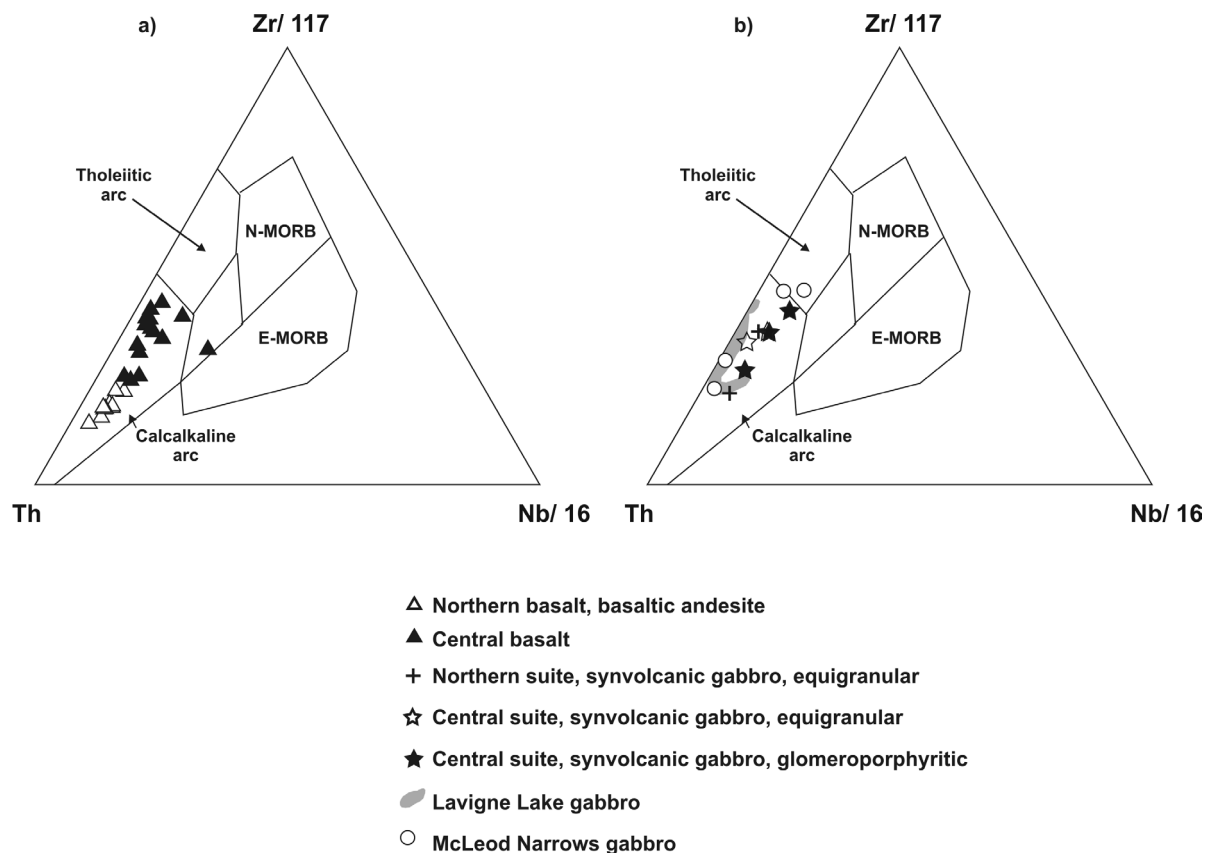


Figure 21: Plots of Th-Zr-Nb, southeast Max Lake–Aswapiswanan Lake area: **a)** mafic volcanic rocks, and **b)** gabbro. Compositional fields of modern volcanic rocks after Wood (1980). Abbreviations: E-MORB, enriched mid-ocean ridge basalt; N-MORB, normal mid-ocean ridge basalt.

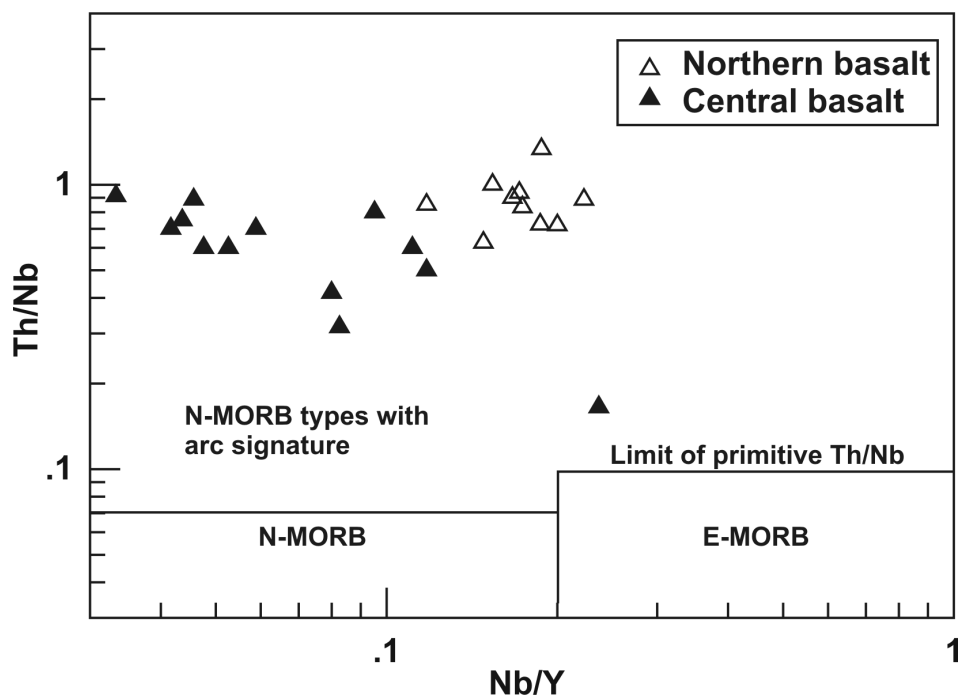


Figure 22: Plot of Th/Nb versus Nb/Y for mafic volcanic rocks in the central and northern sections in the southeast Max Lake–Aswapiswanan Lake area. Normal mid-ocean ridge basalt (N-MORB)–type central basalt is characterized by Th/Nb ratios above the limit of ‘primitive’ values, due to strongly depleted Nb. Compositional fields after Stern et al. (1995b). Abbreviations: E-MORB, enriched mid-ocean ridge basalt; N-MORB, normal mid-ocean ridge basalt.

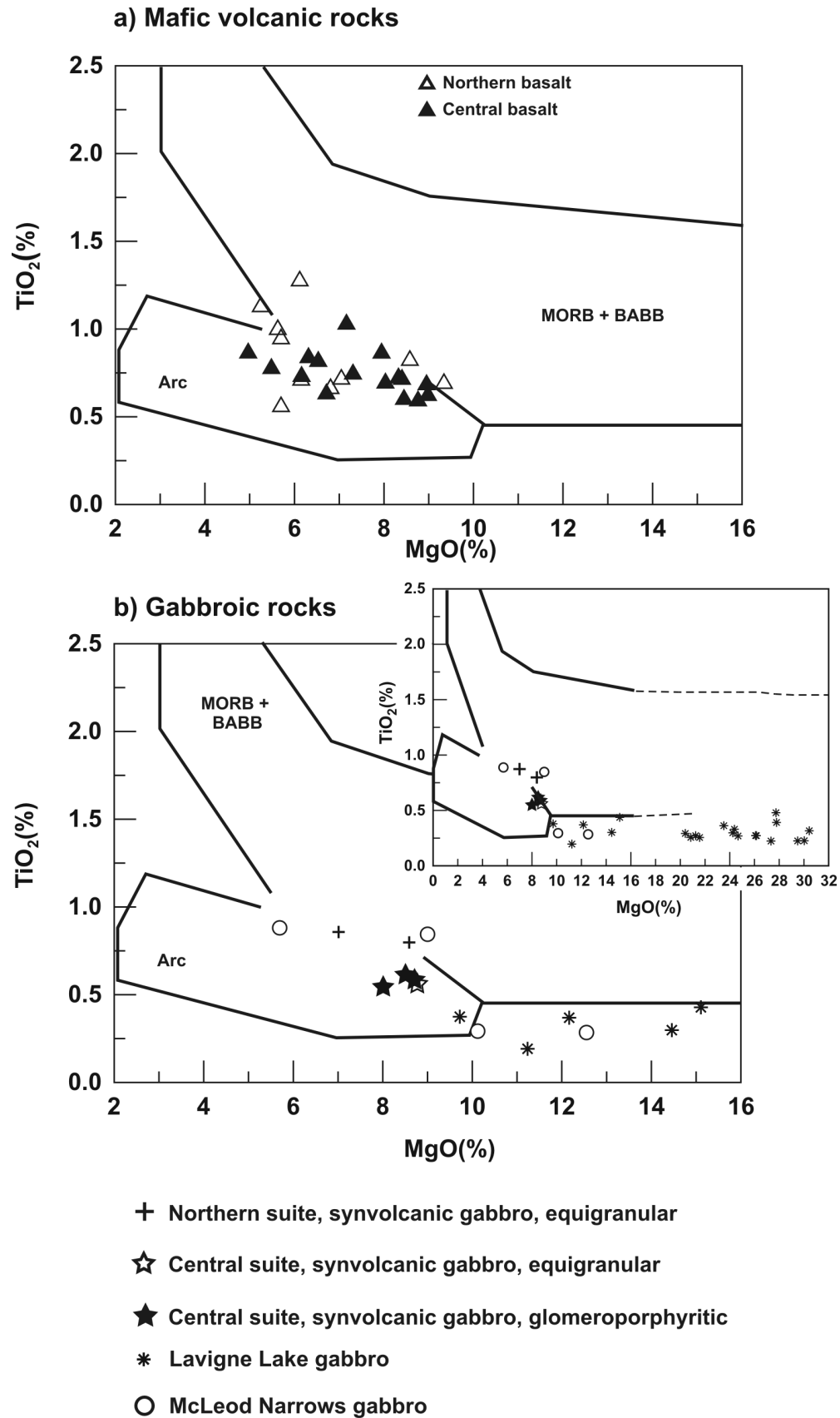


Figure 23: Plots of TiO_2 versus MgO , southeast Max Lake–Aswapiswanan Lake area: **a)** mafic volcanic rocks, and **b)** gabbroic rocks. Compositional fields of modern intraoceanic rocks from Stern et al. (1995b). Abbreviations: MORB, mid-ocean ridge basalt; BABB, back-arc basin basalt.

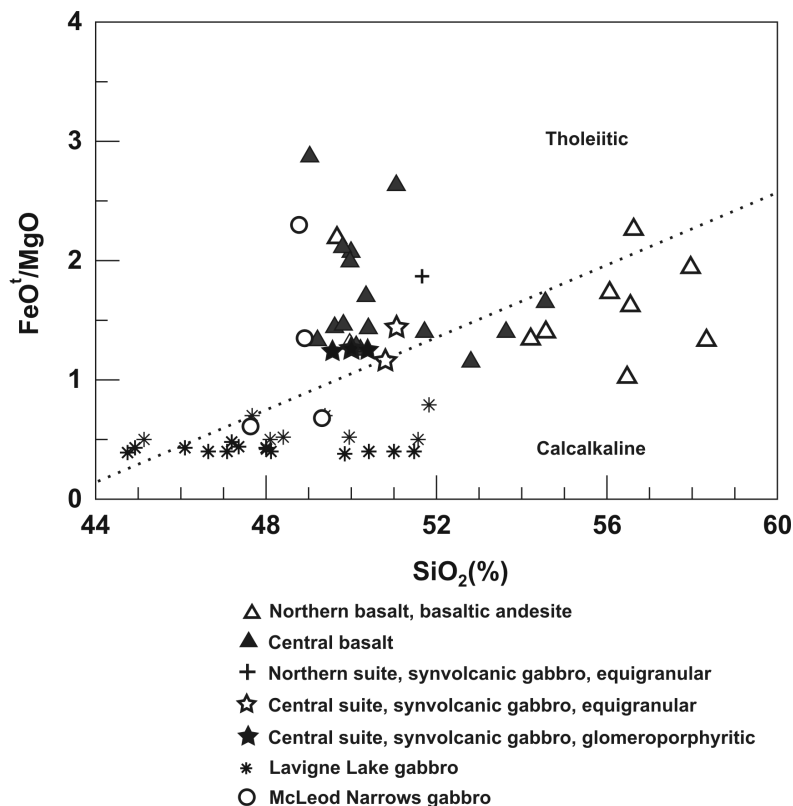


Figure 24: Plots of FeO^t/MgO versus SiO_2 for mafic volcanic and gabbroic rocks in the southeast Max Lake–Aswapiswanan Lake area. $\text{FeO}^t = \text{FeO} + 0.8998\text{Fe}_2\text{O}_3$.

The Lavigne Lake intrusion is geochemically distinctive, with strongly depleted REE and a magmatic trend from the komatiite to high-Mg tholeiite fields on the Jensen cation diagram (Figure 25d). There is virtually no geochemical overlap between the Lavigne Lake intrusion and mafic volcanic rocks of the greenstone belt (Figures 20–26). There is, however, a conspicuous negative Nb anomaly in the REE signature of the mafic-ultramafic intrusion (Figure 20g), in common with all other mafic rock suites in the Ralph Anderson Lake belt. Although the Lavigne Lake intrusion could represent a primitive component of the magmatic system that generated the volcanic rocks, a separate magmatic source appears more likely. This is based on geochemical zonation in the intrusion that indicates the facing direction of the sill is opposite to that of the host volcanic sequence. The opposed facing directions are best explained by inferring a postvolcanic age for the Lavigne Lake gabbro (*see* ‘Structural geology’ section).

Geochemical zonation of the Lavigne Lake gabbro indicates a southward facing direction for the intrusion (Figure 27). The ‘western section’ of the Lavigne Lake sill is located at the west end of MacVicar Lake, whereas the ‘eastern lens’ (believed to be equivalent to the lower part of the Lavigne Lake sill) is the ultramafic intrusion that extends along the creek east of Franklin Murray Lake (Maps GR2004-2-1, GR2004-2-2, in back pocket). Both sections are characterized by gradation from Mg-rich ultramafic rocks at their north margin to more evolved ultramafic or gabbroic rocks to the south. The ‘western section’ grades from ultramafic komatiite in the north, through komatiitic basalt to high-Mg tholeiite in the south (Figure 27a), equivalent to the peridotite-pyroxenite-basalt gradation in Figure 27c. The trend is associated with progressive increases in FeO^t/MgO and overall REE content (Figure 27b). The eastern lens (Figure 27d, e, f) also displays a southward direction of younging, with moderate increases in overall REE content and FeO^t/MgO ; more evolved, gabbroic rock types are absent in the eastern lens. Flat, depleted REE signatures are characteristic of both the western section and the eastern lens; the least depleted rocks are the most southerly in both sections (Figure 28a, b). Furthermore, modal variation in plagioclase composition is consistent with a southward facing direction; hornblende at the north margin of the Lavigne Lake intrusion that contains calcic plagioclase (An_{85}) is apparently gradational with mesocratic gabbro (with plagioclase of An_{52}) in the south part of the sill (C. McGregor, pers. comm., 2001). In summary, the Lavigne Lake intrusion is characterized by systematic geochemical variation attributed to magmatic fractionation within the closed system of the sill. The most Mg-rich ultramafic rocks, which occur at the north margin of the sill, are gradational with more evolved rock types to the south that are assumed to represent the upper part of the intrusive unit.

Intermediate to felsic volcanic rocks and related porphyry intrusions

Intermediate to felsic rocks within the supracrustal sequence in the southeast Max Lake area include massive to fragmental

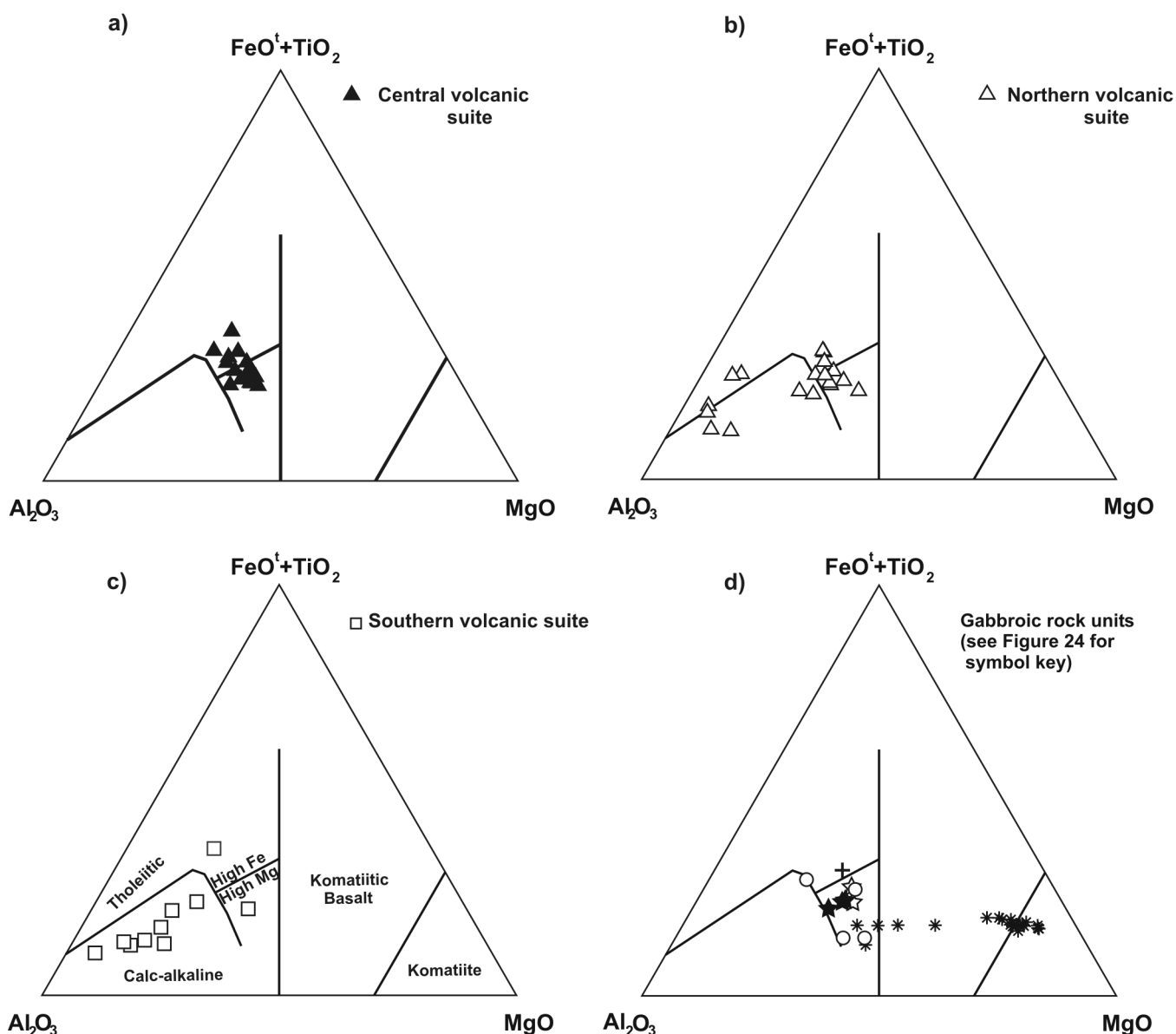


Figure 25: Ternary Al_2O_3 – $(\text{FeO}^t+\text{TiO}_2)$ – MgO diagram for mafic to felsic volcanic rocks and related intrusive rocks in the southeast Max Lake–Aswapiswanan Lake area (Jensen, 1976): **a)** central volcanic suite, **b)** northern volcanic suite, **c)** southern volcanic suite, and **d)** gabbroic rocks. $\text{FeO}^t = \text{FeO} + 0.8998\text{Fe}_2\text{O}_3$.

Table 4: Averages of selected geochemical parameters for mafic volcanic rocks and major gabbroic intrusions in the southeast Max Lake area. Chondrite-normalized La/Yb ratios are based on normalizing values in Sun and McDonough (1989).

	SiO_2 (%)	MgO (%)	Ni (ppm)	Cr (ppm)	TiO_2 (%)	Th (ppm)	Nb (ppm)	Hf (ppm)	Zr (ppm)	Th/Nb	Nb/Y	$(\text{La}/\text{Yb})_{\text{ch}}$
Northern basalt	53.6	6.4	51	88	0.8	3.2	3.7	2.5	87	0.9	0.16	3.7
Central basalt	49.3	7.2	78	250	0.7	0.8	1.3	1.5	49	0.6	0.07	1.0
Southern basalt	51.5	5.8	48	155	1.2	3.1	4.2	2.9	104	0.7	0.16	3.9
Lavigne Lake gabbro	45.5	21.3	570	2614	0.3	0.5	0.2	0.6	21	0.6	0.06	2.0
MacLeod Narrows gabbro	47.5	9.1	153	309	0.6	0.6	0.7	1.3	40	0.8	0.07	1.6

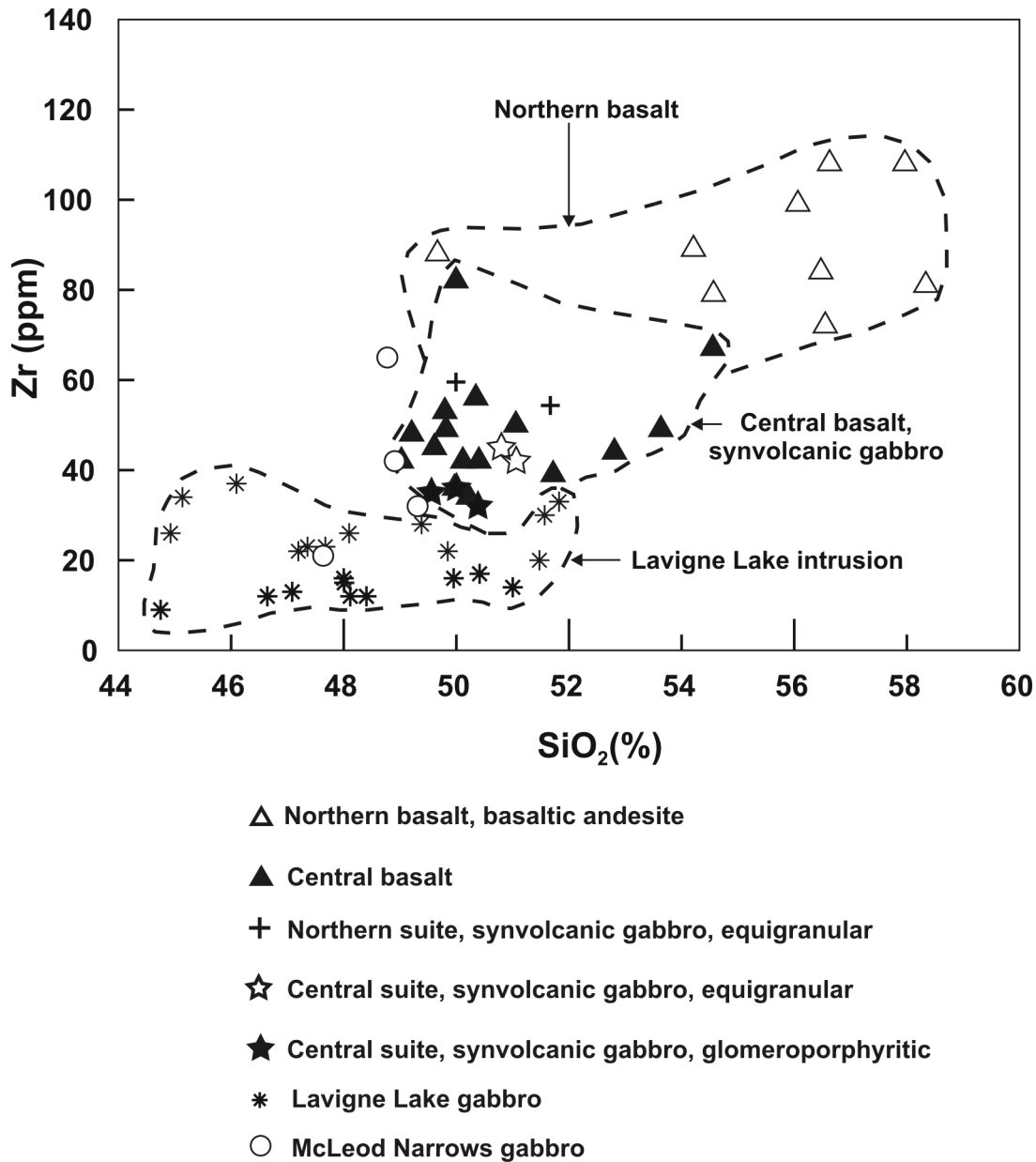


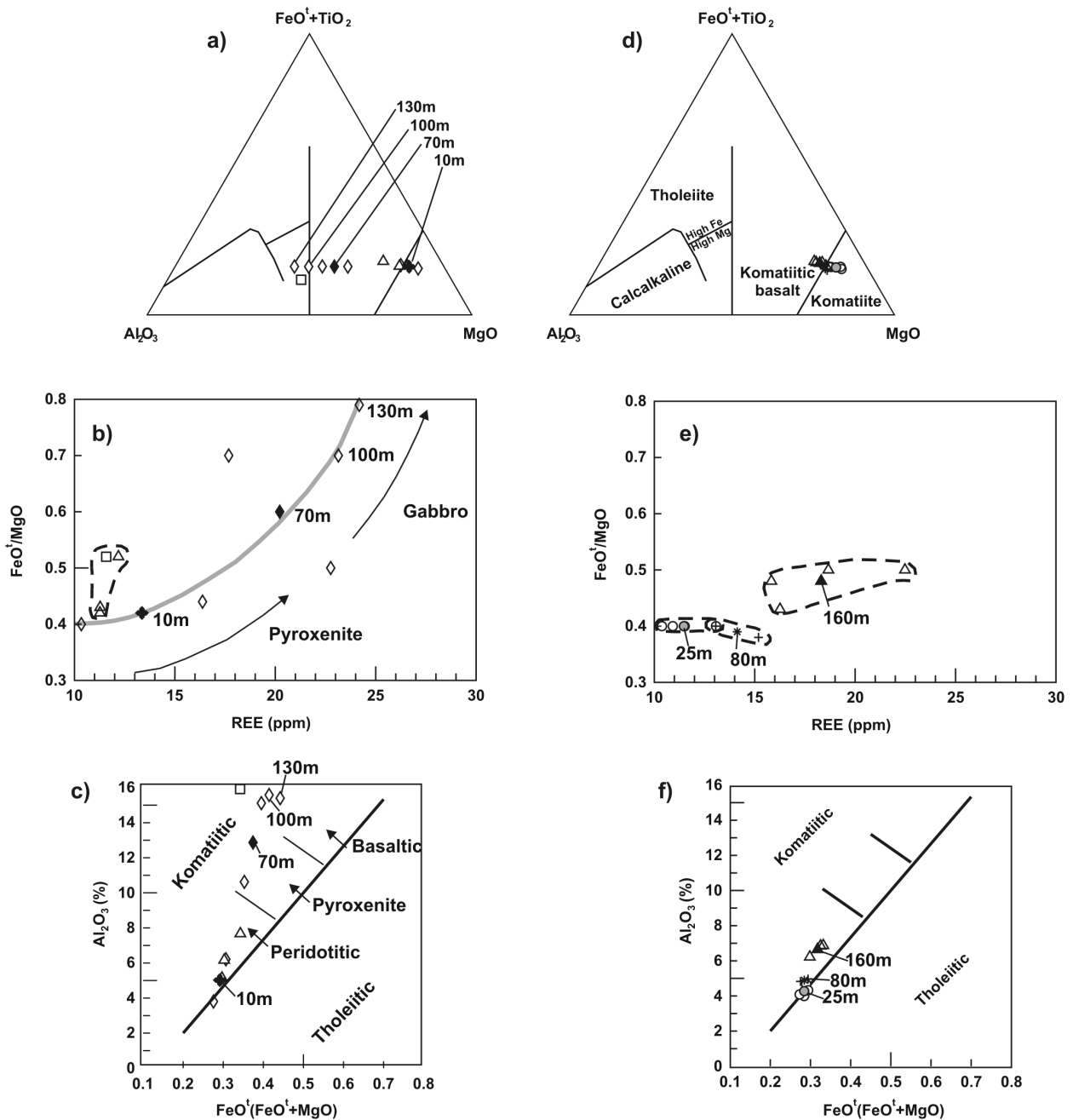
Figure 26: Plot of Zr versus SiO_2 for mafic volcanic and gabbroic rocks in the southeast Max Lake–Aswapiswanan Lake area.

volcanic extrusive types and plagioclase-quartz porphyry intrusions. Analytical data support the field interpretation that most of the felsic porphyry intrusions are compositionally similar and genetically related to the volcanic extrusive rocks. Furthermore, the felsic volcanic and intrusive rocks within the northern section are geochemically very similar to those in the southern section (Figure 2). Whereas felsic volcanic rocks are confined to the arc-type northern and southern stratigraphic sections, several prominent felsic porphyry dikes occur within mafic volcanic flows in the central section, consistent with the interpretation that the felsic dikes are coeval with arc-type volcanic rocks, which are relatively more evolved and younger than the ocean-floor-type central basalt.

Intermediate to felsic volcanic rocks in both the northern and southern sections are classified as calcalkaline in the Jensen cation diagram (Figure 25b, c). Rare earth element geochemical data indicate these rocks are of FI type, according to the classification scheme of Leshner et al. (1986) for Archean felsic volcanic rocks. The FI types display more fractionated REE patterns and have very low potential for base-metal mineralization, compared to the economically more significant FII and FIII types (Leshner et al., 1986). The FI types are characteristic of stratigraphic sequences that are barren of base-metal sulphides, or barren horizons within mineralized sections. In the Ralph Anderson Lake belt, the distinctive geochemical features of the FI-type felsic volcanic rocks include 1) a smooth REE profile that lacks a negative Eu anomaly (Figure 29a, b), 2) a high $(\text{La}/\text{Yb})_N$ ratio (Table 5; Figure 30), 3) high Zr/Y and Sr, and 4) low Zr and Hf.

Lavigne Lake intrusion - western section

Lavigne Lake intrusion - eastern lens



Lavigne Lake intrusion

Western section: \diamond rock sample (metres above base)
 130m
 \blacklozenge average of 2 samples at 10m
 \blacklozenge average of 2 samples at 70m

Other localities: \triangle Lavigne Lake
 \square Aswapiswanan Lake

Lavigne Lake intrusion - eastern lens

Metres above base:

160m \triangle Rock sample
 \blacktriangle Average composition of 4 rock samples

80m $+$ Rock sample
 $*$ Average composition of 2 rock samples

25m \circ Rock sample
 \bullet Average composition of 4 rock samples

Figure 27: Plots of Al_2O_3 –($\text{FeO}^{\text{I}} + \text{TiO}_2$)– MgO (Jensen, 1976), $\text{FeO}^{\text{I}}/\text{MgO}$ versus REE ('REE' is the sum [in ppm] of incompatible elements shown in Figure 20), and Al_2O_3 versus $\text{FeO}^{\text{I}}/(\text{FeO}^{\text{I}} + \text{MgO})$ (Arndt et al., 1977) for various localities throughout the Lavigne Lake intrusion: **a), b) and c)** pyroxenite and gabbro in the western section and at other localities (Lavigne Lake, Aswapiswanan Lake); **d), e) and f)** olivine-bearing pyroxenite and peridotite in the eastern lens. $\text{FeO}^{\text{I}} = \text{FeO} + 0.8998\text{Fe}_2\text{O}_3$.

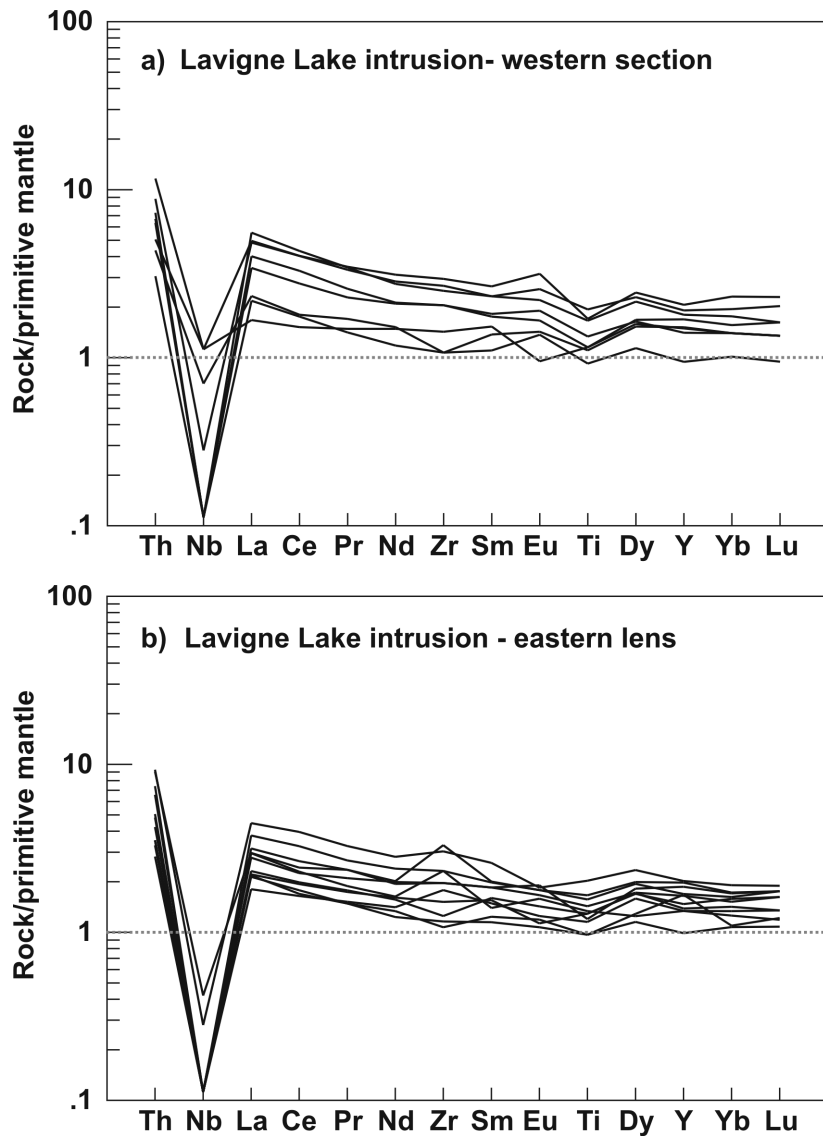


Figure 28: ‘Primitive mantle’–normalized extended-element plots for the Lavigne Lake intrusion: **a)** pyroxenite and gabbro in the western section, and **b)** olivine-bearing pyroxenite and peridotite in the eastern lens. Normalizing values from Sun and McDonough (1989).

A minority of felsic volcanic rocks in the study area is REE enriched. These rocks, identified as FI type by high $(La/Yb)_N$ ratios (Table 5; Figures 29c, 30), are distinguished from the predominant FI-type rocks by negative Eu anomalies (Figure 29c, a) and anomalously high Th contents (‘high-Th felsic rock’ in Table 5). The REE-enriched rocks are also characterized by higher SiO_2 , Zr/TiO_2 , Zr and Hf, and lower Sr, compared to the other FI-type felsic rocks in the belt (Figure 31). In these respects, the REE-enriched rocks are similar to FII-type rocks in the Wabigoon and Abitibi belts (Leshner et al., 1986). Archean FII-type felsic volcanic rocks are occasionally associated with base-metal mineralization (Leshner et al., 1986); thus, the REE-enriched felsic rocks in the Ralph Anderson Lake belt, which exhibit some FII features, may be considered to have limited economic potential. Furthermore, some of the REE-enriched felsic rocks are akin to extension-related rhyolite units that are locally implicated in the development of VMS deposits (e.g., in the Proterozoic Flin Flon belt; Syme, 1998). In contrast, FI-type (not enriched) rocks in the Ralph Anderson Lake belt are compositionally similar to Flin Flon arc-assemblage rhyolite units that are devoid of ore deposits.

In summary, most felsic volcanic rocks and the majority of felsic porphyry intrusions in the southeast Max Lake area are similar to Archean FI-type rocks, which have been interpreted as partial melts of deep-seated magmas that underwent little or no modification during their ascent through the crust. These rocks have low economic potential, whereas several distinctive felsic porphyry dikes (and possibly some volcanic extrusive rocks) in the southeast Max Lake area may be more prospective because they are, in part, akin to FII-type Archean volcanic rocks associated with massive, base-metal sulphide deposits (Leshner et al., 1986). The geochemical signatures of some FII Archean rocks reflect magma modification in high-level magma chambers, which in turn are associated with ore-forming hydrothermal systems (Leshner et al., 1986).

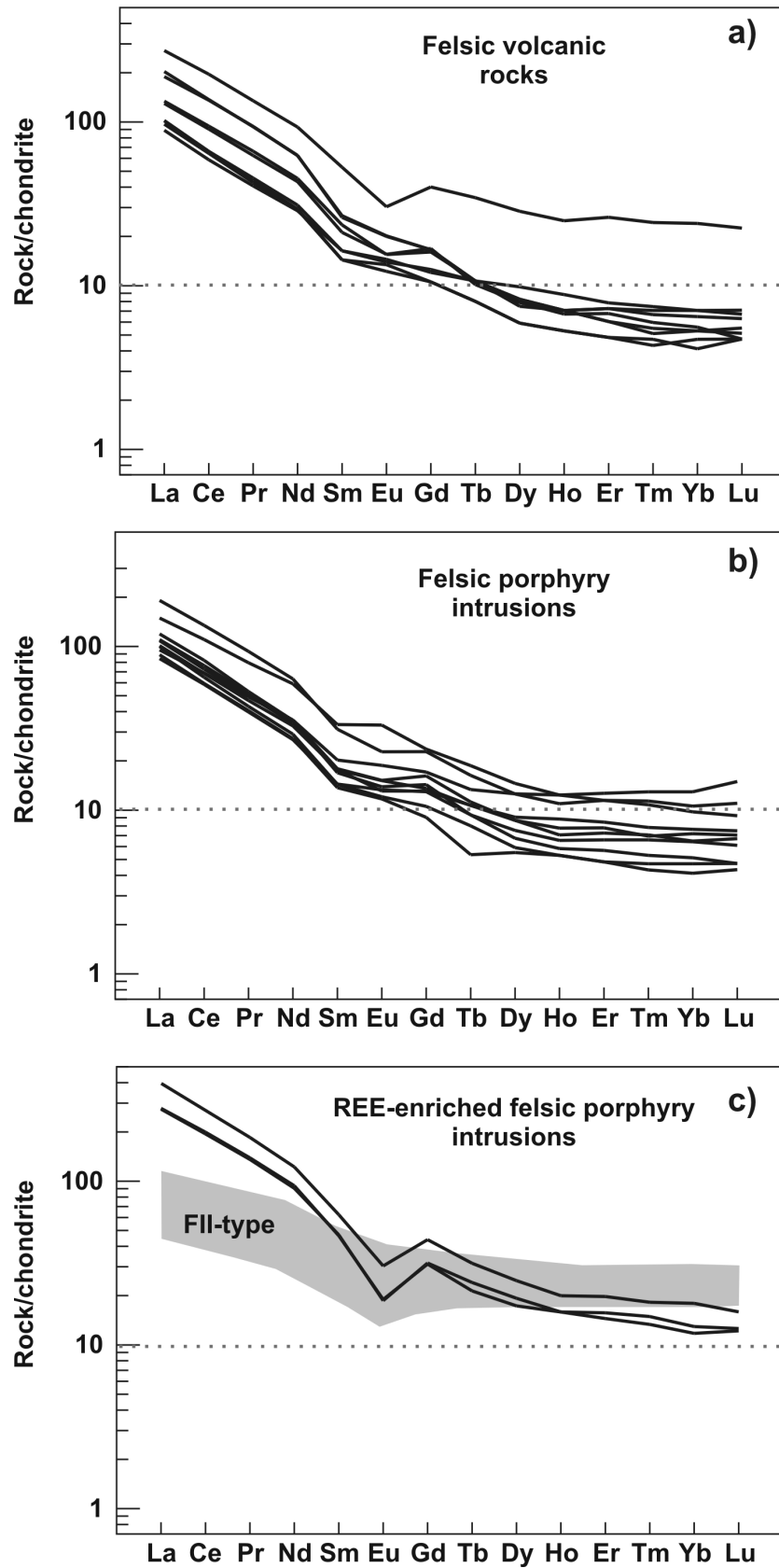


Figure 29: Chondrite-normalized rare earth element plots, southeast Max Lake area: **a)** felsic volcanic rocks, **b)** plagioclase-quartz porphyry intrusions, and **c)** REE-enriched plagioclase-quartz porphyry intrusions. Shaded field shows the range of FII-type Archean rocks in the Abitibi and Wabigoon belts (after Lesher et al., 1986). Chondrite-normalizing values from Sun and Donough (1989).

Table 5: Averages of selected geochemical parameters for felsic volcanic and related intrusive rocks, southeast Max Lake area.

Area	Rock unit	Type	SiO ₂ (%)	(La/Yb)/ 1.394	Zr/Y	Zr (ppm)	Hf (ppm)	Sr (ppm)	Th (ppm)
Southeast Max Lake	Felsic volcanic, massive to fragmental	FI	65.1	23.8	12.3	136	3.4	339	10.8
	Felsic plagioclase-quartz porphyry	FI	64.4	16.5	10.9	150	3.8	250	9.0
	High-Th felsic rock	Enriched FI	72.1	18.1	9.0	225	6.9	140	33.9
Abitibi Belt (data after Leshner et al., 1986)	Felsic tuff, Blake River Group	FI	66.7	6.3	9.2	110	2.7	257	0.6
	Felsic lava, Misema Subgroup.	FII	68.4	2.8	7.0	265	6.9	109	4.3
	Felsic lava, Rouyn-Noranda area	FIIIa	71.3	2.3	5.2	362	8.6	61	7.3

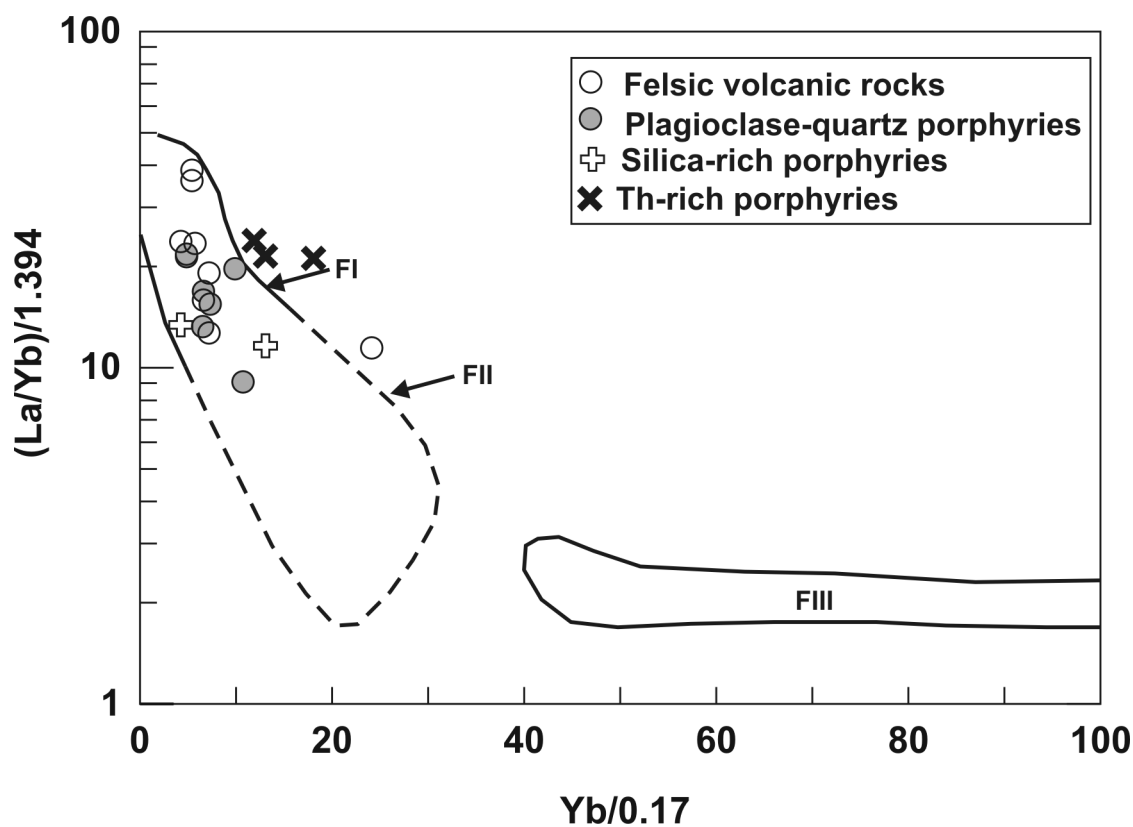


Figure 30: $(La/Yb)_N$ versus Yb_N plot of felsic volcanic rocks and related plagioclase-quartz porphyry intrusions in the southeast Max Lake area. Fields of Archean felsic volcanic rock types are after Leshner et al. (1986). Chondrite-normalizing values from Sun and McDonough (1989).

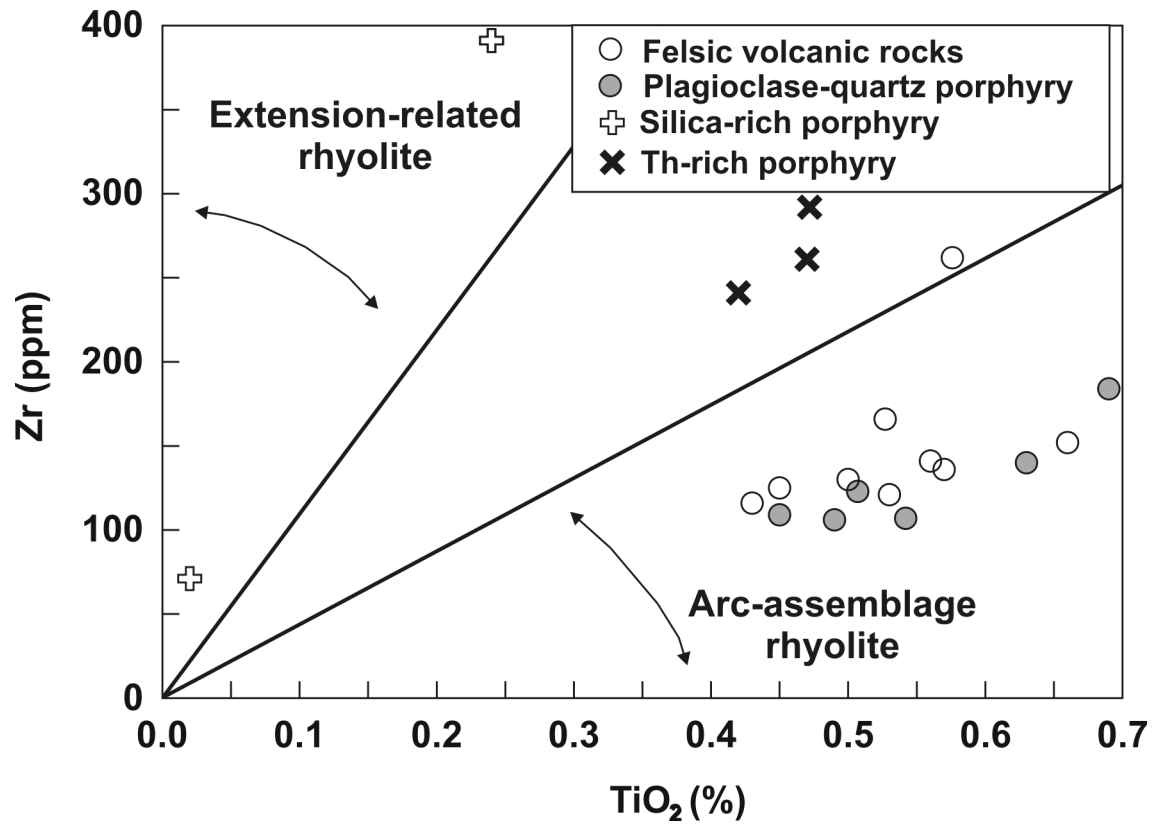


Figure 31: Plot of Zr versus TiO₂ for felsic volcanic rocks and related plagioclase-quartz porphyry intrusions in the southeast Max Lake area. REE-enriched felsic rocks (outside the 'arc assemblage' field) are more fractionated than the rest, with higher Zr/TiO₂ and Th, and negative Eu anomalies. Arc-assemblage and extension-related rhyolite fields for the Proterozoic Flin Flon Belt after Syme (1998).

Metamorphism

Sedimentary and altered volcanic rocks in the southeast Max Lake area contain a variety of porphyroblastic minerals and textural features that document two amphibolite-facies metamorphic events, followed by greenschist-facies retrogressive metamorphism (Table 6). The M_1 metamorphism is associated with regional biotite and/or hornblende foliation (S_1), and syn- to postkinematic porphyroblasts of cordierite, garnet and staurolite. These minerals are distinct from later porphyroblasts (M_2 biotite, amphibole; M_3 chlorite) that overprint the earlier fabric. At the north margin of the McLeod Narrows gabbro, M_2 anthophyllite porphyroblasts overprint the mylonitic fabric at the tectonized basalt-gabbro contact, indicating that peak M_2 metamorphism postdated the faulting at that locality. Retrogressive, greenschist-facies M_3 metamorphism is recognizable throughout the greenstone belt, but is pervasive only in localized sheared and/or metasomatized zones.

M_1 metamorphism

The M_1 metamorphism locally produced the assemblage cordierite-biotite-quartz-plagioclase in altered felsic volcanic and fine-grained sedimentary rocks. These cordierite-bearing units occur within both the northern and southern stratigraphic sections in the Ralph Anderson Lake belt. Cordierite occurs as ovoid, syn- to postkinematic porphyroblasts up to 1.5 cm long, commonly in elongate, lensoid aggregates up to 10 cm by 3 cm (Figure 32). Cordierite formation is generally late- to postkinematic, with porphyroblasts containing an internal foliation (S_{int}) parallel to S_1 (S_{ext}). Synkinematic cordierite, which is less common, contains an internal biotite foliation (S_{int}) that is locally deformed and discordant to the external biotite fabric (S_{ext}). Cordierite blasts are elongate parallel to F_1 minor fold axes in the northern sedimentary formation (Figure 12). Strongly foliated siltstone at the north margin of the southern section contains highly elongate, synkinematic cordierite poikiloblasts parallel to S_1 .

Syn- to late-kinematic M_1 garnet is abundant in the MacVicar Lake alteration zone, and occurs elsewhere in both the northern and southern stratigraphic sections, notably within and at the margins of the northern sedimentary formation. In the alteration zone, the assemblage is garnet-quartz±plagioclase±biotite±staurolite±amphibole±K-feldspar±magnetite±pyrite. Synkinematic garnets contain an internal rotational fabric (S_{int}) defined by quartz and/or opaque minerals (Figure 33); garnets are also commonly rotated and, in some cases, display rolled, ‘snowball’ texture. Elsewhere, slightly younger garnets overprint the mildly deformed bedding lamination (S_0).

M_2 metamorphism

The M_2 amphibolite-facies metamorphism is defined by randomly oriented, postkinematic porphyroblasts (biotite, amphibole and rare plagioclase) that overprint the earlier S_1 foliation; the foliation is also, in part, recrystallized by M_2 . The diagnostic assemblage is biotite-quartz-plagioclase±anthophyllite±cummingtonite. The M_2 biotite occurs as randomly oriented to subparallel

Table 6: Summary of the structural and metamorphic histories of the southeast Max Lake–Aswapiswanan Lake area.

Event	Deformation	Metamorphism
D ₁	Major F_1 nappe structure due to convergent crustal movement ('MacVicar Lake syncline'; hinge line is located close to the north margin of the greenstone belt, roughly coincident with the MacVicar Lake alteration zone). Axes of associated minor folds plunge 125°/60°. Core of nappe may have been removed by tectonic transport on thrusts during the collisional tectonism. Fault and associated mylonite at south margin of central volcanic section probably initiated as a thrust at this time.	Intermediate-grade metamorphism. Regional S_1 foliation and tectonic lamination. Alteration of pyroxene to amphibole in mafic volcanic and intrusive rocks. Syn- to postkinematic garnet, cordierite (locally lineated) and rare staurolite in sedimentary and altered volcanic rocks.
D ₂	Continued convergent tectonic movement, possibly contemporaneous with granitoid plutonism at belt margins. Rotation and steepening of earlier D ₁ structures, resulting in overturned NNE-facing monocline. Minor SE-plunging folds (average 123°/55°) are mainly asymmetric S-shaped. Folding, disruption and boudinage of S_1 foliation at the belt margins and locally within the greenstone belt (e.g., at MacVicar Lake alteration zone).	Intermediate-grade metamorphism. Rotation and crenulation of M_1 porphyroblasts. Postkinematic biotite and amphibole blasts (anthophyllite±cummingtonite; green hornblende). Regional S_1 foliation is locally recrystallized.
D ₃	Shearing and folding in narrow (0.5–5 m) conformable high-strain zones. Strain-slip cleavage and sporadic, narrow tectonic breccia layers in volcanic, sedimentary and gabbroic rocks.	Greenschist-facies metamorphism. Alteration of M_1 , M_2 porphyroblasts (cordierite to pinite; anthophyllite to tremolite±chlorite). Localized alteration and metasomatism
D ₄	NNE- to NE-trending, subvertical faults (estimated displacement up to 100 m).	throughout the greenstone belt: chloritization, silicification, carbonatization and epidotization.

porphyroblasts that overprint the first generation foliation within cordierite (S_{int}). Postkinematic anthophyllite occurs as subhedral prisms, needles and radiating aggregates (Figure 34) that locally appear to be later than M_2 biotite (Figure 35), but these two minerals are interpreted as penecontemporaneous products of the same M_2 metamorphic event. Cummingtonite is very similar to anthophyllite in texture, and the occurrence of one or the other amphibole is probably determined by the host rock composition; a few units contain both cummingtonite and anthophyllite. The M_2 event also produced green hornblende, both in intermediate to mafic volcanic rocks and in metasomatically altered felsic volcanic rocks.

Porphyroblastic minerals that may be either M_1 or M_2 in age include andalusite and muscovite. The assemblage andalusite-quartz-plagioclase-biotite occurs in a felsic porphyry dike close the southeast shore of MacVicar Lake. Elongate, poikiloblastic andalusite xenoblasts are aligned parallel to the biotite foliation, and are partly altered to sericite and muscovite. Muscovite poikiloblasts occur locally in siltstone and felsic porphyry intrusions.

M_3 metamorphism

The M_3 retrogressive, greenschist-facies metamorphism is characterized by randomly oriented chlorite blades that overprint both the regional foliation and earlier porphyroblasts. The M_3 event is also characterized by widespread chloritic, sericitic and saussuritic alteration of the earlier mineral assemblages, and localized carbonatization in shear zones. Cordierite is commonly completely altered to pinitite by M_3 metamorphism (Figure 36); anthophyllite is variously altered to tremolite (\pm chlorite). Sporadic clinozoisite and stilpnomelane are also attributed to M_3 retrogression. Whereas M_3 alteration of the earlier M_1 and M_2 minerals is commonly only partial, the retrogressive metamorphism is pervasive within discrete zones of contemporaneous (D_3) shearing (e.g., alteration of basalt to chloritic schist). Ultramafic rocks (unit P5b) consist largely of tremolitic amphibole of probable M_3 age, derived from original pyroxene+olivine-bearing assemblages.



Figure 32: Ovoid aggregates of pinitized cordierite porphyroblasts are coplanar with S_1 and deformed by an F_2 minor fold. The host rock, of felsic volcanic origin, is located 1.5 km south of the west end of Ralph Anderson Lake.

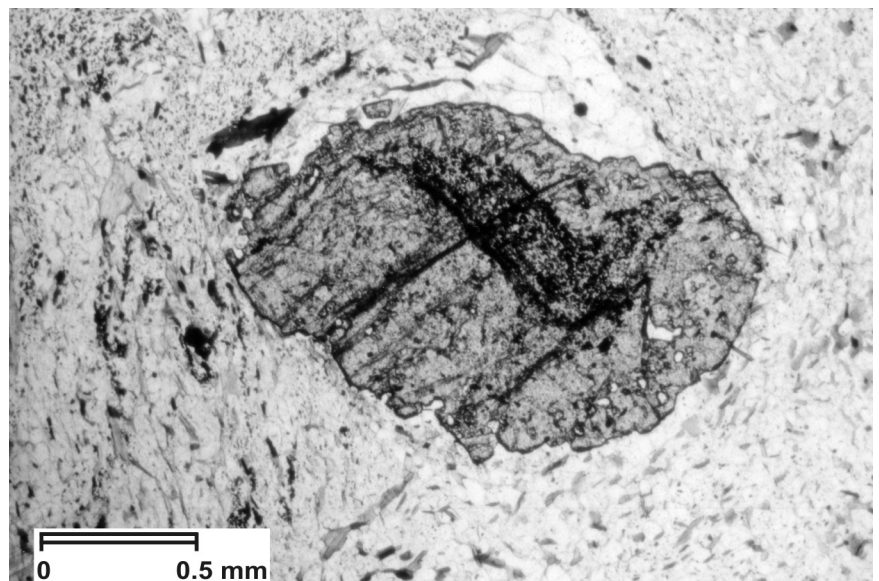


Figure 33: Photomicrograph of a rotational M_1 garnet porphyroblast in magnetite-bearing paragneiss, in the alteration zone (subunit 2c) in the east part of MacVicar Lake. Sample 2125-2, plane polarized light.

Figure 34: Photomicrograph of fascicular M_2 anthophyllite porphyroblasts, overprinting the S_1 micaceous foliation in pebble conglomerate (subunit 4c), located within the southern stratigraphic section, 1.5 km south of the west end of Ralph Anderson Lake. Sample 2197-6, crossed polarizers.

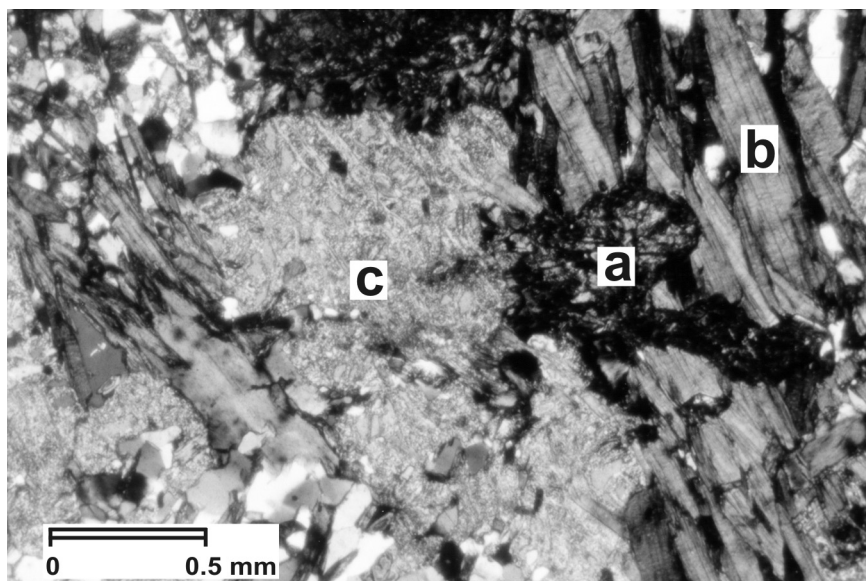
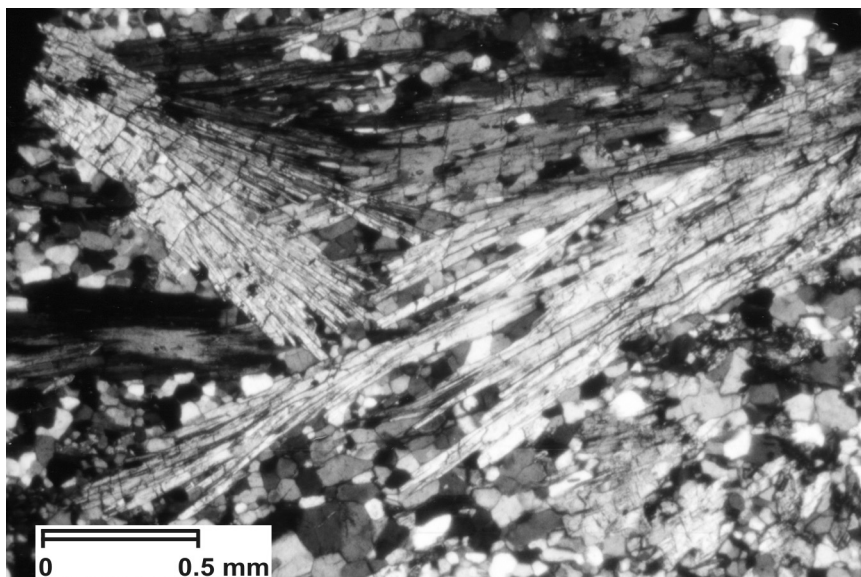
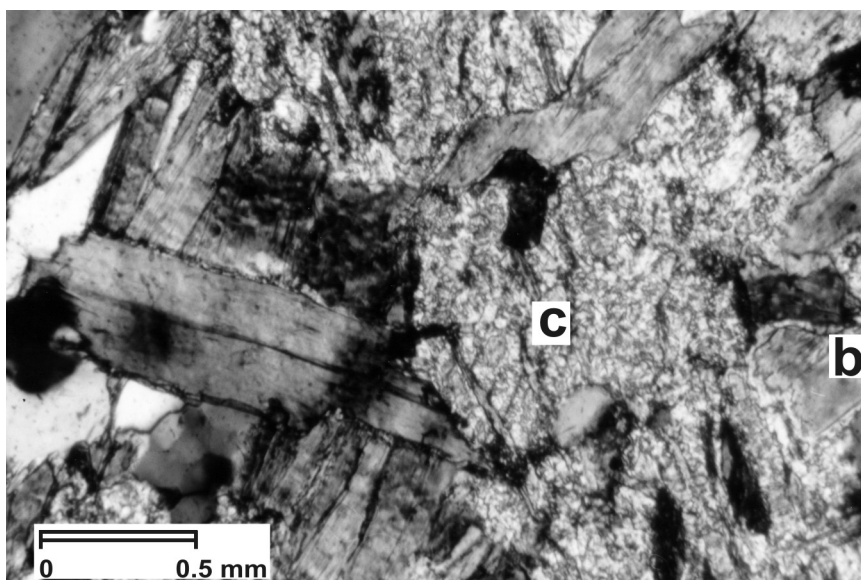


Figure 35: Photomicrograph of a pinitized M_1 cordierite porphyroblast with later M_2 biotite and anthophyllite in siltstone (subunit 4c), located within the southern stratigraphic section, 1.5 km south of the west end of Ralph Anderson Lake. Abbreviations: a, anthophyllite; b, biotite; c, cordierite. Sample 2197-4, crossed polarizers.

Figure 36: Photomicrograph of randomly oriented M_2 biotite within an altered M_1 cordierite porphyroblast in siltstone (subunit 4c), located within the southern stratigraphic section, 1.5 km south of the west end of Ralph Anderson Lake; M_3 pinitization of cordierite postdates the biotite porphyroblasts. Abbreviations: b, biotite; c, cordierite. Station 2197, crossed polarizers.



Structural geology

Structural fabrics are well preserved in the west part of the greenstone belt, south of MacVicar and Ralph Anderson lakes. The mafic volcanic sequence in that area (central stratigraphic section) is overturned and dips steeply to the south; abundant pillow tops and sporadic flow contacts consistently face north to north-northeast. Northward tops are also indicated by graded turbidite deposits within the southern section (Figure 2). Structural indicators are somewhat less abundant in the MacVicar Lake area and north of Ralph Anderson Lake (northern section), but top directions are again consistently north to north-northeast, except near the margin of the belt, where a synclinal fold ('MacVicar Lake syncline') is located north of the west lobe of MacVicar Lake (Figure 4). At that locality, a south-facing turbidite unit with local graded bedding occurs within the northernmost panel of mafic volcanic rocks; the hinge line of the fold is approximately coincident with the MacVicar Lake alteration zone. The fold cannot be traced east of MacVicar Lake as a result of poor exposure and a lack of primary structural features due to strong tectonic attenuation along the north flank of the belt. The MacVicar Lake syncline is interpreted as a product of the first event (D_1) in a multiphase history of deformation (Table 6).

D_1 deformation

The MacVicar Lake syncline is a major F_1 fold, the hinge line of which extends east-west, parallel and close to the north margin of the Ralph Anderson Lake greenstone belt (Figure 4). Typically, the north limb of this fold, which constitutes the northernmost stratigraphic panel of the belt, is tectonically attenuated and much narrower than the southern limb. The northern limb may also be relatively diminished due to assimilation by the granitoid rocks that intrude the north margin of the greenstone belt. Data are insufficient to clearly define the attitude of the F_1 major structure because minor F_1 folds are rare. Several early folds are recognized where bedding in sedimentary units is deformed (Figure 37); for example, a 1.2 m thick turbidite layer within basalt close to the north margin of the greenstone belt displays southeast-plunging F_1 folds (fold plunge 60° ; interlimb angle 60 – 120°). Elsewhere, F_1 minor folds are tight to isoclinal (Figure 38). The F_1 event is assumed to be contemporaneous with M_1 intermediate-grade metamorphism (cordierite±garnet±staurolite) and regional S_1 foliation; lineated M_1 cordierite plunges moderately east ($101^\circ/36^\circ$) at central MacVicar Lake (Figure 12; Table 6).

There is some evidence, based on the southward facing direction of the Lavigne Lake gabbro (*see* 'Geochemistry' section), that the MacVicar Lake syncline represents the core of a major nappe structure, of which the south limb was recumbent. Evidence in support of a major F_1 nappe is provided by geochemical data that indicate the Lavigne Lake gabbro is a south-facing intrusion within regionally north-facing supracrustal rocks. Such an occurrence may be explained if the supracrustal sequence was deformed prior to emplacement of the mafic-ultramafic sill. In this interpretation, the main part of the Ralph Anderson Lake greenstone belt, comprising the central section and most of the northern section (Figure 2), constitutes the recumbent limb of a regional F_1 nappe structure (Figure 39). The other component of the fold consists of the highly attenuated, northernmost panel of the greenstone belt (north of the MacVicar Lake synclinal axis). The structurally overlying southern section, represented by north-facing skialithic enclaves within the McLeod Narrows gabbro, is interpreted as the recumbent limb of the nappe that was juxtaposed by major thrust faults against the central volcanic section. In this model, one segment of the series of nappes was tectonically removed by thrust faults that are now represented by the mylonitized fault zone between the McLeod Narrows gabbro and the central volcanic section (Figures 2, 4, 39).



Figure 37: Minor F_1 fold in bedded turbidite, north of the west part of MacVicar Lake.

Figure 38: Minor F_1 fold in oxide-facies iron formation, close to the north margin of the southern stratigraphic section, 1 km south-southeast of the southeast end of MacVicar Lake.

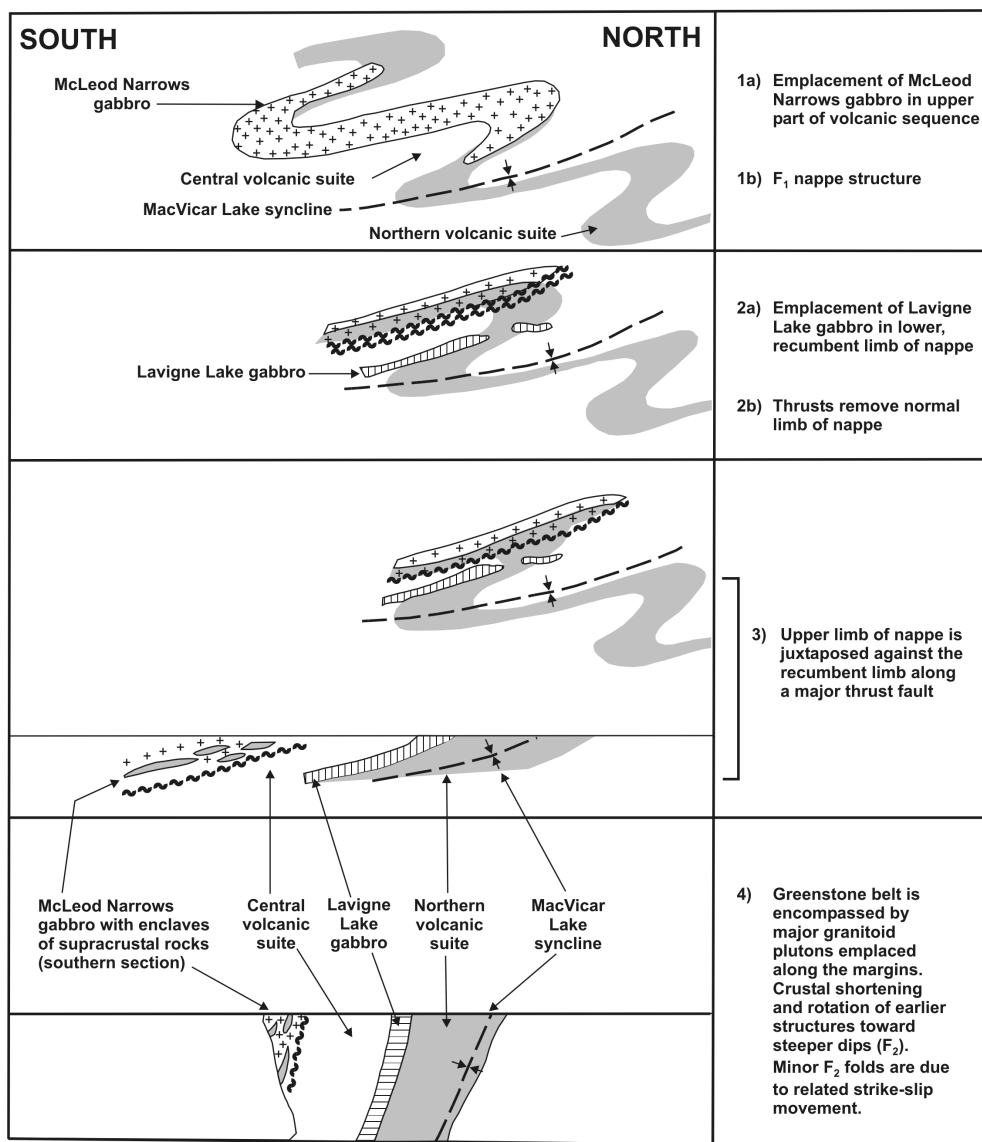
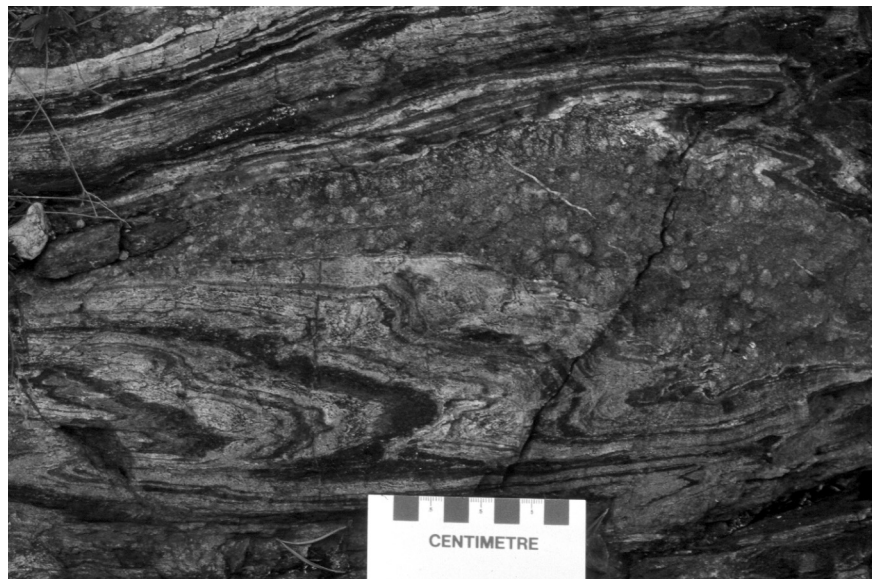


Figure 39: Sequential north-south transverse sections showing the proposed structural model for the evolution of the Ralph Anderson Lake greenstone belt. Early horizontal tectonics resulted in F_1 nappe structures and low-angle thrusts; further collisional movement resulted in crustal shortening and steepening of earlier F_1 structures.

Faulting and mylonitization at the contact between the southern and central sections (or, locally, between the McLeod Narrows gabbro and the central basalt; Figure 2) are interpreted as early (D_1) features because the sheared fabric is overprinted by M_2 porphyroblasts (*see* 'Metamorphism' section). This fault, initiated as an early thrust plane during nappe development (Figure 39, part 2b), has been traced laterally for 7 km in the west part of the map area and is inferred to extend along the south flank of the greenstone belt further to the east. The fault was subsequently rotated and steepened, together with the stratigraphic units, during D_2 crustal shortening (Figure 39).

D_2 deformation

The regional S_1 foliation and related tectonic lamination are deformed by southeast-plunging minor F_2 folds (approximately parallel to F_1 minor fold axes) with steeply dipping to vertical axial planes (Figure 40). The F_2 minor folds are interpreted as part of a regional deformation event that produced the monoclinical configuration of the present-day greenstone belt. The D_2 deformation is inferred to have been associated with compression and crustal shortening, possibly coincident with the emplacement of major granitoid intrusions along the north and south flanks of the greenstone belt. The emplacement of the intrusions resulted in oversteepening of earlier D_1 structures. The D_2 deformation is interpreted as a rotation of earlier structures, rather than large-scale folding, because major F_2 folds are absent. Minor F_2 folds, caused by stress during the inferred rotational movement, are predominantly asymmetric S-shaped, reflecting sinistral strike-slip movement; subordinate F_2 Z-folds reflect dextral movement (Figure 41). At one locality close to the north margin of the belt, interference patterns due to refolding of F_1 folds occur in well-bedded metasedimentary strata (Figure 42). The F_2 folds are most abundant along the north flank of the greenstone belt, where the early (S_1) tectonic lamination is commonly boudinaged due to strong attenuation (Figure 43). The D_2 folding and disruption of gneissic laminae are especially conspicuous in garnetiferous rocks within the MacVicar Lake alteration zone (Figure 16).

D_3 deformation

The D_3 deformation consists of localized shearing and folding (with associated S_3 strain-slip cleavage) along incompetent horizons such as the contacts of mafic volcanic flows, early alteration zones or thin sedimentary rock units. Elsewhere, D_3 deformation was more brittle and resulted in thin (0.2–0.5 m) conformable tectonic breccia units, associated with retrogressive M_3 metamorphism (chloritization, silicification, carbonatization and saussuritization).

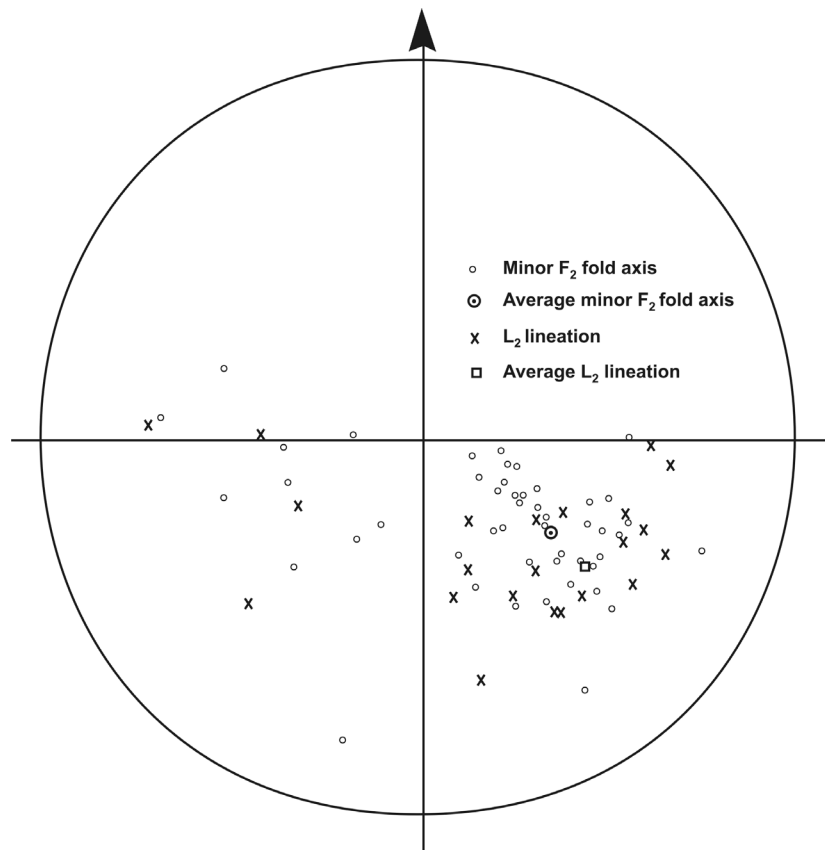


Figure 40: Lower-hemisphere stereographic projection of F_2 minor fold axes and b lineations (mineral stretching and elongation lineations).

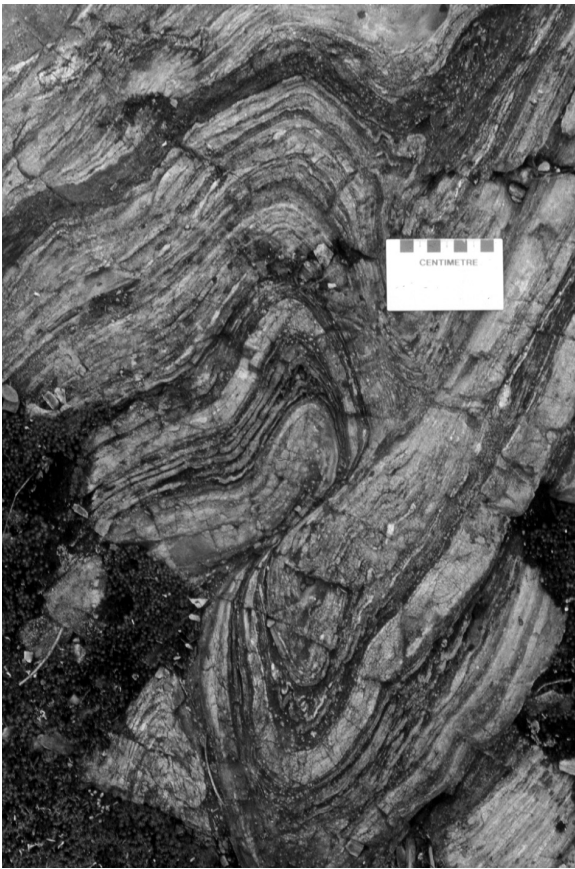


Figure 41: F_2 folding and dislocation of S_1 foliation and related lamination, due to dextral strike-slip movement in strongly attenuated volcanic rocks at McLeod Narrows, Franklin Murray Lake.

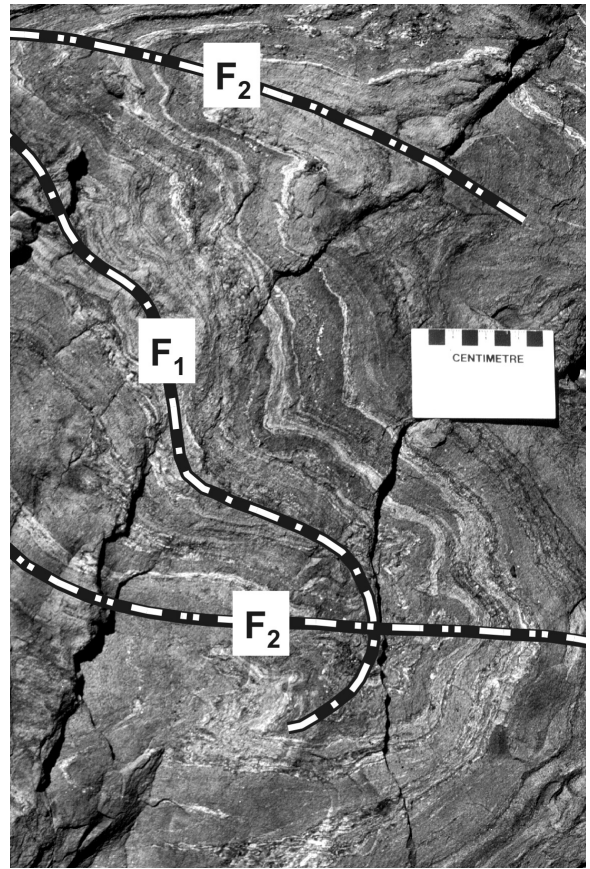


Figure 42: F_1 - F_2 fold interference pattern in layered metasedimentary rocks in the north-central part of the map area.



Figure 43: Boudinage in laminated amphibolite (subunit J1e) derived from mafic volcanic flows at the north margin of the Ralph Anderson Lake belt.

D_4 deformation

The final deformation event produced high-angle faults, which transect the greenstone belt and are commonly associated with north-northeast- to northeast-trending topographic lineaments. At some localities, these faults are associated with displacement of several tens of metres, notably in the major felsic porphyry sill (subunit J4d) in the area north of Ralph Anderson Lake (Figure 2). Elsewhere, the amount of displacement on the late faults appears to have been relatively minor.

Discussion

The model of nappe tectonics proposed in this report for the Ralph Anderson Lake belt is not a new concept for Archean greenstone belts. Although earlier discussions on the origins of these ancient belts have favoured ensialic models where vertical movements are predominant (Anhaeusser et al., 1969; Windley and Bridgwater, 1970; Viljoen and Viljoen, 1971), horizontal tectonic models have also been proposed (e.g., in the Archean of Ontario). Nappe tectonics are the preferred explanation for the downward-facing stratigraphic sequences at Rainy Lake, Ontario (Poulsen, 1979), and Thurston and Breaks (1978) interpreted the entire Red Lake greenstone belt of the Uchi subprovince as an overturned nappe structure. Similarly, in the southeast Max Lake area, a horizontal tectonic model resulting in a major recumbent fold is seen as the most likely explanation for the enigmatic structure in which the south-facing Lavigne Lake intrusion is emplaced within a north-facing volcanic sequence. This model also supports the contention that the volcanic enclaves within the McLeod Narrows gabbro (southern section) are geochemically similar and possibly stratigraphically equivalent to the northern volcanic suite (discussed in the 'Geochemistry' section). The lithologically diverse and chemically evolved northern volcanic suite in the recumbent limb of the overturned fold is thus structurally overlain by the older, geochemically more primitive, central volcanic suite that occupies the core of the inferred nappe structure (Figure 39). The faulted contact between the southern and central sections, the regional foliation and the attitude of stratigraphic units were all initially shallow dipping but have been rotated and steepened by subsequent deformation.

The above model is consistent with the structural and inferred geochemical relationships of the main stratigraphic components of the greenstone belt, except for the assumed age of the McLeod Narrows gabbro. This intrusion is emplaced within the southern stratigraphic section and thus postdates the southern volcanic suite; however, geochemical data suggest the gabbro is coeval with the central volcanic suite (*see* 'Geochemistry' section). The suggested age equivalence between the gabbro and the central basalt is not compatible with the inferred relationships between the main volcanic suites based their comparative geochemistry (i.e., the central suite is geochemically less evolved and older than both the northern and southern volcanic suites). This inconsistency shows that age and genetic relationships between the various stratigraphic components cannot be reliably determined solely on geochemical criteria. Further geochemical investigations, together with new isotopic and geochronological data, are needed to clarify the relationships between the main stratigraphic components and the tectonic history of the Ralph Anderson Lake greenstone belt.

Economic geology

Airborne reconnaissance during a regional geochemical survey in 1996 located conspicuous alteration and mineralization in the area southeast of Max Lake (Fedikow and Nielsen, 1997a). The mineralization at that locality (MacVicar Lake alteration zone) is associated with oxide-facies iron formation within an arc-type mafic volcanic sequence ('northern volcanic section') and is interpreted as a volcanic exhalative deposit. Stratabound mineralization associated with chert occurs further east within the same section, at Ralph Anderson and Franklin Murray lakes (see 'Siltstone, feldspathic greywacke; minor chert' section). Elsewhere, base-metal mineralization at the margins of synvolcanic felsic porphyry and gabbro intrusions is interpreted as hydrothermal in origin, and penecontemporaneous with juvenile-arc volcanism (Table 7). Structurally controlled mineralization occurs at the faulted contact between the southern and central volcanic suites in the area south of the east end of MacVicar Lake (Figure 2).

Minor pyritic mineralization, associated with silicic or chloritic alteration, occurs sporadically throughout arc-type rocks in the west part of the Ralph Anderson Lake belt. The sulphides are mostly altered at these localities, which are interpreted to be due to exhalative and/or hydrothermal activity associated with the volcanism; in some cases, the sulphide minerals have been mobilized and structurally emplaced along faults. Details of the various types of mineralization, classified according to their stratigraphic or structural setting, lithology and/or type of alteration, are given below.

Stratabound mineralization associated with iron formation and basalt (type 1, Table 7)

The most prominent occurrence of stratabound mineralization is a 36 m wide, altered zone of base-metal and gold mineralization, at or close to the top of the northern volcanic section (see 'Altered garnetiferous supracrustal rocks' section). At that locality, hydrothermal alteration and subsequent regional metamorphism have resulted in pervasive garnet porphyroblastesis, which is accompanied by extensive surficial iron staining. Volcanic rocks in the alteration zone contain up to 424 ppm Cu and minor Zn (108 ppm). The mineralized samples are from strongly deformed layers of garnetiferous, silicified basalt with massive garnetite stringers and disrupted quartz veins. Magnetiferous chert beds within and adjacent to the alteration zone contain up to 314 ppb Au and 252 ppm Zn.

Stratabound mineralization associated with chert (types 2A, 2B, 2C, Table 7)

Stratabound mineralization associated with chert-siltstone units occurs at the base of the northern volcanic section, where the sedimentary rocks are in contact with either basalt of the central section or gabbro of the Lavigne Lake intrusion (types 2A and 2B, respectively, in Table 7). At Franklin Murray Lake, an 11 m thick cherty siltstone unit at the base of the northern section contains base-metal sulphides and gold over a 1 m wide section at the south margin of the unit; a grab sample yielded 1700 ppm Zn, 470 ppm Cu, 31 ppb Au and traces of Ag, Ni and Cr. The sedimentary deposit occurs between pillowed basalt of the central section (subunit O1a) to the south and a plagioclase porphyry sill (subunit J4d) to the north (Map GR2004-2-1, in back pocket). At Ralph Anderson Lake, a 2 m thick, laminated chert unit at the contact between basalt of the northern section and (to the south) the Lavigne Lake gabbro contains 828 ppm Cu and traces of Au and Ag. Mineralized chert layers also occur within the northern sedimentary formation at MacVicar Lake (type 2C in Table 7); grab samples yielded 293 ppm Cu and 237 ppm Zn.

Associated with felsic porphyry dikes (type 3, Table 7)

Most felsic porphyry intrusions (subunit J4d) contain minor disseminated pyrite, and some dikes contain concentrations of various other base-metal sulphides. Quartz-plagioclase porphyry within strongly deformed basalt, 0.35 km south of the MacVicar Lake alteration zone, contains up to 478 ppm Zn, 159 ppm Cu and trace Au.

Associated with gabbro (type 4, Table 7)

At Aswapiswanan Lake, gold and base-metal mineralization occurs at the south margin of a 10 m thick synvolcanic gabbro sill in the upper part of the southern volcanic section; a grab sample yielded 1373 ppm Cu, 306 ppm Cr, 124 ppb Au and traces of Ni and Zn. The mineralization occurs in a narrow (30 cm wide) silicified zone at the margin of the sill. In the west part of the project area, both the Lavigne Lake and McLeod Narrows gabbro intrusions contain sporadic pyritic zones with up to 687 ppm Cu and 206 ppm Zn.

Mafic volcanic rock (type 5, Table 7)

Sporadic sulphide mineralization in pillowed flows occurs as irregular zones within and between pillows, and in related volcanic breccia units. Arc-type pillowed basalt in the northern section, 150 m north of the Lavigne Lake intrusion, contains pervasive mineralized zones that yielded up to 248 ppm Cu.

Table 7: Selected geochemical data for mineralized rock samples from the Ralph Anderson Lake greenstone belt.

Sample number	Setting type	Cu (ppm)	Zn (ppm)	Au (ppb)	Ag (ppm)	Ni (ppm)	Cr (ppm)	Location of mineralized zones	Stratigraphic association	Hostrock
Stratabound, associated with iron formation and basalt										
32-99-2019-2	1	110	108	6	0.3	6	-	MacVicar Lake alteration zone, eastern MacVicar Lake		Quartz+felsite vein with chloritic laminae
32-99-2020-1	1	424	8	-5	0.4	33	-	MacVicar Lake alteration zone, eastern MacVicar Lake		Silicified, tectonically laminated basalt; garnet-bearing, with mafic remnants and quartz veins
32-99-2020-3	1	49	82	-5	-0.2	27	-	MacVicar Lake alteration zone, eastern MacVicar Lake	Northern section	Silicified, tectonically laminated basalt; garnet-bearing, with mafic remnants and quartz veins
32-99-2020-6	1	21	10	-5	0.5	6	-	MacVicar Lake alteration zone, eastern MacVicar Lake		Silicified, tectonic laminated basalt; garnet-bearing, with mafic remnants and quartz veins
32-00-3325--2	1	41	145	9	-0.3	13	59	MacVicar Lake alteration zone, central MacVicar Lake		Magnetiferous chert associated with garnetiferous amphibolite
32-00-3281-1	1	23	252	314	-0.3	11	12	20 m south of the alteration zone, west MacVicar Lake		Magnetiferous chert component of oxide-facies iron formation
Stratabound, associated with chert										
32-00-3023-2	2A	189	95	-2	-0.3	74	55	North shore, Franklin Murray Lake		Cherty siltstone with fine bedding lamination
32-00-3023-3	2A	288	1700	29	1.4	50	48	North shore, Franklin Murray Lake		Cherty siltstone with fine bedding lamination
32-00-3025-3	2A	178	206	-2	6.0	119	67	North shore, Franklin Murray Lake		Cherty siltstone with fine bedding lamination
32-00-3025-4	2A	470	978	6	1.2	78	50	North shore, Franklin Murray Lake		Cherty siltstone with fine bedding lamination
32-00-3025-5	2A	211	572	31	0.4	37	103	North shore, Franklin Murray Lake	Northern section	Cherty siltstone with fine bedding lamination
32-99-2321-4	2B	828	64	19	1.6	65	-	200 m north of shore, eastern Ralph Anderson Lake		Chert unit between basalt and gabbro at the base of the northern volcanic suite
32-00-3234-3	2C	68	237	9	0.4	53	89	Northern sedimentary formation, MacVicar Lake		Chert and cherty siltstone associated with porphyroblastic siltstone
32-00-3235-2	2C	293	115	3	-0.3	43	58	Central peninsula, MacVicar Lake		Thin (0.5 m) chert unit within pillowed basalt adjacent to the northern sedimentary formation
Associated with felsic porphyry dikes										
32-99-2024-1	3	99	478	57	0.3	26	-	275 m south of MacVicar Lake alteration zone	Felsic	Quartz-plagioclase porphyry in laminated amphibolite
32-99-2120-2	3	159	134	-5	0.6	14	-	400 m south of MacVicar Lake alteration zone	porphyry	Quartz-plagioclase porphyry in partly altered and sheared basalt

Table 7: Selected geochemical data for mineralized rock samples from the Ralph Anderson Lake greenstone belt. (continued)

Sample number	Setting type	Cu (ppm)	Zn (ppm)	Au (ppb)	Ag (ppm)	Ni (ppm)	Cr (ppm)	Location of mineralized zones	Stratigraphic association	Hostrock
Associated with gabbro										
32-00-3104-1	4	202	146	-2	0.3	-1	-5	North shore, western Aswapiswanan Lake		Gossan zone within gabbro
32-00-3111-1	4	237	112	-2	-0.3	69	81	North shore, western Aswapiswanan Lake		Gossan zone within gabbro
32-00-3142-5	4	301	145	3	-0.3	6	-5	Island, northwest part of Aswapiswanan Lake		Gossan zone at margin of synvolcanic gabbro
32-00-3143-1	4	1373	76	124	0.5	59	306	Island, northwest part of Aswapiswanan Lake	Gabbro	Gossan zone at margin of synvolcanic gabbro
32-00-3260-1	4	166	119	13	0.4	-1	-5	McLeod Narrows gabbro (western part)		Gossan zone in gabbro adjacent to supracrustal enclave
32-00-3264-1	4	177	206	-2	-0.3	28	26	Lavigne Lake gabbro (western part)		Gossan zone in melanocratic gabbro
32-00-3316-1	4	687	5	9	-0.3	70	-5	McLeod Narrows gabbro (western part)		Silicified, epidotized 12 m alteration zone in gabbro
Associated with mafic volcanic rocks										
32-99-2222-1	5	248	38	-5	0.4	12	-	150 m north of central Lavigne Lake gabbro	Northern section	Aphyric pillowed basalt with epidotic domains and minor silicification
Faulted contact										
32-99-2041-3	6	482	29	-5	0.6	859	-	North margin of southern volcanic suite	Southern section	Altered amygdaloidal basalt (quartz-anthophyllite-sericite-chlorite-epidote); locally protomylonitic or gneissic
Intrusive or structural contact										
32-00-3291-5	7	66	146	4	-0.3	107	187	North margin of northern volcanic suite	Northern section	0.5 m gossan zone at contact between basalt and granitoid hybrid gneiss

Note: Minus values indicate an element was not present at the given detection limit.

Faulted contact (type 6, Table 7)

Strike-slip and discordant D₃ and D₄ faults are locally characterized by surficial iron staining due to pyritic mineralization. A tectonized anthophyllite-chlorite-sericite alteration zone at the faulted contact between the southern and central volcanic sections (Figure 2) is silicified and mineralized; samples from this zone yielded up to 482 ppm Cu and 859 ppm Ni.

Intrusive or structural contact (type 7, Table 7)

At the north margin of the Ralph Anderson Lake belt, minor copper-zinc-nickel-chromium mineralization occurs in a narrow, highly sheared zone at the contact between attenuated basalt and amphibolite (subunit J1e) and hybrid gneiss (subunit P6f) derived from the granitoid terrane north of the greenstone belt.

Exploration prospects

The numerous sulphide showings and the varied settings in which mineralization occurs in the arc-type northern and southern stratigraphic sections suggest that these terranes represent viable exploration prospects for both base-metals and gold. Bimodal volcanism, synvolcanic felsic porphyry intrusions, exhalative sedimentary horizons, conformable alteration zones and stratabound mineralization, all present in the southeast Max Lake–Aswapiswanan Lake area, are key features in VMS-hosting terranes of all ages (e.g., Noranda and Timmins, Gibson et al., 1984; Flin Flon, Syme and Bailes, 1993). The stratigraphy in the southeast Max Lake–Aswapiswanan Lake area is also similar to that of some Archean gold camps (e.g., Red Lake, Pirie et al., 1982). In summary, lithostratigraphic and geochemical data suggest that the southeast Max Lake–Aswapiswanan Lake area offers good potential for economic mineralization.

The best prospects for base-metal or precious-metal exploration in the project area are considered to be the stratabound types associated with chert and iron formation within the northern volcanic section that are locally hydrothermally altered (e.g., MacVicar Lake alteration zone, subunit J2c). This mineralization is attributed to exhalative volcanism and hydrothermal alteration, both of which are hallmarks for VMS-type ore deposits; thus, these occurrences are among the most promising exploration targets in the project area.

Copper-nickel mineralization within quartz-sericite-anthophyllite-cordierite-chlorite schist at the north margin of the southern stratigraphic section (type 6, Table 7) is attributed to hydrothermal alteration of volcanic rocks at or close to the sea floor. The mineralization occurs within a 75 m wide zone of extensive silicification and epidotization within arc-type, massive and fragmental volcanic rocks of the southern section, where it is tectonically juxtaposed against ‘central’ ocean-floor basalt to the north. The mineralization at that locality may alternatively be interpreted as postvolcanic; in the latter case, the fault zone that contains the mineralized rocks could have provided a conduit for hydrothermal fluids that are assumed to be the source of the sulphide mineralization.

Acknowledgments

Scott Schoonbaert, Patrick Solylo and Alex Fortin provided assistance in the field and with subsequent data processing; their contribution is gratefully acknowledged. Thanks are extended to Doug Berk and staff in the Rock Preparation Laboratory (Manitoba Industry, Economic Development and Mines) for the cutting of thin sections and preparation of selected rocks for analysis; to Cathy McGregor for measuring plagioclase modal compositions; and to Bonnie Lenton for figure preparation. The report benefited from constructive scientific and technical editing by Alan Bailes and Tim Corkery of the Manitoba Geological Survey and Bob Davie of RnD Technical.

References

- Anhaeusser, C.R., Mason, R., Viljoen, M.J. and Viljoen, R.P. 1969: A reappraisal of some aspects of Precambrian Shield geology; *Geological Society of America Bulletin*, v. 80, p. 2175–2200.
- Arndt, N.T., Naldrett, A.J. and Pyke, D.R. 1977: Komatiitic and iron-rich tholeiitic lavas of Munro township, northeast Ontario; *Journal of Petrology*, v. 18, p. 319–369.
- Bailes, A.H. 1980: Geology of the File Lake area; Manitoba Department of Energy and Mines, Mineral Resources Division, Geological Report GR78-1, 134 p.
- Corkery, T. 1985: Cross Lake supracrustal investigations in the eastern Pipestone Lake area; *in* Report of Field Activities 1985, Manitoba Energy and Mines, Geological Services/Mines Branch, p. 165–172.
- Corkery, M.T., Davis, D.W. and Lenton, P.G., 1992: Geochronological constraints on the development of the Cross Lake greenstone belt, northwest Superior Province, Manitoba; *Canadian Journal of Earth Sciences*, v. 29, p. 2171–2185.
- Currie, K.L. 1961: Oxford House, Manitoba; Geological Survey of Canada, Map 21-1961, scale 1:250 000.
- Elbers, F.J. 1973a: Bolton Lake (NTS 53L/5, north half); Manitoba Mines, Resources and Environmental Management, Preliminary Map 1973 H-10, scale 1:50 000.
- Elbers, F.J. 1973b: Joint Lake (NTS 53L/6, north half); Manitoba Department of Mines, Resources and Environmental Management, Mineral Resources Division, Preliminary Map 1973H-11, scale 1:50 000.
- Elbers, F.J. and Marten, B.E. 1973: Kanuchuan Rapids (NTS 53L/7); Manitoba Department of Mines, Resources and Environmental Management, Mineral Resources Division, Preliminary Map 1973H-12, scale 1:50 000.
- Fedikow, M.A.F. and Nielsen, E. 1997a: Operation Superior: multimedia geochemical surveys in the Edmund Lake and Sharpe Lake greenstone belts, northern Superior Province, Manitoba (NTS 53K); *in* Report of Activities 1997, Manitoba Department of Energy and Mines, Geological Services, p. 4–5.
- Fedikow, M.A.F. and Nielsen, E. 1997b: Multimedia geochemical signatures of precious and base-metal depositional environments, Max Lake area, northern Superior Province (abstract); Manitoba Mining & Minerals Convention 1997, Winnipeg, Manitoba, Nov. 20–22, 1997, Program, p. 35.
- Fedikow, M.A.F. and Nielsen, E. 1998: Operation Superior: multimedia geochemical surveys in the Knife Lake, Webber Lake, Goose Lake and Echimamish River greenstone belts, northern Superior Province, Manitoba (NTS 53L and 53K); *in* Report of Activities 1998, Manitoba Energy and Mines, Geological Services, p. 75–77.
- Fedikow, M.A.F., Nielsen, E. and Conley, G.G. 1997a: Operation Superior: 1996 multimedia geochemical data from the Max Lake area (NTS 63I/8, 9 and 53L/5, 12); Manitoba Energy and Mines, Geological Services, Open File Report OFR97-1, 34 p.
- Fedikow, M.A.F., Nielsen, E., Conley, G.G. and Lenton, P.G. 1999: Operation Superior: multimedia geochemical survey results from the Webber Lake, Knife Lake, Goose Lake and Echimamish River greenstone belts, northern Superior Province, Manitoba (NTS 53L and 53K); Manitoba Energy and Mines, Geological Services, Open File Report OFR99-8, 400 p.
- Fedikow, M.A.F., Nielsen, E., Conley, G.G. and Matile, G.L.D. 1997b: Operation Superior: multimedia geochemical survey results from the Echimamish River, Carrot River and Munro Lake greenstone belts, northern Superior Province, Manitoba (NTS 53L and 63I); Manitoba Energy and Mines, Geological Services, Open File Report OFR97-2, 1501 p.
- Fedikow, M.A.F., Nielsen, E. and Sailerova, E. 1996: Operation Superior: multimedia geochemical surveys in the Echimamish River, Carrot River and Munroe Lake greenstone belts, northern Superior Province, Manitoba (NTS 53L and 63I); *in* Report of Activities 1996, Manitoba Energy and Mines, Geological Services, p. 5–8.
- Fisher R.V. and Schmincke, H.-U. 1984: *Pyroclastic Rocks*; Springer-Verlag, New York, New York, 472 p.
- Gibson, H.L., Walker, S.D., and Coad, P.R. 1984: Surface geology and volcanogenic base metal massive sulphide deposits and gold deposits of Noranda and Timmins; Geological Association of Canada–Mineralogical Association of Canada, Joint Annual Meeting, 1984, London, Ontario, Field Trip Guidebook 14.
- Gilbert, H.P. 1999a: Southeast Max Lake area (parts of NTS 53L/5NW and 12SW); *in* Report of Activities, 1999, Manitoba Industry, Trade and Mines, Manitoba Geological Survey, p. 84–93.
- Gilbert, H.P. 1999b: Geology of the southeast Max Lake area (parts of NTS 53L/5NW, 12SW); Manitoba Industry, Trade and Mines, Manitoba Geological Survey, Preliminary Map 1999S-1, scale 1:20 000.
- Gilbert, H.P. 2000: Geology of the southeast Max Lake area (parts of NTS 53L/5N, 6/NW and 12/SW); Manitoba Industry, Trade and Mines, Manitoba Geological Survey, Preliminary Map 2000S-3, scale 1:20 000.
- Hawkesworth, C.J., Gallagher, K., Hergt, J.M. and McDermott, F. 1994: Destructive plate margin magmatism: geochemistry and melt generation; *Lithos*, v. 33, p. 169–188.

- Hubregtse, J.J.M.W. 1985a: Geology of the Oxford Lake–Carrot River area; Manitoba Energy and Mines, Geological Services Branch, Geological Report GR83-1A, 73 p.
- Hubregtse, J.J.M.W. 1985b: Windy Lake; Map GR83-1-10 in Geological Report GR83-1A, Manitoba Energy and Mines, Geological Services Branch, scale 1:50 000.
- Jensen, L.S. 1976: A new cation plot for classifying subalkaline volcanic rocks; Ontario Geological Survey, Miscellaneous Paper 66, 22 p.
- Jones, J.G. 1969: Pillow lavas as depth indicators; *American Journal of Science*, v. 267, p. 181–195.
- Manitoba Energy and Mines 1987: Oxford House; Manitoba Energy and Mines, Geological Services, Bedrock Geology Compilation Map Series, NTS 53L, scale 1:250 000.
- Manitoba Energy and Mines 1996: Cross Lake; Manitoba Energy and Mines, Geological Services, Bedrock Geology Compilation Map Series, NTS 63I, scale 1:250 000.
- Moore, J.G. 1970: Water content of basalt erupted on the ocean floor; *Contributions to Mineralogy and Petrology*, v. 28, p. 272–279.
- Leshner, C.M., Goodwin, A.M., Campbell, I.H. and Gorton, M.P. 1986: Trace-element geochemistry of ore-associated and barren felsic metavolcanic rocks in the Superior Province, Canada; *Canadian Journal of Earth Sciences*, v. 23, p. 222–241.
- Percival, J.A., Bailes, A.H., Corkery, M.T., Dubé, B., Harris, J., McNicoll, V., Panagapko, D., Parker, J.R., Rogers, N., Sanborn-Barrie, M., Skulski, T., Stone, D., Stott, G.M., Tomlinson, K.Y., Whalen, J.B. and Young, M.D. 2000: Western Superior NATMAP: an integrated view of Archean crustal evolution; in *Report of Activities 2000*, Manitoba Industry, Trade and Mines, Manitoba Geological Survey, p. 108–116.
- Pirie, J., Durocher, M. and Wallace, H. 1982: Volcanic stratigraphy, alteration and gold deposits of the Red Lake area, northwestern Ontario; Geological Association of Canada–Mineralogical Association of Canada, Joint Annual Meeting, 1982, Winnipeg, Manitoba, Field Trip Guidebook 8.
- Poulsen, H. 1979: Polyphase deformation of Archean rocks at Rainy Lake, Ontario (abstract); 25th Annual Institute on Lake Superior Geology, Duluth, Minnesota, Technical Session and Abstracts, 42 p.
- Saunders, A.D. and Tarney, J. 1991: Back-arc basins; in *Oceanic Basalts*, P.A. Floyd (ed.), Blackie and Son, Glasgow, United Kingdom, p. 219–263.
- Schledewitz, D.C.P. 1980: Oxford House southwest; Manitoba Energy and Mines, Mineral Resources Division, Preliminary Map 1980 K-3, scale 1:100 000.
- Sinton, J.M. and Fryer, P. 1987: Mariana Trough lavas from 18°N: implications for the origin of back-arc basin basalts; *Journal of Geophysical Research*, v. 92, no. B12, p. 12 782–12 802.
- Skulski, T., Corkery, M.T., Stone, D., Whalen, J.B. and Stern, R.A. 2000: Geological and geochronological investigations in the Stull Lake–Edmund Lake greenstone belt and granitoid rocks of the northwestern Superior Province; in *Report of Activities 2000*, Manitoba Industry, Trade and Mines, Manitoba Geological Survey, p. 117–128.
- Stern, R.A., Syme, E.C., Bailes, A.H. and Lucas, S.B. 1995a: Paleoproterozoic (1.90–1.86 Ga) arc volcanism in the Flin Flon Belt, Trans-Hudson Orogen, Canada; *Contributions to Mineralogy and Petrology*, v. 119, p. 117–141.
- Stern, R.A., Syme, E.C. and Lucas, S.B. 1995b: Geochemistry of 1.9 Ga MORB- and OIB-like basalts from the Amisk collage, Flin Flon belt, Canada: evidence for an intra-oceanic origin; *Geochimica et Cosmochimica Acta*, v. 59, p. 3131–3154.
- Sun, S.S. and McDonough, W.F. 1989: Chemical and isotopic systematics of oceanic basalts: implications for mantle composition and processes; in *Magmatism in the Ocean Basins*, A.D. Saunders and M.J. Norry (ed.), The Geological Society, Special Publication 42, p. 313–345.
- Syme, E.C. 1998: Ore-associated and barren rhyolites in the central Flin Flon Belt: case study of the Flin Flon Mine sequence; Manitoba Energy and Mines, Open File Report OF98-9, 26 p.
- Syme, E.C. and Bailes, A.H. 1993: Stratigraphic and tectonic setting of volcanogenic massive sulfide deposits, Flin Flon, Manitoba; *Economic Geology*, v. 88, p. 566–589.
- Thurston, P.C. and Breaks, F.W. 1978: Metamorphic and tectonic evolution of the Uchi–English River subprovince; in *Metamorphism in the Canadian Shield*, J.A. Fraser and W.W. Heywood (ed.), Geological Survey of Canada, Paper 78-10, p. 49–62.
- Thurston, P.C., Osmani, I.A. and Stone, D. 1991: Northwestern Superior Province: review and terrane analysis; Chapter 5 in *Geology of Ontario*, Ontario Geological Survey, Special Volume 4, pt. 1, p. 81–144.
- Viljoen, R.P. and Viljoen, M.J. 1971: The geological and geochemical evolution of the Onverwacht volcanic group of the Barberton Mountain Land, South Africa; in *Symposium on Archean Rocks*, Geological Society of Australia, Special Publication 3, p. 133–149.

- White, W.M. and Dupré, B. 1986: Sediment subduction and magma genesis in the Lesser Antilles: isotopic and trace element constraints; *Journal of Geophysical Research*, v. 91, p. 5927–5941.
- Windley, B.F. and Bridgwater, D. 1970: Some aspects of Archean crustal evolution; *in* *The Archean Rocks*, G.J.H. McCall (ed.), Geological Society of Australia, Precambrian Symposium, Perth, Australia, p. 16–17.
- Wood, D.A. 1980: The application of a Th-Hf-Ta diagram to problems of tectonomagmatic classification and to establishing the nature of crustal contamination of basaltic lavas of the British Tertiary volcanic province; *Earth and Planetary Science Letters*, v. 50, p. 11–30.
- Wright, J.F. 1928: Island Lake area, Manitoba; Geological Survey of Canada, Summary Report, 1927, Part B, p. 54–80.
- Wright, J.F. 1932: Oxford House area, Manitoba; Geological Survey of Canada, Summary Report, 1931, Part C, p. 1–25.

Appendix: Major-, minor- and trace-element data for volcanic and intrusive rocks in the southeast Max Lake–Aswapiswanan Lake area

Sample number	Rock type	UTM Easting	UTM Northing	UTM Zone	SiO ₂ (%)	Al ₂ O ₃ (%)	Fe ₂ O ₃ (%)	MnO (%)	MgO (%)	CaO (%)	Na ₂ O (%)	K ₂ O (%)	TiO ₂ (%)	P ₂ O ₅ (%)	LOI (%)	TOTAL (%)	Ba (ppm)	Sr (ppm)	Sc (ppm)	V (ppm)	S (ppm)	CO ₂ (%)	Cr (ppm)	Co (ppm)	Ni (ppm)	Cu (ppm)	Zn (ppm)	Ga (ppm)	Ge (ppm)	As (ppm)		
NORTHERN VOLCANIC SUITE																																
32-99-2012-3	Basalt	311758	6043413	14U	48.94	15.23	14.62	0.20	6.00	10.27	2.97	0.39	1.25	0.12	0.42	99.24	67	221	36	270	0.08	-0.05	221	46	101	116	65	18	-10	18		
32-00-3265-1	Basalt	308790	6043261	14U	53.65	15.11	10.33	0.12	6.95	9.57	3.15	0.32	0.70	0.09	0.8	98.54	70	136	36	207	0.03	0.22	59	48	59	112	62	19	16	5		
32-00-3009-1	Basalt	321660	6041822	14U	53.99	14.88	10.44	0.17	6.71	7.96	4.38	0.81	0.66	0.08	0.54	98.64	178	100	33	193	0.01	-0.05	26	38	41	74	53	13	1.5	-5		
32-99-2201-1	Basalt	316602	6042503	14U	55.47	14.88	10.62	0.19	5.54	8.31	3.43	0.48	0.98	0.10	0.35	98.73	104	92	32	204	0.06	-0.05	73	32	45	111	49	17	-10	-5		
32-00-3280-1	Basalt	308349	6043265	14U	55.88	14.49	10.46	0.13	9.22	6.48	2.39	0.17	0.68	0.09	0.76	99.08	38	219	34	201	0.1	-0.05	55	48	46	98	50	20	12	-5		
32-00-3004-1	Basalt	322303	6041312	14U	55.90	13.34	12.93	0.18	5.15	6.77	3.81	0.66	1.11	0.14	0.46	98.53	127	142	29	247	0.03	0.11	52	39	30	27	99	17	1.5	-5		
32-99-2023-1	Basalt	311960	6043022	14U	55.94	14.37	10.92	0.17	6.06	8.32	3.03	0.41	0.70	0.09	0.25	98.83	124	135	33	188	0.04	-0.05	-20	26	29	93	-30	13	-10	-5		
32-99-2066-1	Andesite	313159	6042670	14U	57.26	13.83	12.11	0.17	5.60	7.21	2.23	0.51	0.94	0.15	0.24	98.94	119	154	32	193	0.02	-0.05	-20	21	16	77	-30	11	-10	-5		
32-99-2021-1	Andesite	312048	6043208	14U	57.85	14.76	8.33	0.17	5.63	9.88	2.39	0.36	0.55	0.08	0.26	99.80	111	255	30	190	0.07	-0.05	127	43	75	131	78	17	10	8		
32-99-2139-5	Basalt, altered	313950	6042820	14U	54.16	16.38	8.66	0.15	5.20	8.96	4.47	0.22	1.08	0.72	0.55	100.18	84	1421	21	176	0.02	0.25	125	27	88	54	119	20	10	-5		
32-99-2120-1	Basalt, altered	311694	6042877	14U	63.34	14.83	4.51	0.18	0.79	12.56	2.74	0.16	0.83	0.06	0.89	100.26	49	180	27	206	0.03	3.80	114	15	35	92	-30	11	-10	-5		
32-99-2018-1	Gabbro	311892	6042937	14U	49.35	15.88	12.20	0.16	8.44	10.79	2.06	0.21	0.81	0.09	0.40	99.15	57	164	31	160	0.04	0.07	270	21	68	102	-30	8	-10	-5		
32-99-2224-1	Gabbro	314715	6042368	14U	50.88	13.76	14.36	0.30	6.92	10.58	2.05	0.21	0.85	0.09	0.41	100.27	46	107	50	300	0.02	-0.05	71	47	90	97	194	18	10	6		
32-99-2175-1	Dacite	315807	6042997	14U	62.64	15.48	8.26	0.13	1.52	5.53	3.77	1.34	1.06	0.27	0.27	98.04	352	110	14	71	0.01	-0.05	-20	18	26	28	125	19	-10	-5		
32-99-2231-1	Dacite	315049	6042904	14U	63.79	18.79	3.94	0.05	1.60	3.47	6.06	1.66	0.52	0.13	0.61	100.67	465	257	11	94	0.01	-0.05	30	14	26	28	65	21	-10	-5		
32-99-2084-1	Dacite	313588	6042858	14U	64.51	17.54	3.68	0.07	2.38	4.85	4.14	2.01	0.56	0.27	0.64	100.29	446	574	8	81	0.01	0.15	28	19	24	35	50	20	10	-5		
32-00-3266-1	Felsic volcanic breccia	308773	6043323	14U	70.98	12.45	6.57	0.09	0.94	2.07	3.53	2.66	0.58	0.12	1.12	100.46	435	131	12	28	0.05	0.81	37	10	-20	29	70	23	1.5	-5		
32-99-2167-1	Popo, major sill	315681	6042967	14U	63.35	17.47	5.51	0.10	2.81	4.22	3.48	2.41	0.49	0.15	0.95	99.70	299	171	10	80	0.01	-0.05	24	17	-15	49	208	14	-10	-5		
32-99-2173-1	Popo, major sill	315112	6042741	14U	64.13	17.04	5.09	0.04	2.37	4.12	4.56	1.94	0.55	0.15	0.67	100.42	399	228	12	89	0.01	-0.05	49	18	41	21	39	19	10	-5		
32-00-3011-1	Popo	320970	6041591	14U	63.25	16.59	5.63	0.08	1.42	5.81	4.95	1.47	0.63	0.19	1.38	98.02	447	349	11	109	0.09	1	47	14	39	49	69	14	0.8	-5		
32-99-2206-1	Popo	316911	6042671	14U	68.42	16.01	4.68	0.10	0.93	6.78	3.98	1.37	0.51	0.23	1.81	100.18	523	791	8	85	0.02	1.54	25	13	23	16	101	19	-10	-5		
32-99-2340-1	Popo	317697	6041908	14U	73.72	13.13	3.32	0.04	0.77	2.05	3.55	2.87	0.42	0.12	0.92	100.23	554	110	5	27	0.02	0.48	207	9	98	-10	44	19	10	17		
32-99-2008-1	Popo	310834	6043682	14U	78.04	10.97	2.90	0.04	0.20	1.08	3.54	2.94	0.24	0.03	0.32	99.93	1032	73	3	6	0.06	-0.05	-20	4	-15	22	40	15	-10	-5		
32-99-2010-2	Popo	311218	6043710	14U	79.63	11.82	0.61	0.01	0.07	1.28	4.02	2.52	0.02	0.02	0.26	100.24	236	77	1	-5	0.02	-0.05	-20	-1	-15	14	-30	18	-10	-5		
CENTRAL VOLCANIC SUITE																																
32-99-2254-1	Basalt	317917	6041950	14U	48.19	13.28	17.11	0.36	5.36	11.61	2.66	0.62	0.76	0.06	0.27	98.88	101	66	42	212	0.01	-0.05	132	45	93	18	-30	11	-10	-5		
32-00-3124-1	Basalt	337029	6040445	14U	48.57	14.82	13.00	0.20	8.81	11.29	2.52	0.07	0.67	0.06	0.72	98.84	21	134	43	258	0.02	-0.05	826	61	107	92	64	16	20	-5		
32-00-3047-1	Basalt	324239	6040650	14U	48.95	14.49	13.20	0.22	8.26	12.09	1.86	0.13	0.71	0.07	0.55	98.69	25	78	43	263	0.02	-0.05	248	57	92	130	59	15	1.8	-5		
32-99-2342-1	Basalt	318617	6041237	14U	49.07	15.03	14.49	0.29	6.19	10.88	2.87	0.25	0.83	0.09	0.58	98.92	56	90	47	257	0.01	-0.05	132	39	78	13	102	14	-10	-5		
32-00-3070-1	Basalt	323286	6040728	14U	49.18	14.79	12.85	0.21	7.90	13.08	1.20	0.06	0.68	0.06	0.5	98.7	28	92	43	258	0.01	-0.05	275	60	99	71	64	16	1.8	-5		
32-99-3220-1	Basalt	349740	6039356	14U	49.19	15.17	16.12	0.23	7.02	7.53	3.53	0.10	1.01	0.09	1.62	99.64	90	92	55	329	0.01	-0.05	117	67	42	137	96	18	20	-5		
32-99-2000-1	Basalt	310666	6042777	14U	49.30	14.83	13.39	0.23	6.05	13.59	1.60	0.23	0.72	0.07	0.64	99.31	46	107	43	147	0.03	0.33	171	18	42	11	-30	6	-10	-5		
32-00-3331-1	Basalt	308970	6042804	14U	49.53	14.80	11.80	0.18	8.32	12.85	1.81	0.06	0.59	0.06	0.7	98.79	26	92	41	230	0.08	0.22	527	66	97	112	52	21	20	-5		
32-99-3021-1	Basalt	323193	6040942	14U	49.61	14.83	14.73	0.17	7.80	8.78	3.03	0.13	0.85	0.08	0.3	100.42	65	168	47	278	0.16	-0.05	123	56	97	149	93	14	1.2	-5		
32-99-2032-1	Basalt	311960	6042504	14U	49.62	15.11	12.03	0.18	8.63	11.40	2.24	0.15	0.58	0.06	0.39	98.21	51	89	42	238	0.09	-0.05	399	47	93	110	64	15	10	-5		
32-99-2164-1	Basalt	317225	6041341	14U	49.74	14.69	12.98	0.22	8.19	10.89	2.46	0.06	0.71	0.06	0.35	98.78	27	94	46	274	0.01	-0.05	214	54	96	128	104	17	10	-5		
32-99-2120-5	Basalt	311894	6042877	14U	50.33	14.77	14.23	0.28	4.87	13.00	1.24	0.34	0.85	0.08	0.81	99.53	84	102	48	271	0.02	0.47	105	36	56	18	-30	13	-10	21		
32-99-2071-1	Basalt	312507																														

Appendix: Major-, minor- and trace-element data for volcanic and intrusive rocks in the southeast Max Lake–Aswapiswanan Lake area

Sample number	Rock type	UTM Easting	UTM Northing	UTM Zone	SiO ₂ (%)	Al ₂ O ₃ (%)	Fe ₂ O ₃ (%)	MnO (%)	MgO (%)	CaO (%)	Na ₂ O (%)	K ₂ O (%)	TiO ₂ (%)	P ₂ O ₅ (%)	LOI (%)	TOTAL (%)	Ba (ppm)	Sr (ppm)	Sc (ppm)	V (ppm)	S (ppm)	CO ₂ (%)	Cr (ppm)	Co (ppm)	Ni (ppm)	Cu (ppm)	Zn (ppm)	Ga (ppm)	Ge (ppm)	As (ppm)	
SOUTHERN VOLCANIC SUITE																															
32-99-2092-1	Basalt	312102	6040225	14U	46.76	15.08	16.12	0.34	4.79	11.86	2.34	0.41	2.06	0.23	0.35	98.50	61	130	44	302	0.03	-0.05	110	17	43	36	30	10	-1.0	-5	
32-00-3196-1	Basalt	348424	6037375	14U	53.94	14.20	9.40	0.18	8.04	10.13	3.16	0.25	0.63	0.07	0.66	98.54	40	235	38	199	0.04	-0.05	258	52	68	94	76	16	1.7	-5	
32-99-2080-2	Basalt, altered	311935	6041440	14U	56.74	16.01	8.97	0.32	4.81	6.89	4.59	0.36	1.11	0.22	1.09	99.66	215	242	29	183	0.08	-0.05	96	30	32	81	207	19	-1.0	-5	
32-99-2086-1	Basalt, altered	312001	6040691	14U	60.34	16.01	7.25	0.12	3.48	7.37	3.81	0.42	0.94	0.26	0.36	99.89	175	235	13	109	0.01	-0.05	62	19	55	11	44	20	-1.0	-5	
32-99-2287-1	Dacite	317124	6040417	14U	64.12	16.43	5.73	0.04	3.28	5.04	3.49	1.16	0.57	0.14	0.82	100.18	226	251	11	85	0.11	-0.05	47	18	47	12	-30	19	-1.0	-5	
32-99-2106-2	Dacite	310130	6041596	14U	64.81	16.67	4.31	0.06	3.79	4.34	4.26	1.19	0.44	0.13	1.39	100.11	284	257	11	79	0.01	-0.05	39	15	39	28	38	19	-1.0	-5	
32-99-2082-1	Dacite	311930	6041227	14U	65.18	16.87	4.42	0.04	2.79	4.38	5.18	0.55	0.45	0.14	0.65	100.06	86	291	10	80	0.02	-0.05	34	15	39	97	49	20	-1.0	-5	
32-00-2559-3	Felsic volcanic breccia	306429	6041768	14U	69.54	15.30	3.27	0.05	2.03	2.16	6.08	0.87	0.54	0.16	1.74	99.27	160	149	9	63	-0.01	-0.05	64	12	35	14	31	16	0.6	-5	
32-99-2161-1	Dacite clast in breccia	314220	6040854	14U	68.65	15.31	3.36	0.06	1.71	4.05	4.75	1.21	0.67	0.23	1.03	100.29	336	153	10	77	0.01	0.22	28	15	31	29	58	15	-1.0	-5	
32-99-2353-2	Felsic flow/sill	318081	6040060	14U	70.10	15.68	2.58	0.05	0.90	5.46	3.89	0.85	0.38	0.11	0.82	100.40	283	367	7	59	0.01	0.18	45	8	24	-10	-30	18	-1.0	-5	
32-00-3072-7	Pg2ppz	321016	6039866	14U	64.79	15.89	5.52	0.08	2.18	4.84	3.59	2.19	0.70	0.21	0.88	99.18	345	335	11	83	-0.01	0.11	47	17	23	26	72	20	1.2	-5	
32-99-2048-1	Pg2ppz	311125	6041389	14U	65.61	16.47	4.48	0.07	2.15	4.46	5.78	0.43	0.45	0.11	0.60	100.32	266	244	8	80	0.01	0.18	33	14	36	-10	58	18	-1.0	-5	
MAJOR GABBROIC INTRUSIONS																															
McLeod Narrows gabbro																															
32-00-3028-4	Gabbro	321429	6039931	14U	47.24	18.16	8.37	0.13	12.44	11.96	1.30	0.07	0.28	0.04	1.48	99.13	14	89	20	101	0.04	-0.05	216	54	245	61	37	10	1.0	-5	
32-00-3072-3	Gabbro	321016	6039866	14U	48.07	17.67	14.32	0.20	5.61	10.70	2.24	0.24	0.87	0.06	0.48	100.16	21	171	24	237	0.01	-0.05	42	80	64	135	79	26	2.0	-5	
32-00-3028-6	Gabbro	321429	6039931	14U	48.25	14.77	13.29	0.19	8.87	11.27	2.15	0.12	0.84	0.24	0.8	99.87	37	108	33	243	0.01	-0.05	164	58	158	100	55	15	1.3	-5	
32-00-3072-10	Gabbro	321016	6039866	14U	48.94	18.16	7.59	0.13	10.04	12.98	1.30	0.53	0.29	0.04	1.88	100.19	77	99	29	132	-0.01	-0.05	812	56	144	39	45	15	1.6	-5	
Lavigne Lake gabbro																															
32-00-3041-1	Pyroxenite	325131	6041013	14U	44.28	5.29	14.36	0.19	29.99	5.20	0.32	0.02	0.32	0.03	6.46	99.59	8	32	22	87	0.02	-0.05	3170	117	948	54	66	4	1.0	-5	
32-00-3062-4	Pyroxenite	326086	6040919	14U	44.50	6.54	14.10	0.17	27.35	6.54	0.25	0.04	0.47	0.04	5.91	99.08	7	41	32	128	0.06	-0.05	3720	96	934	-10	56	6	1.3	-5	
32-00-3062-1	Pyroxenite	326086	6040919	14U	45.50	6.13	12.97	0.17	27.42	7.03	0.33	0.02	0.39	0.03	5.71	98.98	8	37	31	109	0.02	0.15	3980	102	865	32	43	6	1.4	-5	
32-00-3064-2	Pyroxenite	325906	6041032	14U	46.04	3.94	12.84	0.19	29.11	7.41	0.18	0.03	0.22	0.03	5.32	99.94	9	12	32	101	0.03	-0.05	3020	102	766	-10	56	4	1.4	-5	
32-00-3064-3	Pyroxenite	325906	6041032	14U	46.50	4.04	12.38	0.20	29.66	6.82	0.14	0.01	0.22	0.03	5.14	99.26	7	12	30	89	0.02	-0.05	3050	108	786	-10	60	4	1.6	-5	
32-00-3062-2	Pyroxenite	326086	6040919	14U	46.59	6.75	12.86	0.19	24.07	8.65	0.44	0.06	0.33	0.04	4.43	99.79	7	30	35	123	0.03	-0.05	3220	97	739	74	75	6	1.3	-5	
32-00-3242-1	Pyroxenite	307129	6043004	14U	46.76	6.13	12.66	0.18	25.76	7.95	0.18	0.06	0.27	0.03	7.23	100.21	7	29	29	93	0.04	1.58	3600	113	790	49	61	7	1.7	-5	
32-00-3242-4	Pyroxenite	307129	6043004	14U	47.18	14.95	10.39	0.16	14.30	11.39	1.21	0.07	0.30	0.04	2.15	99.41	28	94	27	116	0.05	-0.05	143	70	318	84	53	10	1.3	-5	
32-99-2121-3	Pyroxenite	311215	6043011	14U	47.43	5.08	12.13	0.16	25.84	9.05	0.02	-0.01	0.27	0.03	5.73	98.88	4	21	33	132	0.03	2.37	3290	99	822	55	76	6	1.3	-5	
32-99-2028-2	Pyroxenite	311797	6042701	14U	47.44	6.09	11.75	0.17	24.38	9.77	0.07	0.03	0.27	0.03	4.72	98.69	6	10	30	120	0.06	1.53	1880	66	501	97	35	6	0.6	-5	
32-00-3062-3	Pyroxenite	326086	6040919	14U	47.48	6.78	12.81	0.19	23.22	8.87	0.27	-0.01	0.35	0.03	4.29	99.42	7	33	38	145	0.05	-0.05	2910	93	738	77	109	6	1.5	-5	
32-00-3242-2	Pyroxenite	307129	6043004	14U	47.57	3.76	11.43	0.18	27.02	9.70	0.11	-0.01	0.22	0.02	8.25	99.04	7	42	34	96	0.04	4.95	3250	83	850	26	61	3	1.5	-5	
32-99-2028-1	Pyroxenite	311797	6042701	14U	47.81	7.57	12.34	0.20	21.30	10.26	0.21	0.04	0.25	0.02	3.59	98.67	9	10	37	139	0.03	0.66	2300	63	416	56	-30	6	0.7	-5	
32-00-3242-6	Gabbro	307129	6043004	14U	48.91	15.43	9.47	0.16	12.04	11.32	2.04	0.19	0.37	0.06	1.71	100.11	50	110	39	164	0.03	0.11	280	54	196	88	65	11	1.2	-5	
32-00-3063-1	Gabbro	325974	6041998	14U	49.40	4.78	8.89	0.20	21.06	14.86	0.52	-0.01	0.27	0.03	2.48	98.97	6	12	52	153	-0.01	-0.05	4290	76	335	41	35	5	1.9	-5	
32-00-3213-1	Gabbro	340622	6040851	14U	48.63	16.09	6.44	0.13	11.16	15.26	1.05	0.03	0.19	0.02	1.02	98.63	16	93	41	150	0.01	-0.05	473	45	127	89	-30	11	1.7	-5	
32-00-3064-1	Gabbro	325906	6041032	14U	49.87	4.82	10.85	0.17	23.98	9.93	0.19	0.06	0.30	0.03	3.91	98.97	5	13	48	153	0.01	-0.05	3380	72	329	-10	61	4	1.7	-5	
32-00-3063-2	Gabbro	325974	6041998	14U	50.52	4.51	9.36	0.17	20.22	14.20	0.28	0.02	0.29	0.03	2.96	99.51	13	20	55	169	0.05	-0.05	3110	59	340	34	41	5	1.7	-5	
32-99-3064-4	Gabbro	325906	6041032	14U	50.98	4.28	9.56	0.18	20.64	13.72	0.33	0.02	0.25	0.02	1.87	100.40	6	23	56	169	0.04	-0.05	3510	68	399	61	39	4	1.8	6	
32-00-3242-5	Gabbro	307129	6043004	14U	51.10	10.53	9.06	0.16	14.97	12.15	1.43	0.08	0.43	0.08	1.59	98.67	33	98	44	182	0.03	0.15	1460	51	237	107	49	8	1.5	-5	
32-00-3242-7	Gabbro	307129	6043004	14U	51.39	15.26	8.48	0.16	9.63	12.39	2.09	0.17	0.38	0.04	0.89	99.43	36	112	41	181	0.01	0.07	151	57	94	156	41	14	1.8	-5	
MISCELLANEOUS INTRUSIVE UNITS																															
32-99-2282-2	Dabase (subunit P5c)	316787	6040728	14U	51.17	5.53	14.66	0.38	14.42	12.35	0.41	0.17	0.64	0.07	0.79	98.66	27	24	20	100	0.01	-0.05	1290	26	273	-10	-30	5	-1.0	-5	
32-99-2104-1	Quartz diorite, MT-bearing (subunit P5b)	308670	6041860	14U	58.52	12.41	16.55	0.27	3.01	3.48	3.92	0.36	1.13	0.34	0.06	100.24	436	89	25	7	0.02	-0.05	-20	25	-15	-10	174	32	1.0	-5	

Appendix: Major-, minor- and trace-element data for volcanic and intrusive rocks in the southeast Max Lake–Aswapiswanan Lake area

Sample number	Rock type	UTM Easting	UTM Northing	UTM Zone	Rb (ppm)	Sr (ppm)	Y (ppm)	Zr (ppm)	Nb (ppm)	Mo (ppm)	Ag (ppm)	In (ppm)	Sn (ppm)	Sb (ppm)	Cs (ppm)	La (ppm)	Ce (ppm)	Pr (ppm)	Nd (ppm)	Sm (ppm)	Eu (ppm)	Gd (ppm)	Tb (ppm)	Dy (ppm)	Ho (ppm)	Er (ppm)	Tm (ppm)	Yb (ppm)	Lu (ppm)		
NORTHERN VOLCANIC SUITE																															
32-99-2012-3	Basalt	311758	6043413	14U	5	227	27.0	88	4.0	-2	-0.5	-0.2	-1	0.7	-0.5	6.10	14.70	2.18	10.00	3.00	1.13	3.90	0.70	4.50	0.90	2.80	0.41	2.60	0.39		
32-00-3265-1	Basalt	308790	6043261	14U	9	139	21.0	89	3.6	2	-0.5	-0.1	-1	0.9	0.9	14	27.6	3.24	12.5	2.87	0.845	3.37	0.54	3.42	0.69	2.08	0.292	1.93	0.308		
32-00-3009-1	Basalt	321669	6041821	14U	17	107	19.0	79	3.3	-2	-0.5	-0.1	-1	0.3	0.8	6.17	14.4	1.98	8.47	2.17	0.784	2.79	0.45	2.78	0.57	1.8	0.262	1.76	0.263		
32-99-2201-1	Basalt	316602	6042503	14U	9	88	25.0	99	5.0	-2	-0.5	-0.2	-1	-0.5	-0.5	10.80	22.90	3.06	13.60	3.60	1.13	4.00	0.70	4.30	0.80	2.60	0.39	2.50	0.39		
32-00-3280-1	Basalt	308349	6043265	14U	3	220	18.4	84	4.1	2	-0.5	-0.1	1	0.2	0.2	10.7	22.1	2.74	11	3.01	1.03	3.66	0.59	3.46	0.72	2.25	0.313	2.17	0.313		
32-00-3004-1	Basalt	322303	6041312	14U	15	144	28.4	108	5.3	-2	-0.5	-0.1	1	0.5	0.9	16.1	33.3	4.06	16	3.82	1.2	4.59	0.74	4.35	0.89	2.74	0.391	2.54	0.397		
32-99-2023-1	Basalt	311960	6043022	14U	8	135	18.0	72	3.0	-2	-0.5	-0.2	-1	-0.5	-0.5	9.30	19.10	2.40	9.90	2.40	0.82	2.90	0.50	3.10	0.60	1.90	0.28	1.90	0.28		
32-99-2066-1	Andesite	313159	6042670	14U	9	155	26.0	108	4.0	-2	-0.5	-0.2	-1	-0.5	0.5	15.70	30.90	3.81	15.10	3.30	1.07	4.10	0.70	4.40	0.90	2.70	0.39	2.60	0.39		
32-99-2021-1	Andesite	312048	6043208	14U	7	269	16.0	81	3.0	-2	-0.5	-0.2	-1	1.2	-0.5	12.70	23.90	2.77	10.00	2.10	0.72	2.50	0.40	2.60	0.50	1.60	0.24	1.50	0.23		
32-99-2139-5	Basalt, altered	313950	6042820	14U	6	1330	27.0	216	13.0	-2	-0.5	-0.2	-1	1.2	-0.5	99.40	189.00	21.80	75.90	11.20	3.13	9.50	1.10	5.20	1.00	2.50	0.34	2.20	0.33		
32-99-2120-1	Basalt, altered	311694	6042877	14U	3	173	16.0	43	1.0	-2	-0.5	-0.2	-1	-0.5	-0.5	3.10	6.90	1.01	4.80	1.60	0.64	2.20	0.40	2.80	0.60	1.80	0.28	1.80	0.25		
32-99-2019-1	Gabbro	311892	6043268	14U	5	160	17.0	59	2.0	-2	-0.5	-0.2	-1	0.5	-0.5	6.20	13.70	1.86	8.30	2.20	0.82	2.80	0.50	3.10	0.70	1.90	0.28	1.80	0.27		
32-99-2224-1	Gabbro	314715	6042368	14U	-2	108	23.0	54	1.0	-2	-0.5	-0.2	-1	1.0	-0.5	2.50	6.00	0.95	4.70	1.70	0.70	2.60	0.50	3.60	0.80	2.60	0.39	2.50	0.39		
32-99-2175-1	Dacite	315807	6042597	14U	36	108	31.0	158	7.0	-2	-0.5	-0.2	1	-0.5	0.6	22.30	42.90	5.03	19.40	4.20	1.33	5.00	0.90	5.20	1.10	3.30	0.50	3.20	0.48		
32-99-2231-1	Dacite	315049	6042504	14U	52	273	13.0	121	5.0	-2	-0.5	-0.2	-1	-0.5	2.0	21.10	36.00	3.87	13.40	2.50	0.81	2.50	0.40	2.10	0.40	1.20	0.18	1.20	0.17		
32-99-2064-1	Dacite	313588	6042658	14U	63	557	11.0	141	7.0	-2	-0.5	-0.2	-1	-0.5	1.0	44.90	83.10	8.93	29.10	4.10	1.17	3.30	0.40	2.10	0.40	1.00	0.13	0.90	0.14		
32-00-3266-1	Felsic volcanic breccia	308773	6043323	14U	106	139	37.1	262	17.6	3	-0.5	-0.1	3	1.5	2.6	64.7	120	12.8	43.5	8.1	1.76	7.98	1.29	7.24	1.41	4.33	0.621	4.08	0.571		
32-99-2167-1	Pgpp, major sill	315681	6042367	14U	75	168	8.0	88	4.0	-2	-0.5	-0.2	-1	-0.5	1.3	21.10	36.40	3.85	12.80	2.10	0.68	1.80	0.20	1.40	0.30	0.80	0.11	0.70	0.11		
32-99-2173-1	Pgpp, major sill	315112	6042741	14U	51	232	14.0	133	6.0	-2	-0.5	-0.2	-1	-0.5	1.4	24.00	41.90	4.44	15.30	2.70	0.88	2.70	0.40	2.30	0.50	1.40	0.20	1.30	0.19		
32-00-3011-1	Pgpppp	320970	6041591	14U	39	332	10.3	114	5.7	-2	-0.5	-0.1	-1	1.7	0.7	28.3	50.4	5.04	16.5	2.59	0.807	2.85	0.35	1.71	0.33	0.94	0.135	0.87	0.12		
32-99-2206-1	Pgpppp	316811	6042767	14U	28	753	11.0	130	7.0	-2	-0.5	-0.2	-1	0.7	-0.5	48.20	83.90	8.89	29.20	4.00	1.16	3.30	0.40	1.90	0.40	1.00	0.14	0.80	0.13		
32-99-2340-1	Pgpppp	317597	6041908	14U	94	111	26.0	241	15.0	-2	-0.5	-0.2	-1	-0.5	0.6	65.40	119.00	12.90	42.30	7.20	1.08	6.30	0.90	4.90	0.80	2.60	0.38	2.20	0.32		
32-99-2006-1	Pgpppp	310334	6043682	14U	43	75	21.0	391	4.0	2	-0.5	-0.2	1	-0.5	0.8	35.40	67.50	7.56	27.60	5.10	1.92	4.70	0.70	3.70	0.70	2.10	0.33	2.20	0.38		
32-99-2010-2	Pgpppp	311218	6043710	14U	47	78	8.0	71	2.0	-2	-0.5	-0.2	-1	-0.5	1.0	13.00	24.20	2.79	9.60	2.30	0.39	2.10	0.30	1.30	0.30	0.70	0.11	0.70	0.10		
CENTRAL VOLCANIC SUITE																															
32-99-2254-1	Basalt	317917	6041950	14U	4	67	21.0	42	1.0	-2	-0.5	-0.2	-1	-0.5	-0.5	1.80	4.90	0.78	3.80	1.40	0.63	2.20	0.50	3.20	0.70	2.20	0.36	2.30	0.35		
32-00-3124-1	Basalt	337029	6040445	14U	3	139	16.9	48	4.0	4	-0.5	-0.1	-1	0.4	0.8	2.89	6.46	0.94	4.4	1.55	0.677	2.43	0.46	3.08	0.66	2.15	0.32	2.19	0.342		
32-00-3047-1	Basalt	324239	6040650	14U	1	82	20.8	45	0.5	3	-0.5	-0.1	-1	0.8	0.4	2.92	6.58	1	4.56	1.57	0.674	2.39	0.47	3.13	0.7	2.08	0.321	2.14	0.329		
32-99-2342-1	Basalt	318617	6041237	14U	6	88	23.0	53	1.9	-2	-0.5	-0.2	-1	-0.5	-0.5	2.80	6.60	0.92	4.90	1.90	0.65	2.50	0.60	3.90	0.80	2.60	0.42	2.50	0.39		
32-00-3070-1	Basalt	323288	6040728	14U	1	102	17.3	49	0.5	-2	-0.5	-0.1	-1	0.5	0.3	2.7	6.35	0.93	4.54	1.56	0.676	2.34	0.48	3.16	0.7	2.19	0.321	2.17	0.336		
32-00-3220-1	Basalt	349140	6039356	14U	10	94	27.5	82	1.2	-2	-0.5	-0.1	1	-0.2	0.8	4.05	9.66	1.4	7.05	2.26	0.953	3.79	0.74	5.13	1.11	3.45	0.514	3.5	0.529		
32-99-2000-1	Basalt	310666	6042777	14U	2	104	18.0	36	0.5	-2	-0.5	-0.2	-1	-0.5	-0.5	2.10	5.30	0.81	4.10	1.40	0.62	2.10	0.40	2.90	0.70	1.90	0.30	2.00	0.29		
32-00-3331-1	Basalt	308870	6042804	14U	3	97	17.5	42	0.8	4	-0.5	-0.1	-1	0.3	0.3	3.49	7.57	1.11	5.06	1.66	0.64	2.49	0.5	3.24	0.71	2.18	0.313	2.16	0.361		
32-00-3021-1	Basalt	323193	6040942	14U	-1	164	24.0	56	0.8	-2	-0.5	-0.1	-1	1.0	0.3	3.09	7.36	1.02	4.94	1.63	0.601	2.61	0.51	3.57	0.77	2.45	0.381	2.6	0.406		
32-99-2032-1	Basalt	311860	6042504	14U	-2	93	15.0	34	1.2	-2	-0.5	-0.2	-1	-0.5	-0.5	1.90	4.50	0.69	3.40	1.10	0.50	1.80	0.40	2.50	0.60	1.70	0.26	1.70	0.25		
32-99-2164-1	Basalt	317225	6041341	14U	-2	96	19.0	42	1.0	-2	-0.5	-0.2	-1	-0.5	-0.5	2.50	5.70	0.86	4.10	1.50	0.64	2.20	0.50	3.00	0.70	2.00	0.31	2.00	0.30		
32-99-2120-5	Basalt	311694	6042877	14U	3	105	24.0	50	1.0	-2	-0.5	-0.2	-1	1.5	-0.5	2.90	6.50	1.00	4.90	1.70	0.75	2.70	0.50	3.70	0.90	2.50	0.40	2.90	0.38		
32-99-2071-1	Basalt	312507	6042427	14U	-2	100	17.0	39	1.0	-2	-0.5	-0.2	-1	-0.5	-0.5	2.90	6.20	0.88	4.10	1.30	0.58	2.00	0.40	2.70	0.60	1.80	0.28	1.80	0.26		
32-99-2295-1	Basalt	317429	6040969	14U	-2	94	17.0	44	2.0	-2	-0.																				

Appendix: Major-, minor- and trace-element data for volcanic and intrusive rocks in the southeast Max Lake–Aswapiswanan Lake area

Sample number	Rock type	UTM Easting	UTM Northing	UTM Zone	HF (ppm)	Ta (ppm)	W (ppm)	Ti (ppm)	Pb (ppm)	Bi (ppm)	Th (ppm)	U (ppm)	(La/Yb)ch
NORTHERN VOLCANIC SUITE													
32-99-2012-3	Basalt	311758	6043413	14U	2.40	0.30	-0.5	-0.10	-5	-0.20	2.50	0.50	1.68
32-00-3265-1	Basalt	308790	6043261	14U	2.7	0.35	-0.5	-0.05	-5	0.2	3.37	0.87	5.20
32-00-3009-1	Basalt	321660	6041822	14U	2.2	0.3	-0.5	-0.05	-5	0.2	2.75	0.65	2.51
32-99-2201-1	Basalt	316602	6042503	14U	2.80	0.40	-0.5	-0.10	-5	-0.20	3.60	1.00	3.10
32-00-3280-1	Basalt	308340	6043265	14U	2.8	0.38	0.9	-0.05	-5	0.4	3.63	0.94	3.54
32-00-3004-1	Basalt	322303	6041312	14U	3.3	0.49	1.2	0.08	7	0.5	3.84	1.03	4.55
32-99-2023-1	Basalt	311960	6043022	14U	2.00	0.30	-0.5	-0.10	-5	-0.20	2.70	0.70	3.51
32-99-2066-1	Andesite	313159	6042670	14U	2.90	0.40	-0.5	-0.10	-5	-0.20	4.00	1.00	4.33
32-99-2021-1	Andesite	312048	6043208	14U	2.10	0.30	-0.5	0.10	22	-0.20	4.00	1.10	6.07
32-99-2139-5	Basalt, altered	313950	6042820	14U	4.90	0.90	-0.5	-0.10	-5	1.00	18.90	3.90	32.41
32-99-2120-1	Basalt, altered	311894	6042877	14U	1.30	-0.10	-0.5	-0.10	-5	-0.20	0.70	0.20	1.24
32-99-2019-1	Gabbro	311892	6043268	14U	1.70	0.20	-0.5	-0.10	-5	-0.20	1.70	0.40	2.47
32-99-2224-1	Gabbro	314715	6042368	14U	1.60	-0.10	-0.5	-0.10	15	-0.20	0.80	0.20	0.72
32-99-2175-1	Dacite	315807	6042997	14U	4.10	0.70	1.3	0.40	23	0.40	6.70	1.80	5.00
32-99-2231-1	Dacite	315049	6042904	14U	3.10	0.60	-0.5	0.30	34	-0.20	8.10	2.30	12.61
32-99-2084-1	Dacite	313588	6042858	14U	3.40	0.80	-0.5	0.30	22	0.30	16.60	4.40	35.79
32-00-3266-1	Felsic volcanic breccia	308773	6043323	14U	9.9	1.77	1.8	0.16	16	0.7	21.4	6.78	11.36
32-99-2167-1	Pygpp, major sill	315681	6042367	14U	2.20	0.50	-0.5	-0.10	8	-0.20	7.30	2.20	21.62
32-99-2173-1	Pygpp, major sill	315112	6042741	14U	3.20	0.70	-0.5	0.30	12	-0.20	8.90	2.40	13.24
32-00-3011-1	Pygpp	320970	6041591	14U	2.9	0.61	-0.5	0.26	24	3.3	9.61	2.74	23.33
32-99-2001-1	Pygpp	316911	6042677	14U	3.20	0.70	0.5	0.20	45	1.20	15.30	4.10	38.42
32-99-2340-1	Pygpp	317697	6041908	14U	6.40	1.60	-0.5	0.50	16	-0.20	34.30	7.10	21.33
32-99-2006-1	Pygpp	310354	6043682	14U	8.50	0.50	-0.5	0.20	13	-0.20	10.00	2.00	11.54
32-99-2010-2	Pygpp	311218	6043710	14U	2.70	0.40	-0.5	0.40	64	-0.20	33.30	7.50	13.32
CENTRAL VOLCANIC SUITE													
32-99-2254-1	Basalt	317917	6041950	14U	1.20	-0.10	-0.5	-0.10	-5	-0.20	0.60	0.20	0.56
32-00-3124-1	Basalt	337029	6040445	14U	1.5	0.09	0.6	-0.05	-5	0.4	0.66	0.14	0.95
32-00-3047-1	Basalt	324239	6040650	14U	1.5	0.08	-0.5	-0.05	-5	0.2	0.59	0.16	0.98
32-99-2342-1	Basalt	318617	6041237	14U	1.50	-0.10	-0.5	-0.10	-5	-0.20	0.60	0.20	0.80
32-00-3070-1	Basalt	323286	6040728	14U	1.6	0.1	-0.5	-0.05	-5	1.1	0.59	0.14	0.89
32-99-3220-1	Basalt	349140	6039356	14U	2.5	0.14	0.5	0.05	-5	1.5	0.9	0.22	0.83
32-99-2000-1	Basalt	310666	6042777	14U	1.20	-0.10	-0.5	-0.10	-5	-0.20	0.50	0.10	0.75
32-00-3331-1	Basalt	308970	6042804	14U	1.6	0.11	-0.5	-0.05	-5	0.3	0.71	0.18	1.16
32-99-3021-1	Basalt	323193	6040942	14U	1.7	0.11	-0.5	-0.05	9	0.4	0.73	0.17	0.85
32-99-2032-1	Basalt	311860	6042504	14U	1.00	-0.10	-0.5	-0.10	7	-0.20	0.50	0.10	0.80
32-99-2164-1	Basalt	317225	6041341	14U	1.20	-0.10	-0.5	-0.10	8	-0.20	0.60	0.10	0.90
32-99-2120-5	Basalt	311894	6042877	14U	1.40	-0.10	-0.5	-0.10	-5	-0.20	0.70	0.20	0.83
32-99-2071-1	Basalt	312507	6042427	14U	1.20	-0.10	-0.5	-0.10	12	-0.20	0.70	0.20	1.16
32-99-2295-1	Basalt	317429	6040969	14U	1.30	0.10	-0.5	-0.10	10	-0.20	1.00	0.20	1.52
32-99-2163-1	Basalt	314222	6041310	14U	1.40	0.10	-0.5	-0.10	12	-0.20	1.20	0.30	1.47
32-99-2036-1	Basalt	311809	6042001	14U	1.80	0.20	-0.5	-0.10	14	-0.20	1.60	0.40	1.98
32-00-3240-1	Gabbro	307458	6042696	14U	1.2	0.1	-0.5	-0.05	-5	0.2	0.75	0.17	1.32
32-99-2071-2	Gabbro	312507	6042427	14U	1.30	-0.10	-0.5	-0.10	12	-0.20	0.60	0.10	0.90
32-99-2238-1	Megaphytic gabbro	315922	6041669	14U	1.00	-0.10	-0.5	-0.10	9	-0.20	0.50	0.10	0.94
32-99-2362-1	Megaphytic gabbro	316792	6041454	14U	1.00	-0.10	-0.5	-0.10	-5	-0.20	0.40	0.10	0.94
32-99-2183-4	Megaphytic gabbro	315215	6041759	14U	0.90	-0.10	-0.5	-0.10	8	-0.20	0.70	0.10	0.90
32-99-2045-1	Pygpp	311065	6041619	14U	3.20	0.60	0.7	0.30	11	-0.20	6.00	1.60	9.01
32-00-3024-1	Pygpp	322890	6041018	14U	2.8	0.82	0.8	0.13	9	0.3	7.79	2.42	13.16
32-00-3245-1	Pygpp	307171	6042739	14U	3.6	0.68	1.3	0.16	6	0.4	8.81	2.55	15.35
32-99-2000-3	Pygpp	310666	6042777	14U	2.70	0.50	-0.5	-0.10	-5	-0.20	6.80	2.10	16.76
32-00-3231-1	Pygpp	310167	6042997	14U	9	2.02	0.7	0.48	10	0.8	47.8	9.05	20.98
32-99-2182-1	Pygpp	315327	6041815	14U	6.40	1.50	-0.5	0.70	24	-0.20	32.60	7.80	23.71

Appendix: Major-, minor- and trace-element data for volcanic and intrusive rocks in the southeast Max Lake–Aswapiswanan Lake area

Sample number	Rock type	UTM Easting	UTM Northing	UTM Zone	HF	Ta	W	Ti	Pb	Bi	Th	U	(La/Yb)ch
SOUTHERN VOLCANIC SUITE													
32-99-2092-1	Basalt	312102	6040225	14U	3.10	0.40	-0.5	-0.10	-5	-0.20	1.40	0.30	1.27
32-00-3196-1	Basalt	348424	6037375	14U	2.8	0.36	2.2	-0.05	6	0.6	3.63	1.03	3.61
32-99-2090-2	Basalt, altered	311935	6041440	14U	2.90	0.50	-0.5	-0.10	17	-0.20	4.20	1.00	6.93
32-99-2096-1	Basalt, altered	312001	6040691	14U	4.20	0.90	-0.5	-0.10	12	1.10	7.30	1.60	7.65
32-99-2287-1	Dacite	317124	6040417	14U	3.40	0.70	-0.5	0.20	23	-0.20	9.50	2.60	15.78
32-99-2106-2	Dacite	310130	6041596	14U	2.90	0.60	-0.5	0.20	15	-0.20	8.50	2.40	23.57
32-99-2082-1	Dacite	311930	6041227	14U	3.10	0.70	-0.5	0.10	22	0.40	9.70	2.60	21.61
32-00-3259-3	Felsic volcanic breccia	306429	6041768	14U	4.2	0.7	1.0	0.13	-5	1.1	8.64	2.16	23.26
32-99-2161-1	Dacite clast in breccia	314220	6040854	14U	3.80	0.80	-0.5	0.10	15	-0.20	10.20	2.80	19.01
32-99-2353-2	Felsic flow/sill	318081	6040060	14U	3.30	0.80	1.3	-0.10	11	0.50	10.90	2.70	42.61
32-00-3072-7	Pgzzpp	321016	6039866	14U	5.9	1.15	0.8	0.39	11	1.8	16.3	4.27	19.58
32-99-2048-1	Pgzzpp	311126	6041389	14U	2.80	0.60	-0.5	-0.10	27	-0.20	8.30	2.00	21.25
MAJOR GABBROIC INTRUSIONS													
McLeod Narrows gabbro													
32-00-3028-4	Gabbro	321429	6039931	14U	0.6	0.05	-0.5	-0.05	-5	0.6	0.44	0.11	1.88
32-00-3072-3	Gabbro	321016	6039866	14U	2.3	0.17	2.3	-0.05	-5	0.7	0.58	0.4	1.15
32-00-3028-6	Gabbro	321429	6039931	14U	1.4	0.09	0.8	-0.05	-5	1.8	0.41	0.11	1.23
32-00-3072-10	Gabbro	321016	6039866	14U	1	0.1	-0.5	0.18	10	3	0.93	0.18	2.10
Lavigne Lake gabbro													
32-00-3041-1	Pyroxenite	325131	6041013	14U	0.6	0.16	0.7	0.05	-5	0.8	0.43	0.12	2.35
32-00-3062-4	Pyroxenite	326086	6040919	14U	0.90	0.10	-0.5	0.09	13	-0.10	0.79	0.19	2.30
32-00-3062-1	Pyroxenite	326086	6040919	14U	0.90	0.09	-0.5	0.10	-5	0.30	0.77	0.19	1.72
32-00-3064-2	Pyroxenite	325906	6041032	14U	0.30	0.04	-0.5	-0.05	8	-0.10	0.28	0.13	2.00
32-00-3064-3	Pyroxenite	325906	6041032	14U	0.40	0.05	-0.5	-0.05	7	-0.10	0.30	0.09	2.00
32-00-3062-2	Pyroxenite	326086	6040919	14U	0.70	0.08	-0.5	0.18	-5	0.30	0.63	0.18	2.08
32-00-3242-1	Pyroxenite	307129	6043004	14U	0.70	0.06	-0.5	-0.05	-5	0.10	0.57	0.15	2.19
32-00-3242-4	Pyroxenite	307129	6043004	14U	0.50	0.08	-0.5	-0.05	-5	-0.10	0.54	0.15	2.90
32-99-2121-3	Pyroxenite	311215	6043011	14U	0.50	-0.10	-0.2	-0.05	12	-0.08	0.37	0.10	1.98
32-99-2028-2	Pyroxenite	311797	6042701	14U	0.50	-0.10	-0.2	-0.05	-5	-0.08	0.43	0.11	1.20
32-00-3062-3	Pyroxenite	326086	6040919	14U	0.70	0.07	2.9	0.17	-5	-0.10	0.56	0.19	2.30
32-00-3242-2	Pyroxenite	307129	6043004	14U	0.30	0.05	-0.5	-0.05	-5	-0.10	0.26	0.08	2.20
32-99-2028-1	Pyroxenite	311797	6042701	14U	0.40	-0.10	-0.2	-0.05	-5	-0.08	0.37	0.17	1.68
32-00-3242-6	Gabbro	307129	6043004	14U	0.70	0.09	-0.5	-0.05	-5	-0.10	0.62	0.18	3.10
32-00-3063-1	Gabbro	325974	6041998	14U	0.60	0.05	0.6	-0.05	-5	1.40	0.41	0.12	1.63
32-00-3213-1	Gabbro	340622	6040851	14U	0.40	0.19	-0.5	-0.05	-5	0.50	0.25	0.07	1.76
32-00-3064-1	Gabbro	325906	6041032	14U	0.50	0.05	-0.5	-0.05	12	0.10	0.36	0.10	1.40
32-00-3063-2	Gabbro	325974	6041998	14U	0.40	0.06	-0.5	-0.05	9	0.10	0.30	0.09	1.60
32-00-3064-4	Gabbro	325906	6041032	14U	0.40	0.03	-0.5	-0.05	7	0.10	0.24	0.07	1.30
32-00-3242-5	Gabbro	307129	6043004	14U	0.80	0.11	-0.5	-0.05	6	-0.10	0.75	0.21	2.50
32-00-3242-7	Gabbro	307129	6043004	14U	1.00	0.13	-0.5	-0.05	-5	0.40	0.99	0.26	2.15
MISCELLANEOUS INTRUSIVE UNITS													
32-99-2282-2	Diorite (subunit P5c)	316787	6040728	14U	1.80	0.50	-0.5	-0.10	-5	-0.20	2.60	0.50	5.09
32-99-2104-1	Quartz diorite, MT-bearing (subunit P5d)	309870	6041860	14U	6.20	0.40	-0.5	0.20	12	-0.20	2.00	0.60	1.16
Major elements (wt %) calculated to 100% volatile-free. Trace elements in ppm. Total iron as Fe ₂ O ₃ .													
Minus values indicate an element was not present at the given detection limit.													
Chondrite-normalizing values from Sun and McDonough (1989)													